SEMI-SYNTHESIS AND EVALUATION OF FUSIDIC ACID DERIVATIVES AS POTENTIAL ANTITUBERCULOSIS AGENTS

A dissertation submitted to the University of Cape Town in fulfillment of the requirements for the degree

Master in Chemistry

By

Petrus Siningu Shanika

Supervisor: Prof. Kelly Chibale

Co–supervisor: Dr. Suthananda Sunassee

Department of Chemistry
University of Cape Town
Rondebosch, 7700
South Africa

June 2017

Declaration

I declare that the thesis entitled, "***Semi-synthesis and evaluation of fusidic acid derivatives as potential antituberculosis agents"*** is my original work and has not been submitted for the award of any degree at any university. I know the meaning of plagiarism and declare that all of the work in the document, except for that which is properly acknowledged, is my own.

Signed by candidate

.....

Petrus S. Shanika

June 2017

Dedicated to my parents:

My late dad

Mr. Petrus Marovhu Shaanika "Siningu"

And my mum

Ms. Leena Nasira Mwendela

Acknowledgement

Let me take this opportunity to extend my sincere heartfelt thanks to my supervisors, Prof. Kelly Chibale and Dr. Suthananda Sunassee. Thanks to Prof. Kelly Chibale for the opportunity, support, guidance and supervisory input from the beginning of the research to its conclusion. I wish to thank Dr. Suthananda Sunassee for the support and advice I received, I am forever grateful to both of them.

I also wish to acknowledge the following: Dr. Kawaljit Singh, Dr. Gurminder Kaur, Peter Cheuka and Dr. Mathew Njoroge for their useful suggestions, introducing me and teaching me on the chemistry and biological aspects of my research. I wish to thank Godwin Akpeko, Duane Knowles, Edward Kativu and Pete Roberts for their assistance with LC-MS and spectroscopic analysis. I appreciate Ms. Ronnett Seldon for the in vitro antimycobacterial testing of all compounds.

Special thanks to Peter Cheuka and Dr. Gurminder Kaur for proof-reading my chapters before submission. I am also indeed grateful to the other KC and Natural Product research group members for their support, especially the FA group members for support and ideas.

I am also thankful to Elaine Rutherfoord-Jones, Saroja Naicker and Deirdre Brooks for the generous assistance with administrative arrangements.

Lastly, my deepest appreciation goes to my mum (Ms. Leena Mwendela), my siblings, the whole Mwendela and Marovhu family members, Dr. Hans Renate and my friends for their love, support, encouragement, faith and affection throughout my study.

Conferences

Shanika P, Kaur G, Sunassee S, Chibale K. *Semi-synthesis and profiling of fusidic acid derivatives as potential antituberculosis agents*. Poster presentation at a *H3D*: Progress in Drug Discovery and Development on Malaria, Tuberculosis and Neglected Tropical Diseases symposium, 15 – 18 November 2016, Goudini Spa, Western Cape, South Africa.

Abstract

The causative agent of tuberculosis (TB), *Mycobacterium tuberculosis* (*Mtb*), still remains one of the most serious infectious diseases with 10 million new reported cases in 2015. Although TB is curable, the ability to acquire resistance to various antibiotics by the *Mtb* organism is well known. The emergence and spread of multidrug resistance (MDR) and extremely drug resistance (XDR) *Mtb* strains, along with HIV/TB co-infections, has put TB control programmes in jeopardy, particularly in developing countries. Therefore, there is a continuous need to search for new structural classes of anti-TB drugs with novel modes of action and ideally no cross resistance to current drugs to treat both sensitive and resistant forms of TB.

Fusidic acid is a naturally occurring antibiotic used to treat Gram-positive bacterial infections. It has potent activity against *S. aureus* and is clinically used to treat mild to moderately severe skin and soft-tissue infections. The mode of action of fusidic acid involves the inhibition of protein synthesis via binding to bacterial elongation factor G (EF-G). Fusidic acid has also been reported to possess *in vitro* antimycobacterial activity but was subsequently found to lack *in vivo* efficacy in a mouse model.

Towards contributing to new antimycobacterial agents, this study focusses on repositioning fusidic acid for tuberculosis by employing prodrug and bioisosterism approaches through structural modifications at the C-3, C-11 and C-21 positions of the drug (Figure 1). Accordingly, C-21 derivatives **3.2** and **3.3** were synthesized by a one-step coupling reaction, while C-3 analogues **3.8** and **3.9** were synthesized by a three step synthetic protocol involving esterification followed by coupling with hydrazine monohydrate and mesylation. The other C-3 esters **3.10**-**3.22** were synthesized via Steglich esterification. The C-3 target compound **3.26** was synthesized

using a 4-step synthetic route. The first step involved an acid-amine coupling reaction, which was followed by mesylation, Jones oxidation and then reductive amination of the resulting ketone.

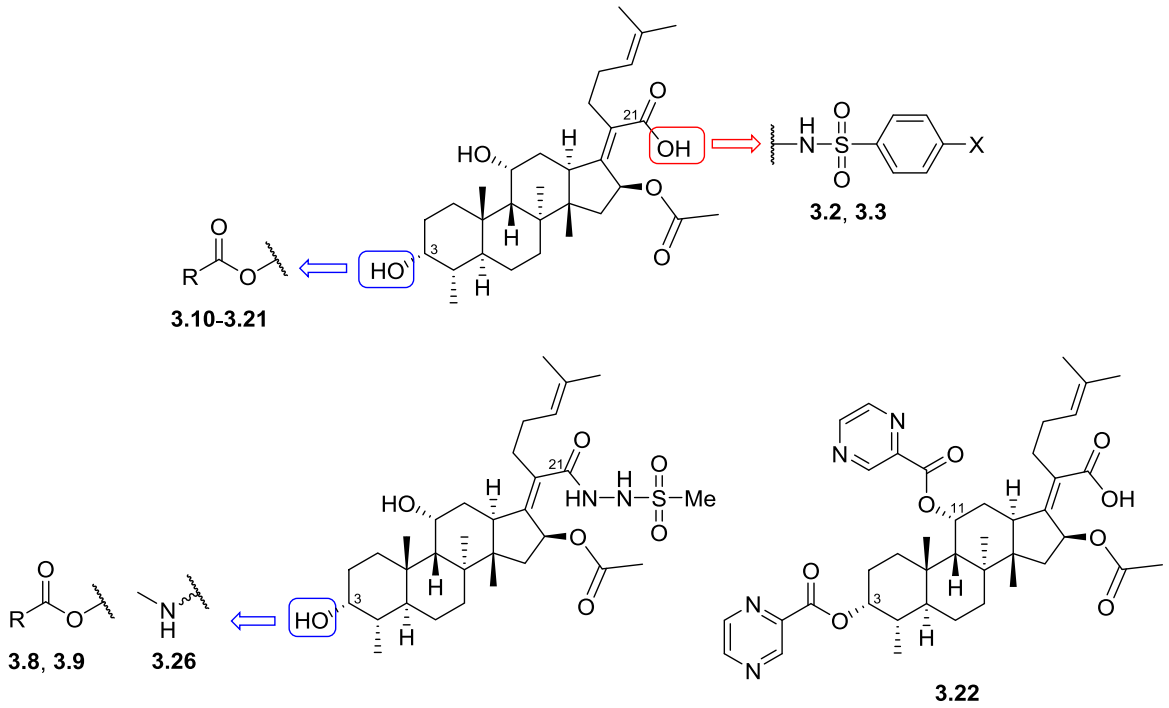

Figure 1: Graphic abstract of synthesized compounds

The synthesized compounds were characterized on the basis of nuclear magnetic resonance (NMR) spectroscopy, mass spectrometry (MS), high performance liquid chromatography (HPLC), thin layer chromatography (TLC) and melting point (m.p.).

Relative to fusidic acid (MIC_{99} of 0.49 µM), this set of analogues exhibited good to poor *in vitro* activity against the H37Rv strain of *Mtb* in glycerol-containing media glycerol-alanine-salt with Tween-80 and iron (GAST/Fe), with compounds **3.4**, **3.5**, **3.8** and **3.21** showing promising MIC_{99} values in the range of 0.49–7.81 µM. However, compounds **3.8** and **3.21** were inactive in the 7H9 GLU/ADC media containing glucose as a carbon source.

Structure-activity relationship (SAR) studies suggested that the C-3 and C-11 hydroxyl, as well as the C-21 carboxylic acid functional groups are necessary for antimycobacterial activity.

Table of Contents

Abbreviations

δ	Chemical shift
ADMET	Absorption, Distribution, Metabolism, Excretion and Toxicity
APCI	Atmospheric Pressure Chemical Ionization
AR	Analytical Reagent
ARV	Antiretroviral
BCG	Bacillus Calmette-Guérin
br s	Broad singlet
^{13}C NMR	Carbon-13 Nuclear Magnetic Resonance
$CDCl_3$	Deuterated chloroform
CD_3OD	Deuterated methanol
CH_3CN	Acetonitrile
COSY	Homonuclear Correlation Spectroscopy
CYP	Cytochrome
d	Doublet
DCM	Dichloromethane
DMAP	4-Dimethylaminopyridine
DMF	Dimethylformamide
dd	Doublet of Doublets
DAD	Diode Array Detector
DCC	*N*,*N*-Dicyclohexylcarbodiimide
DCE	1,2-Dichloroethane
DMSO-d_6	Deuterated dimethyl sulfoxide
DOTS	Directly Observed Treatment, Short Course
DS-TB	Drug-Susceptible Tuberculosis
DR-TB	Drug-Resistant Tuberculosis
E2	Bimolecular Elimination
EDCI	1-Ethyl-3-(3-dimethylaminopropyl)carbodiimide
EF-G	Elongation Factor G
ESI	Electrospray Ionization

EMB	Ethambutol
EtOAc	Ethyl acetate
eq	Equivalent
FDA	Food and Drug Administration
FICI	Fractional Inhibitory Concentration Index
^{1}H NMR	Proton Nuclear Magnetic Resonance
HCl	Hydrochloric acid
HIV	Human Immunodeficiency Virus
Hex	Hexane
HLM	Human Liver Microsome
HMBC	Heteronuclear Multiple Bond Correlation
HOBt	1-Hydroxybenzotriazole
HPLC	High Performance Liquid Chromatography
HSQC	Heteronuclear Single Quantum Correlation
HTS	High-Throughput Screening
Hz	Hertz
IC_{90}	Concentration of a drug that is required for 90% inhibition *in vitro*
IC_{50}	Half-maximal inhibitory concentration
IDM	Institute of Infectious Diseases and Molecular Medicine
IDV	Indinavir
INH	Isoniazid
J	Coupling constant
LC-MS	Liquid Chromatography–Mass Spectrometry
m	Multiplet
MeOH	Methanol
μM	Micro molar
MDR-TB	Multidrug-Resistant Tuberculosis
MHz	Megahertz
MIC	Minimum Inhibitory Concentration
MoA	Mechanism of Action
m.p	Melting point

MS	Mass Spectroscopy
MsCl	Methanesulfonyl chloride
Mtb	Mycobacterium tuberculosis
m/z	Mass over charge ratio
$Na(OAc)_3BH$	Sodium triacetoxyhydroborate
$NaHCO_3$	Sodium hydrogen carbonate
NVP	Nevirapine
NFV	Nelfinavir
OAc	Acetate
ppm	Parts per million
PZA	Pyrazinamide
q	Quartet
R_f	Retardation Factor
s	Singlet
RIF	Rifampicin
RLM	Rat Liver Microsome
SAR	Structure Activity Relationship
SM	Streptomycin
t	Triplet
T3P	n-Propanephosphonic acid anhydride
TAACF	Tuberculosis Antimicrobial Acquisition Coordinating Facility
TB	Tuberculosis
TDR-TB	Totally Drug Resistant Tuberculosis
TLC	Thin Layer Chromatography
TMS	Tetramethyl silane
t_R	Retention Time
UV	Ultra violet
WHO	World Health Organization
w/v	Weight over volume ratio
XDR-TB	Extremely Drug-Resistant Tuberculosis

List of Appendices

List of Figures

List of Tables

List of Schemes

CHAPTER 1

1. Tuberculosis

1.1 Disease and epidemiology

Tuberculosis (TB) is a prevalent and often fatal infectious disease that has existed for millennia.[1] The causative agent of TB in humans is the pathogenic bacteria *Mycobacterium tuberculosis (Mtb)*, which was originally identified by Robert Koch in 1882 as a slow growing, nonmotile, aerobic and rod-shaped bacterium.[2–4] The history of mycobacteria is believed to have come from soil-dwelling ancestors, which subsequently became pathogenic to humans after animal domestication about 70 000 years ago.[5] Other TB causing agents, which are closely related to *Mtb* includes *M. bovis, M. africanum, M. microti* and *M. canetti*, which are referred to as the mycobacterial complex.[6]

Tuberculosis was declared a public health emergency in 1993 by the World Health Organization (WHO) as it was reaching pandemic levels. According to the WHO, in 2015 it was reported that 10.4 million new cases of TB were recorded with 1.8 million TB-related deaths. In the same period, TB was the number one cause of death globally after the human immunodeficiency virus (HIV), with HIV/TB co-infections accounting for more than 0.4 million deaths worldwide.[1,7,8] Overall, 95% of TB related deaths occurred in developing countries, with countries in Asia (India, Indonesia, China and Pakistan) and Africa (Nigeria and South Africa) accounting for 60% of all TB cases. Although, there has been a decline in TB incidences since 2000, complete TB eradication by 2030 is the target for the WHO.[1] **Figure 2** shows the global TB incidence for 2014.

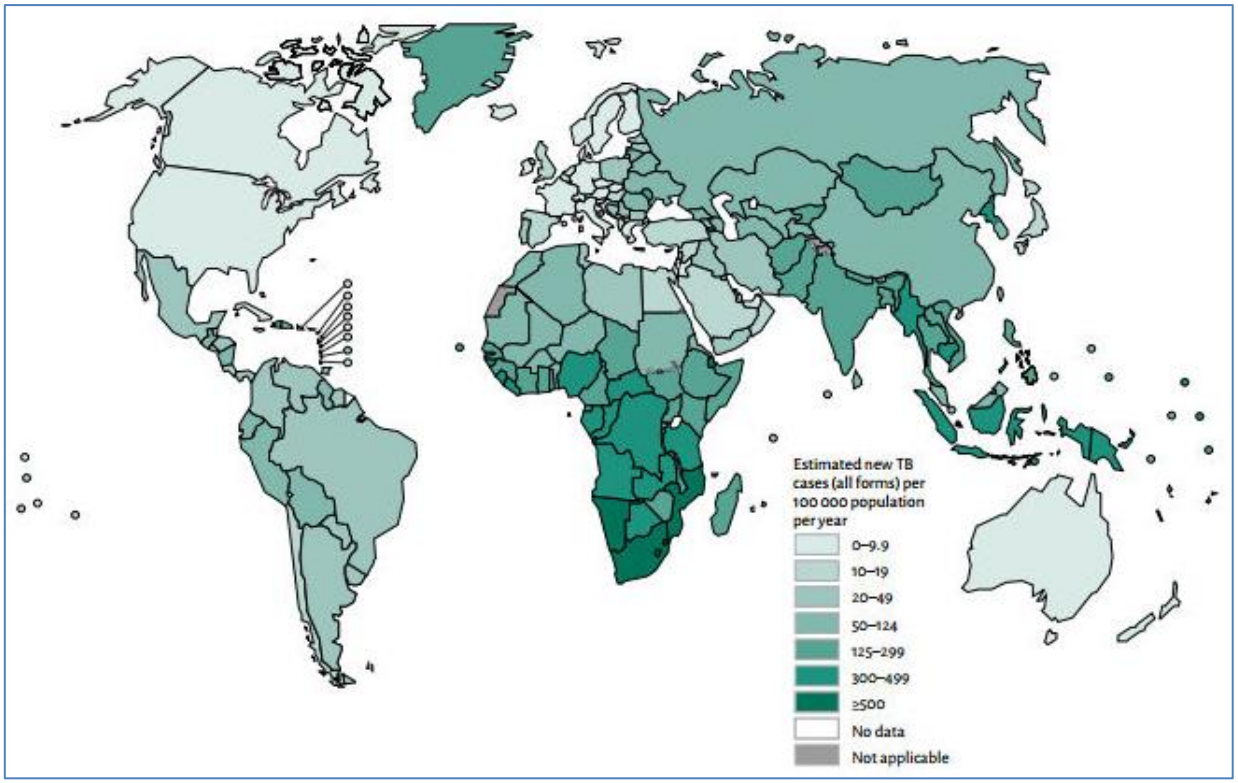

Figure 2: Global TB incidence for 2014.[1]

1.2 Transmission and pathogenesis

Mtb is an airborne pathogen transmitted through coughing and sneezing. The primary site of infection is the lungs (pulmonary TB), from which the bacterium can enter the blood stream and infect other sites such as the lymphatic and genitourinary systems as well as bones and joints as extrapulmonary TB.[2,7] Once in the lung, the *Mtb* bacilli are phagocytosed by alveolar macrophages, the first line of defense against infections (Figure 3).[5]

In the macrophages, phagosome maturation takes place to eradicate the bacterial infection, but *Mtb* has developed mechanisms to escape and survive within these macrophages as compared to other mycobacterial infections. For example, due to the low oxygen tension and limited nutrients in the macrophages, *Mtb* can shut down its own metabolism thus terminating replication and transiting into dormancy, a state known as latent TB.[5,9]

As the macrophages migrate, *Mtb* is transported from the alveolus to pulmonary tissue sites. To prevent further infection and spread of *Mtb*, the infected macrophages forms a granuloma. The cellular composition of granuloma lesions include infected or uninfected macrophages, B and T lymphocytes and fibroblasts (Figure 3).[9,10] The survival of *Mtb* within the granuloma can be attributed to its impermeable thick cell wall that is made up of peptidoglycans, polysaccharides, glycolipids and lipids such as mycolic acid.[5]

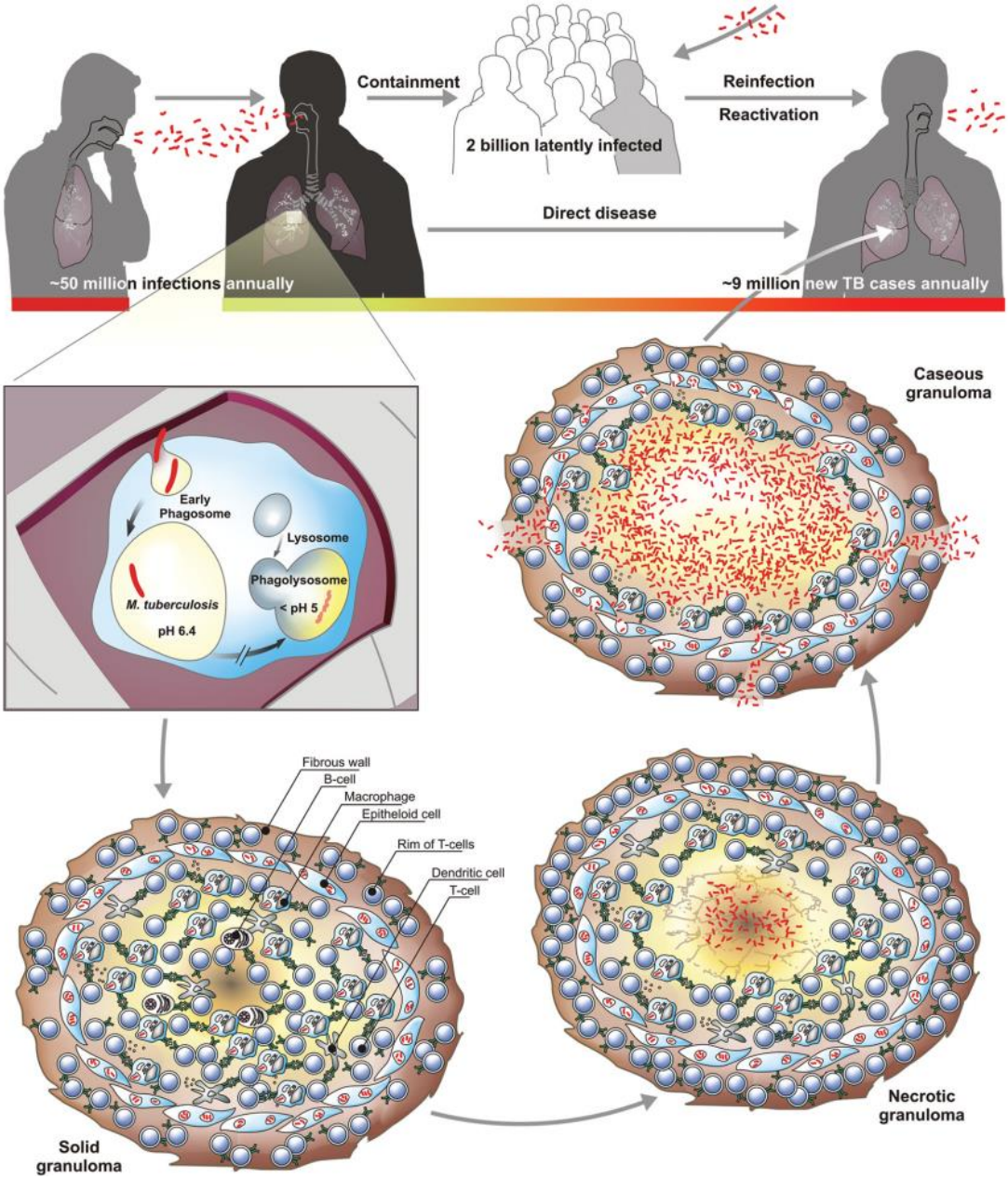

Figure 3: Transmission and pathology of tuberculosis. Transmission of TB between individuals occurs via aerosols of infected bacilli. Upon inhalation of infected bacilli, the pathogen reached the lungs where it is phagocytosed by alveolar macrophages. Healthy

individuals can control the pathogen, but the *Mtb* can grow to a high numbers, realizing the infected bacilli in the airways and coughing them out as aerosol.[5]

In an immunocompetent individual, *Mtb* can persist within the granuloma for decades without symptoms of infection.[5] Once the immune system is compromised, *Mtb* becomes metabolically active and starts to replicate, resulting in the collapse of the granuloma and release of the virulent bacilli to other tissues or transmission to other individuals (Figure 3).[5,6,9–11] Immune compromisation can occur in children or old age populations, individuals on immunosuppressants and people who are HIV positive or malnourished.[12] The symptoms of active TB include weight loss, poor appetite, night sweats, fever, productive or dry cough and chest pains.[12,13]

1.3 Anti-TB drugs

Tuberculosis chemotherapy is based on antibiotic drugs, which were discovered in the 20th century and, since the 1960's, the rate of antibiotic drug discovery has been on the decline.[14] Shortly after the introduction of streptomycin in 1946 as an effective monotherapy treatment for *Mtb,* streptomycin-drug resistance was observed, which led to the adoption of combination therapy.[15] Currently, TB therapy consists of drugs that can be classified based on their efficacy, potency, drug class and experience of use (Table 1). The first-line drugs (Group 1) are used to treat drug-susceptible TB (DS-TB), except streptomycin (SM), which is classified as an injectable drug (Group 2). Drugs in Groups 2-5 (except streptomycin) are all second-line drugs used for resistant TB treatment. These second line drugs are further divided into their respective groups based on features such as cross-resistance.[16]

Table 1: Drugs for TB treatment.[16–20]

Groups	Drugs
Group 1: First-line oral agents	Isoniazid (INH), Rifampicin (RIF), Rifapentine, Pyrazinamide (PZA), Ethambutol (EMB), Rifabutin
Group 2: Injectable agents	Aminoglycosides: Kanamycin, Amikacin, Streptomycin (SM), Polypetide: Capreomycin
Group 3: Fluoroquinolones	Levofloxacin, Moxifloxacin, Ofloxacin, Gatifloxacin
Group 4: Oral bacteriostatic second-line agents	*p*-Aminosalicylic acid, Cycloserine, Terizidone, Ethionamide, Protionamide
Group 5: Drugs with limited efficacy or safety data	Bedaquiline, Delamaid, Clofazimine, Linezolid, Amoxicillin/Clavulanate Thioacetazone, Meropenem, Imipenem/Cilastatin, Clarithromycin

1.4 Treatment

The primary object of TB therapy is to (i) cure the infection without subsequent relapse, (ii) improve efficacy, safety and duration of treatment, (iii) improve the safety of combination therapy for TB patients co-infected with other chronic diseases, and (iv) establish an effective therapy for latent TB.[2,17,21] The WHO therefore recommends a standard chemotherapeutic treatment regime under the "directly observed treatment, short course" (DOTS) and DOTS-Plus strategies. The DOTS strategies are designed to ensure completion of treatment and cure, with the success of these strategies largely dependent on commitment by various government agencies implementing the guidelines.[22]

The regime for new non-multidrug resistant TB cases under DOTS comprises of the intensive and continuation phases. The intensive phase involves the administration of isoniazid (INH), rifampicin (RIF), pyrazinamide (PZA) and ethambutol (ETB) or streptomycin (SM, Figure 4) daily for two months. The tubercle bacilli are killed rapidly during this phase but, to avoid

relapse, the continuation phase is initiated. The continuation phase consists of INH and RIF for an additional four months.[13,17,22]

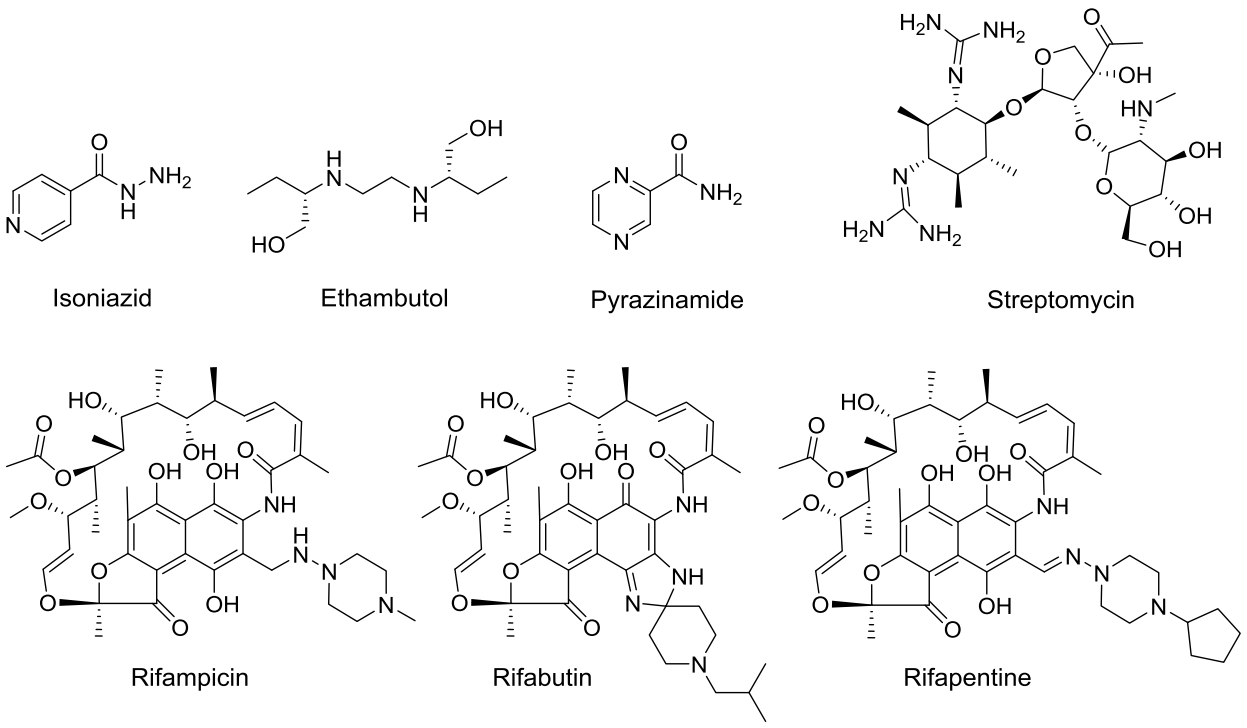

Figure 4: First-line anti-TB drugs.

HIV/TB co-infected patients can be treated using one of the following three regimes; (i) daily INH for six to nine months, (ii) daily INH and RIF for 3 months or (iii) INH and RIF twice weekly for 3 months.[13]

The DOTS-Plus recommends the use of five second-line drugs for multidrug resistant TB (MDR-TB). The choice of drugs is based on susceptibility testing of *Mtb* against available drugs. In the absence of susceptibility test results, the regime is based on factors such as drug resistance patterns in the geographic area, previous drug exposure, other underlying medical conditions or adverse effects of the drugs of choice.[16] The commonly used regime consists of pyrazinamide (PZA), a fluoroquinolone, amikacin or kanamycin, ethionamide or prothionamide and cycloserine (recommended) or *p*-aminosalicylic acid (Figure 5). The regime for extremely drug resistant TB (XDR-TB) is non-existing, therefore, the same procedure as for MDR-TB is

recommended. Drug resistant TB (DR-TB) therapy is recommended for eighteen to twenty months.[13,16] The current vaccine, M. bovis Bacillus Calmette-Guérin (BCG), is used as a protective measure for pediatric TB, but fails for pulmonary TB in adults.[5]

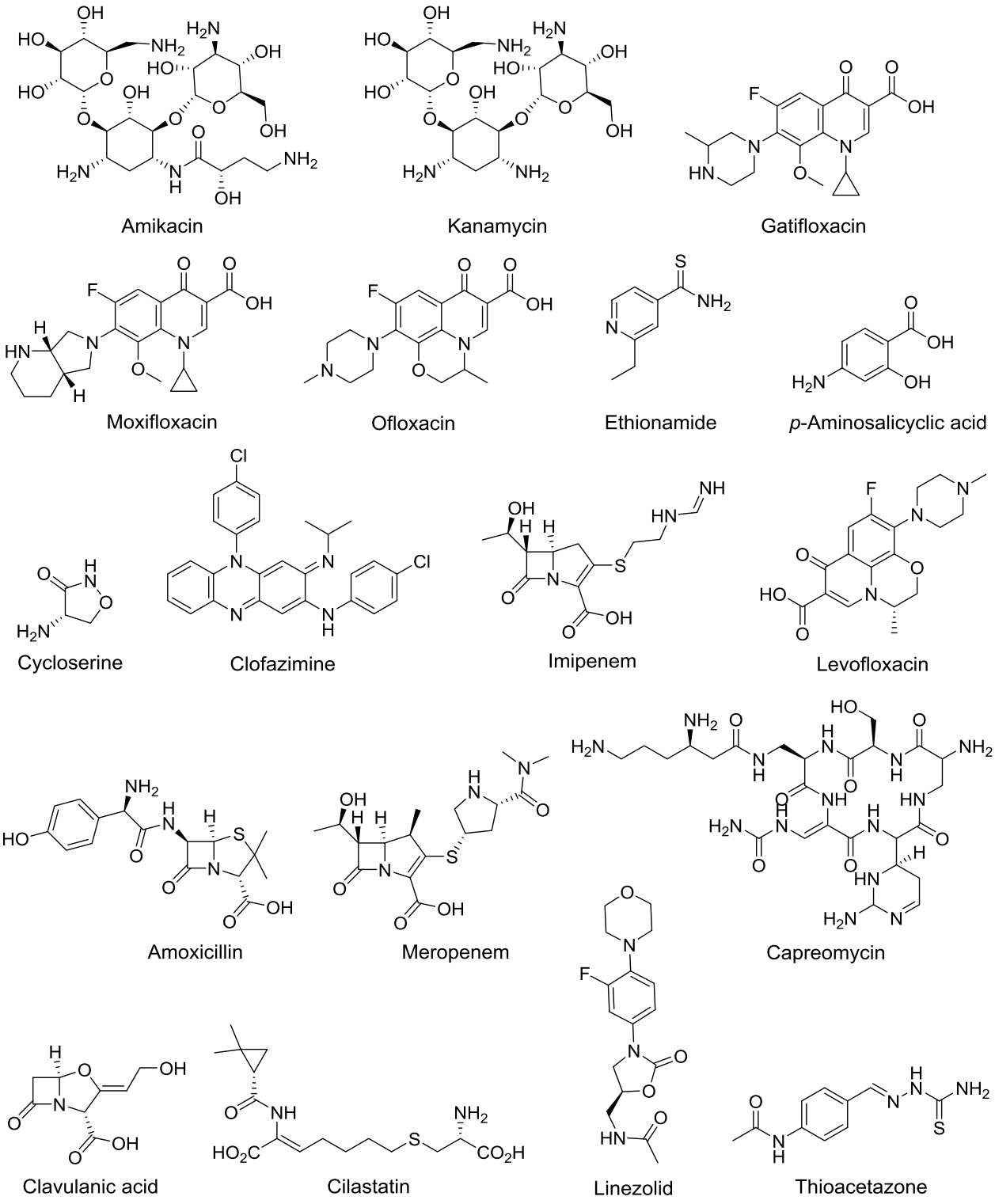

Figure 5: Second-line anti-TB drugs.

1.5 Challenges

Despite the valuable information amassed on the biology of mycobacteria, there are notable discrepancies and challenges that have prevented the complete eradication of TB worldwide. Such challenges include drug resistance, HIV/TB co-infections, drug-drug interactions, long treatment duration and a high pill burden.

The long treatment period of six months to two years for DS-TB and DR-TB respectively, not only burdens the already compromised healthcare facilities found in most developing countries, but also contributes to the development of drug resistance.[1]

Drug resistance in *Mtb* can be traced back to the late 1940s, after the introduction of the first antibiotics for tuberculosis treatment.[23] There are two types of drug resistance; primary resistance, which occur in persons who have been infected with the resistant mycobacterium strain and secondary resistance, which develops during therapy, either by an inadequate regime or noncompliance of patients.[24]

The two types of TB resistant strains that have been recognized by the WHO are MDR- and XDR-TB. MDR-TB is resistant to INH and RIF, the two most effective first-line anti-TB drugs. On the other hand, XRD-TB is characterized by resistance to INH, RIF, any fluoroquinolone and any second line injectable aminoglycoside.[25–27] Some of the reasons for the development of drug resistance include:[28]

- Deficient or deteriorating TB control programs
- Improper prescription of regimens
- Interruption of chemotherapy due to side effects
- Non-adherence of patient to the prescribed drug therapy
- The epidemic of HIV co-infection
- Use of anti-TB drugs for indications other than tuberculosis.

A more concerning issue is the emergence of the more severe drug–resistant forms of TB, which is totally drug resistant (TDR-TB), and is defined as resistance to all first and second-line anti-TB drugs.[3] Although the diagnostic definition of TDR-TB is still pending, it is conceivable that treatment options for TDR-TB will be severely limited or non-existing.[29] In addition, the drugs used for the treatment of drug resistant TB are associated with high toxicity and are expensive as compared to first-line drugs.[30,31]

TB chemotherapy is further impeded by the existence of non-replicating forms of *Mtb*. These latent infections serve as a reservoir for future transmissions and contribute to the severity of the disease through the risk of reactivation as reported for immune-compromised individuals.[32]

Some of the most crucial issues in the treatment of HIV-associated TB include unfavorable drug-drug interactions and the additive toxicities associated with combined antiretroviral (ARV) drugs with TB drugs. For example, RIF cannot be co-administered with ARVs such as nevirapine (NVP), indinavir (IDV) and nelfinavir (NFV, Figure 6), since RIF is a powerful inducer of cytochrome P450 (CYP) enzymes. These enzymes are responsible for metabolizing ARVs to their inactive metabolites, thus reducing the effective serum concentration and exposure. Hence, patients are forced to complete TB treatment before beginning HIV treatment.[2,33] The HIV/TB co-infection causes a faster progression of each other.[7]

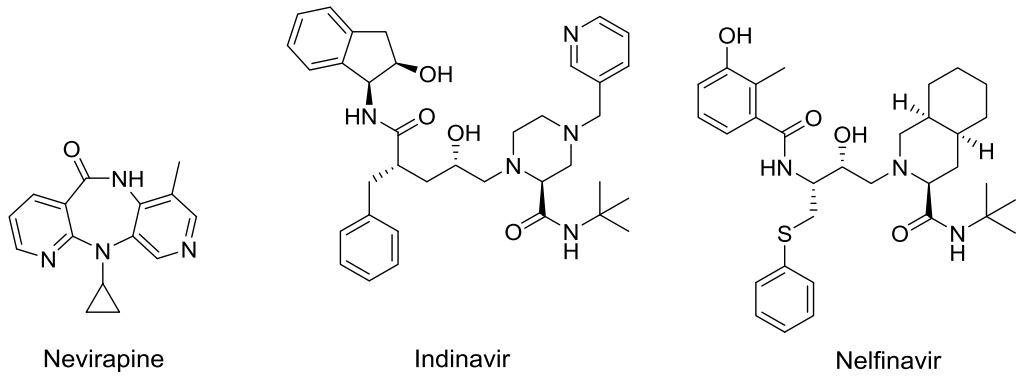

Figure 6: ARV drugs with drug-drug interactions with RIF.

Therefore, the next generation of anti-TB drugs should preferably be fast acting, potent with novel modes of action, be able to shorten the treatment duration, effective against all drug-resistant strains of TB, less toxic and safe to be co-administered with other chronic medications.[34,35]

1.6 Current anti-TB drugs in the drug development pipeline

There are several compounds currently in preclinical and clinical development as potential anti-TB agents. **Figure 7** shows the current anti-TB agents at different stages in the drug discovery and development value chain. These compounds are either new chemical entities or known compounds that have been repurposed for TB.

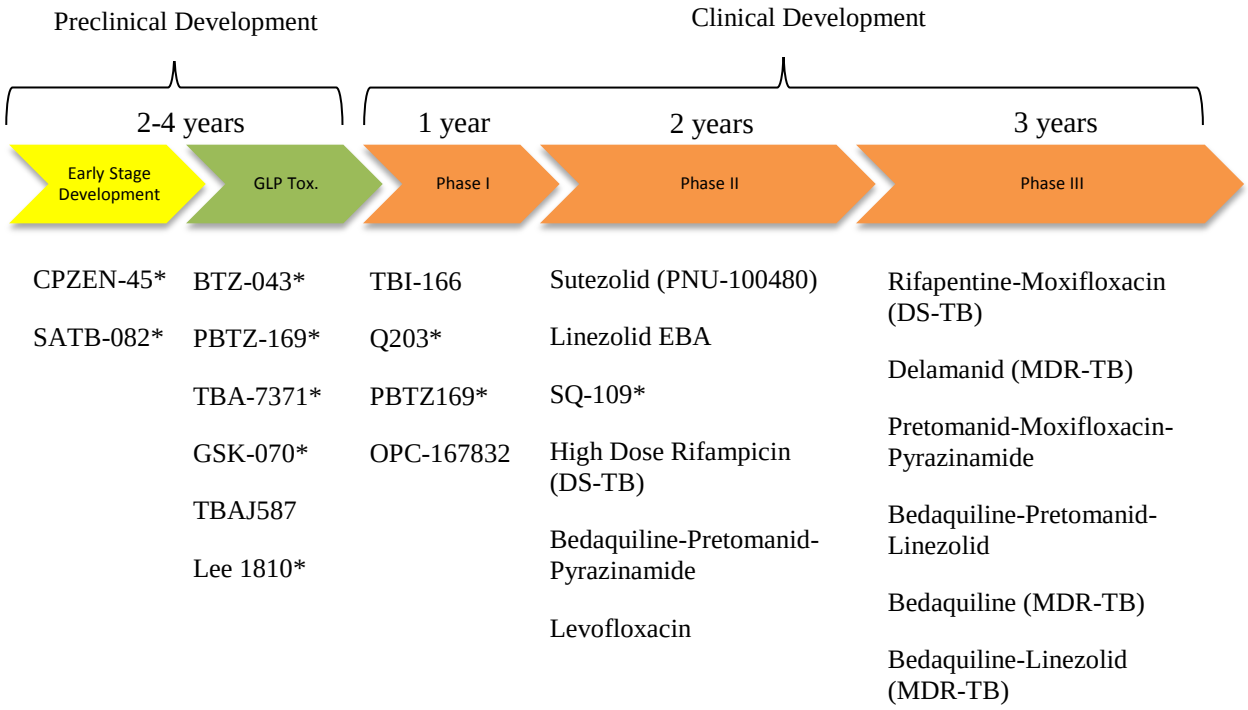

Good Laboratory Practices Toxicity (GLP Tox.); New chemical class*

Figure 7: Global TB drug development pipeline.[20,36,37]

One of the many products in clinical development is Bedaquiline, which is the first compound to be approved by the United States Food and Drug Administration (FDA) in over 40 years as an anti-TB drug. Bedaquiline (Figure 8) was approved to be used in combination with at least 3 or 4

other drugs based on a susceptible *in vitro* test for the treatment of extrapulmonary TB, pediatric TB, TB in pregnant women, HIV/TB patients and MDR-TB in adults. The mechanism of action (MoA) involves inhibition of mycobacterial ATP synthase, an enzyme essential for energy generation (Figure 8).[38]

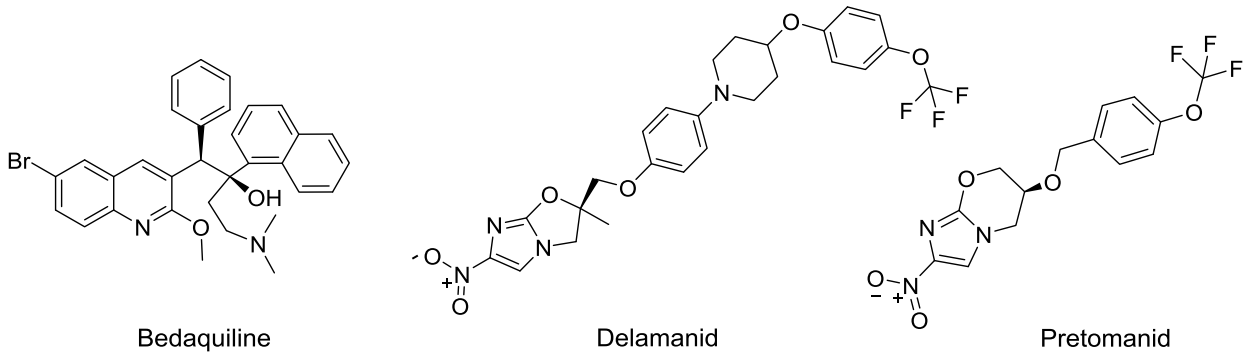

Figure 8: Structure of Bedaquiline, delamanid and pretomanid.

Two of the combination partners of Bedaquiline are nitroimidazoles delamanid and pretomanid (Figure 8). These compounds have inhibitory activity against both replicating and non-replicating *Mtb*. Both of these drugs are activated by the deazaflavin (cofactor F_{420})-dependent nitroreductase enzyme.[39] Pretomanid inhibits the formation of ketomycolate, a constituent of mycobacterial cell wall and by poisoning the bacterium with nitric oxide, a byproduct of nitroimidazole metabolism. Delamanid inhibits mycolic acid biosynthesis, a mycobacterial cell wall component (Figure 9) and was approved in 2014 by the FDA to treat MDR-TB in people who lack effective and tolerable treatments.[39,40] **Figure 9** indicates the MoA of anti-TB drugs in use or in preclinical and clinical stages of drug development.[35]

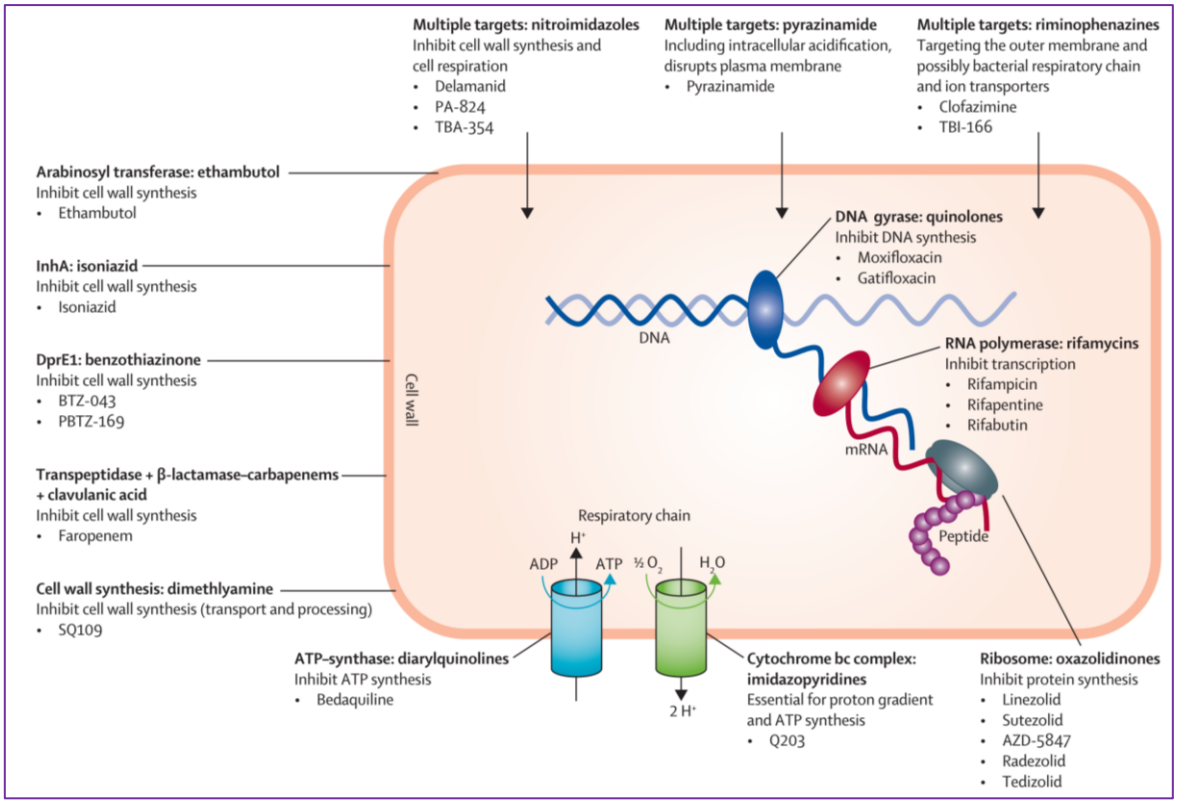

Figure 9: MoA of anti-TB drugs in use or in preclinical and clinical stages of drug development.[35]

In summary, since the high-TB burdened countries are mainly those in developing countries, the availability of inexpensive and easily accessible drugs will always be in demand. In addition, the next generation of anti-TB drugs have to be safe, tolerable and have both bactericidal and sterilizing activity.[41] Most importantly, they should be short acting, to improve patient compliance and active against *Mtb* throughout its different states.[7,42]

CHAPTER 2

2. Natural products

For centuries, mankind has relied on natural products and their Semi-Synthetic derivative for their use in various industries such as in dyes, polymers, fibers, glues, oils, waxes, flavoring agents, perfumes and drugs.[43] Of interest to this study are the medicinal properties of bioactive ingredients in natural products. The term natural product in this context refers to secondary metabolites produced by terrestrial and marine organisms such as plants, bacteria, fungi and algae.[44,45] They are produced as an adaptive strategy to the environment or as a defensive mechanism against herbivores, pathogens, insects or competing plants. On the other hand, primary metabolites are used for cellular functions such as growth, development and reproduction.[44,46]

Secondary metabolites can be characterized based on their composition, synthetic pathway and chemical structures as either (i) phenolic compounds containing benzene, hydrogen and oxygen; (ii) terpenes, which are hydrocarbons, or (iii) alkaloids, which contain nitrogen atoms.[45,46]

This study looks at the involvement of natural products and their synthetic derivatives in drug discovery, especially for *Mtb*.

2.1 Natural products in drug discovery

There are extensive reports on the contribution of natural products and their synthetic derivatives to the drug discovery process. Natural products and their synthetic derivatives have therapeutic uses as exemplified by antibacterial, anticancer, immunosuppressive, cholesterol lowering and antiparasitic agents.[47]

The discovery of penicillin in 1929 by Alexander Fleming from *Penicillium notatum*, brought about the "Golden Age of Antibiotics", the period when most commercially used antibiotics

where discovered.[46,48] Since then, natural products have continued to inspire drug discovery for both infectious and non-infectious diseases. As of 2014, 50% of all new approved drugs between 1981 and 2014 were either natural products, inspired by natural products or natural product derivatives.[46,48,49] Examples of drugs from natural products include, morphine, cocaine, codeine and quinine (Figure 10).[43]

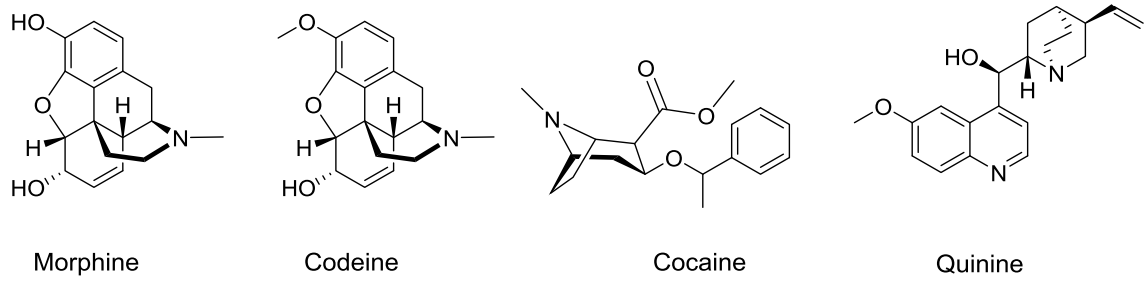

Figure 10: Structures of ancient natural products for medicinal use.

In recent times, synthetic small molecules have taken precedence in drug discovery over natural products, even though nature holds limitless unexplored potential. Some of the reasons that contributed to the decline in natural products-driven drug discovery include; (i) limited natural product material, leading to low isolation yields; (ii) time constraints associated with isolation and structural characterization; (iii) synthetic difficulties during lead optimization or total synthesis due to structural complexity; or (iv) metabolic bioactivation of natural products to their toxic metabolites.[48,50–53] Moreover, the introduction of combinatory chemistry and high throughput screening (HTS) to generate chemical diversity became an inexpensive and favorable route.[50,53]

Although natural products have their limitations, they are still favorable in complementing drug discovery efforts due to, in some cases, their desirable physico-chemical and pharmacokinetic profiles, such as high solubility, appropriate lipophilicity, good oral absorption and low toxicity profile.[25,51] In addition, natural products occupy various chemical spaces with structural features which, for many, are unconceivable to humans and highly desirable in drug discovery as

compared to synthetic compounds. These structural features include chiral centers, aromatic rings, complex ring systems, degree of saturation and heteroatoms.[43,52,54]

2.2 Antimycobacterial natural products

Natural products and their synthetic derivatives have shown to be a reliable source of innovative and effective therapeutic agents, especially between 1940 and 1970 when most anti-TB drugs where discovered. The discovery of the first anti-TB drug, streptomycin (Figure 11), isolated from *Streptomyces griseus* by Selma Abraham and co-workers in 1943, began an era where several natural products were discovered for antitubercular use.[25,46] Other natural product inspired anti-TB agents are shown in **Figure 11**, with the year they were introduced to the market.[2,31,32,42,48]

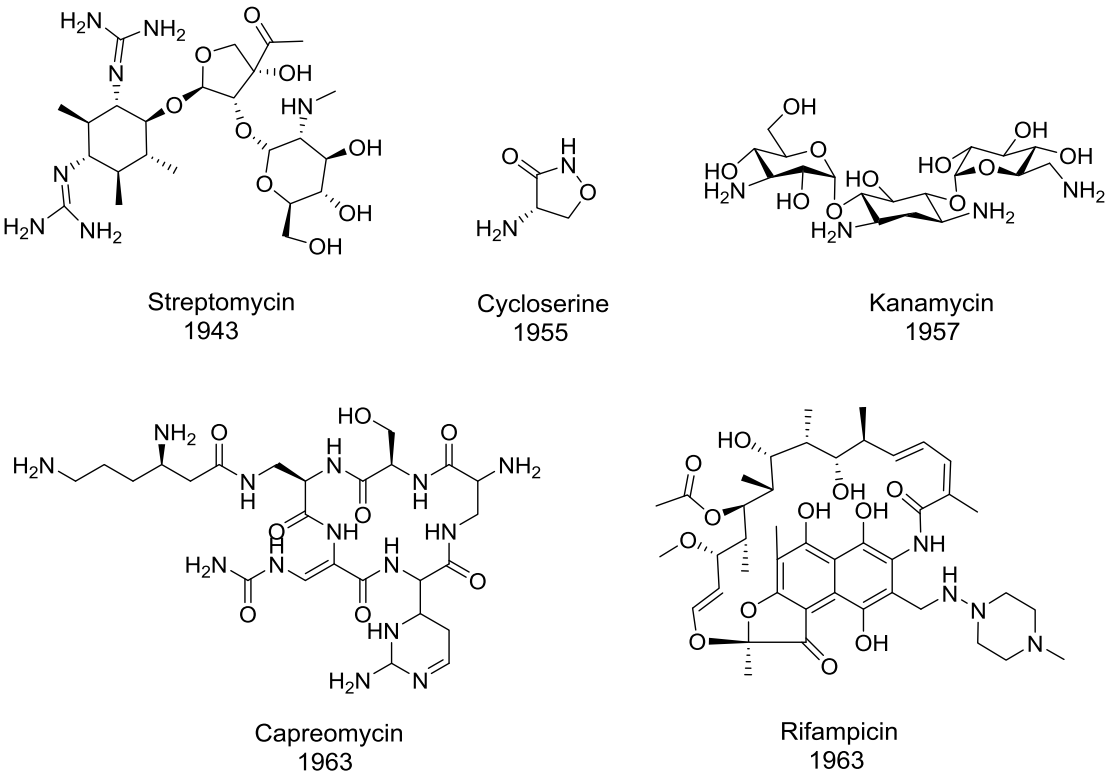

Figure 11: Natural product-inspired TB drugs.

There are various natural products and natural product derivatives that have displayed potent *in vitro* inhibitory activities against susceptible and drug resistant *Mtb*.[48] Of interest to this study are reports on the promising antibacterial activity displayed by the natural product fusidic acid.

2.3 Fusidic acid

2.3.1 Chemistry of Fusidic acid

Fusidic acid (Figure 12) belongs to the fusidane family of compounds and was first isolated from *Fusidium coccineum* fungus in 1960. The structural features of fusidic acid are; a tetracyclic ring system with a chair-boat-chair (*trans-syn-trans*) conformation, a carboxylic acid bearing side chain linked to the ring system at C-17 and an acetate group at C-16 (Figure 12).[55]

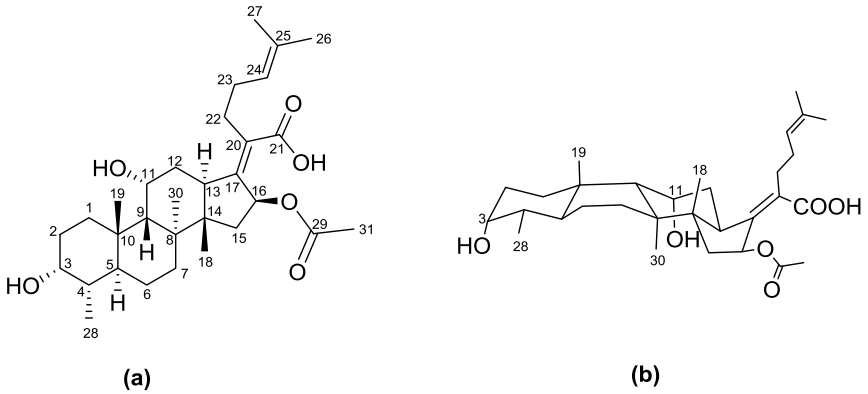

Figure 12: Structures of fusidic acid; (a) numerical numbering of fusidic acid, (b) chair-boat-chair conformation.

2.3.2 Biology of Fusidic acid

Fusidic acid is a narrow-spectrum antibiotic. Since 1962 it has been used to treat infections caused by both Gram-positive and Gram–negative bacteria.[56,57] The various infections that fusidic acid is used against a range from boils, anthrax or carbuncle, erythema, cellulitis, folliculitis, acne, paronychia, hidradenitis, bone and joint infections to soft-tissue infections.[57–59]

Amongst the fusidane family, fusidic acid is the only clinically used antibiotic, as other fusidanes are less active. Other naturally occurring fusidanes with antibiotic activity are shown in **Figure 13**.[60–64]

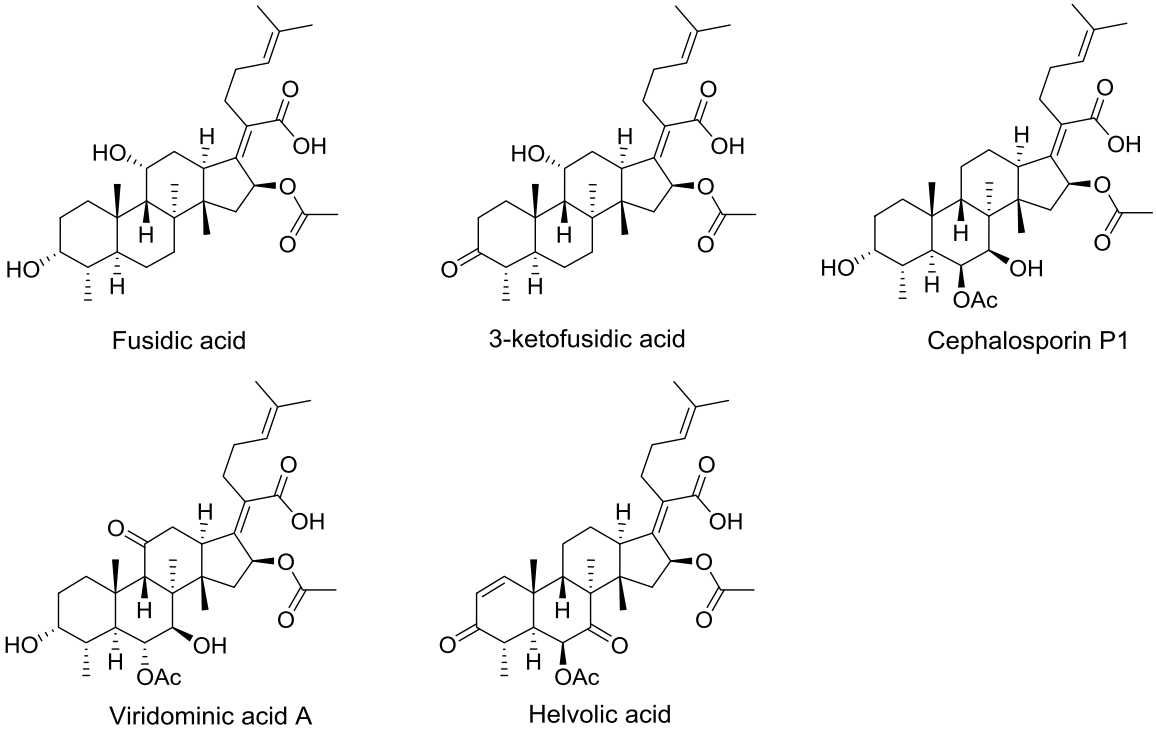

Figure 13: Natural occurring antibiotic fusidanes.

The therapeutic usefulness of fusidic acid is based on its high tissue distribution, good penetration, low toxicity and bacterial resistance, low allergic reaction and no cross-resistance with other clinical antibiotics. The mode of administration of fusidic acid is either oral (tablet and suspension), intravenous or topical (cream and ointment).[57–59]

Although fusidic acid has the above mentioned advantages, there have been some reports of concern. For example, a clinical study of fusidic acid in combination with rifampin (RIF) for prosthetic joint infections was terminated due to drug-drug interactions between these two drugs.[65] This combination was used for the treatment of staphylococci resistant strains.[66] In addition, fusidic acid has been shown to have various side effects, which include gastrointestinal tract discomfort, diarrhea and headaches. A rarely reported side effect of fusidic acid is skin reactions (itching, rashes and dryness), but these adverse effects do not warrant a discontinuation of fusidic acid use.[57,67]

The activity of fusidic acid against various infectious is generally bacteriostatic but bactericidal at high dosage. A bacteriostatic drug effect is the ability of the drug to inhibit bacteria proliferation while a drug bactericidal effect is the ability of a drug to promote microorganism death.[57] The mode of action of fusidic acid is through inhibition of protein synthesis in prokaryotes and eukaryotes at the translocation step during elongation of the polypeptide. Fusidic acid binds to the elongation factor G (EF-G) and stabilizes the ternary complex EF-G-GDP-ribosome. EF-G is essential for bacterial protein elongation on the ribosome after peptide bond formation.[57,68]

Due to its mechanism of action, fusidic acid has been shown to have *in vitro* activity against various pathogens, as shown in **Table 2**. These antibacterial activities of fusidic acid have stimulated interest in the structural modification of this drug.

Table 2: *In vitro* activity of fusidic acid against various species.[69,70]

Species	MIC_{90} (µg/ml)
Staphylococcus aureus (methicillin susceptible)	0.03 – 0.3
Streptococcus pyogenes	4 – 16
Streptococcus pneumoniae	2 – 16
Streptococcus faecalis	1 – 8
Neisseria honorrhoeae	0.03 – 4
Neisseria meningitides	0.015 – 0.5
Clostridium spp	0.06 – 1.0
Peptostrep. spp	0.06 – 2
Bacteroides fragilis	0.25 – 16
Bacteroides spp	0.06 – 6
Corynebacterium spp	0.06 – 12.5

2.3.2.1 Structural Activity Relationship studies of fusidic acid (Antibacterial Study)

Intensive structural-activity relationship (SAR) studies of fusidic acid have revealed that the tetracyclic skeleton and the carboxylic acid functionalities are of importance in order to maintain activity, while the side chain, in addition to the sterol backbone, is responsible for lipophilicity.

The double bond between C-17 and C-20 plays no apparent role in activity compared to the orientation of the lipophilic side-chain and can therefore be reduced. However, only the 17*S*,20*S* isomer shows equipotent biological activity to fusidic acid. The two hydroxyl groups can be substituted with other functional groups such as keto, halogens, sulfoxides and azides, while maintaining antibacterial activity. The acetate group can be substituted with functionalities, such as, O-acyl, S-acyl and ethers and still maintain antibacterial activity (Figure 14).[55,59,71]

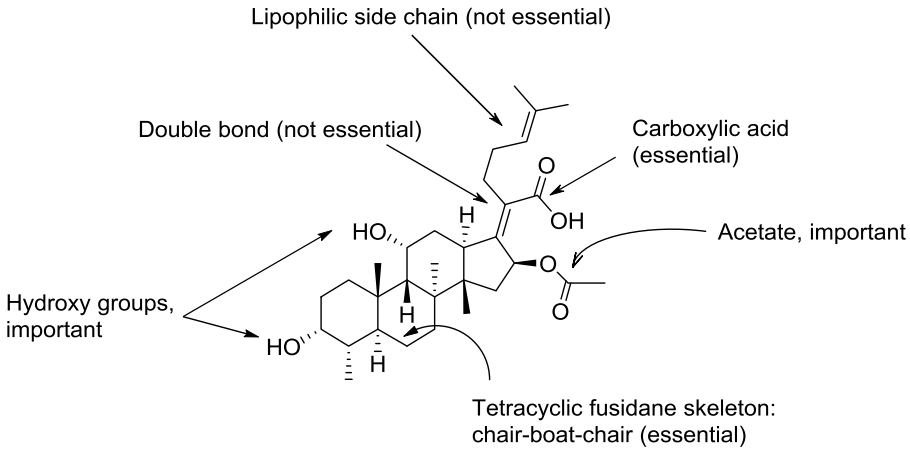

Figure 14: Antibacterial SAR of fusidic acid.

Within the context of TB, fusidic acid was found to have *in vitro* MIC_{90} (minimum concentration that will inhibit 90% of the bacterial population) of 1.2 µM against the H37Rv strain of *Mtb*, with no cross-resistance against first line anti-TB drugs.[72,73] Due to these properties of fusidic acid, this study focusses on utilization of the drug repositioning strategy based on fusidic acid as a template for the semi-synthesis of new derivatives as potential antimycobacterial agents .

2.4 Drug repositioning for TB

A literature review revealed various strategies that have been used in the design and synthesis of potential anti-TB agents. One of the rewarding strategies is drug repositioning, which refers to the use of an existing drug developed for a specific disease indication as a template for further synthetic derivatization to improve on its pharmacological profile in a different disease indication.[74,75] Examples of drugs that have been repositioned for TB are shown in **Figure 15**.

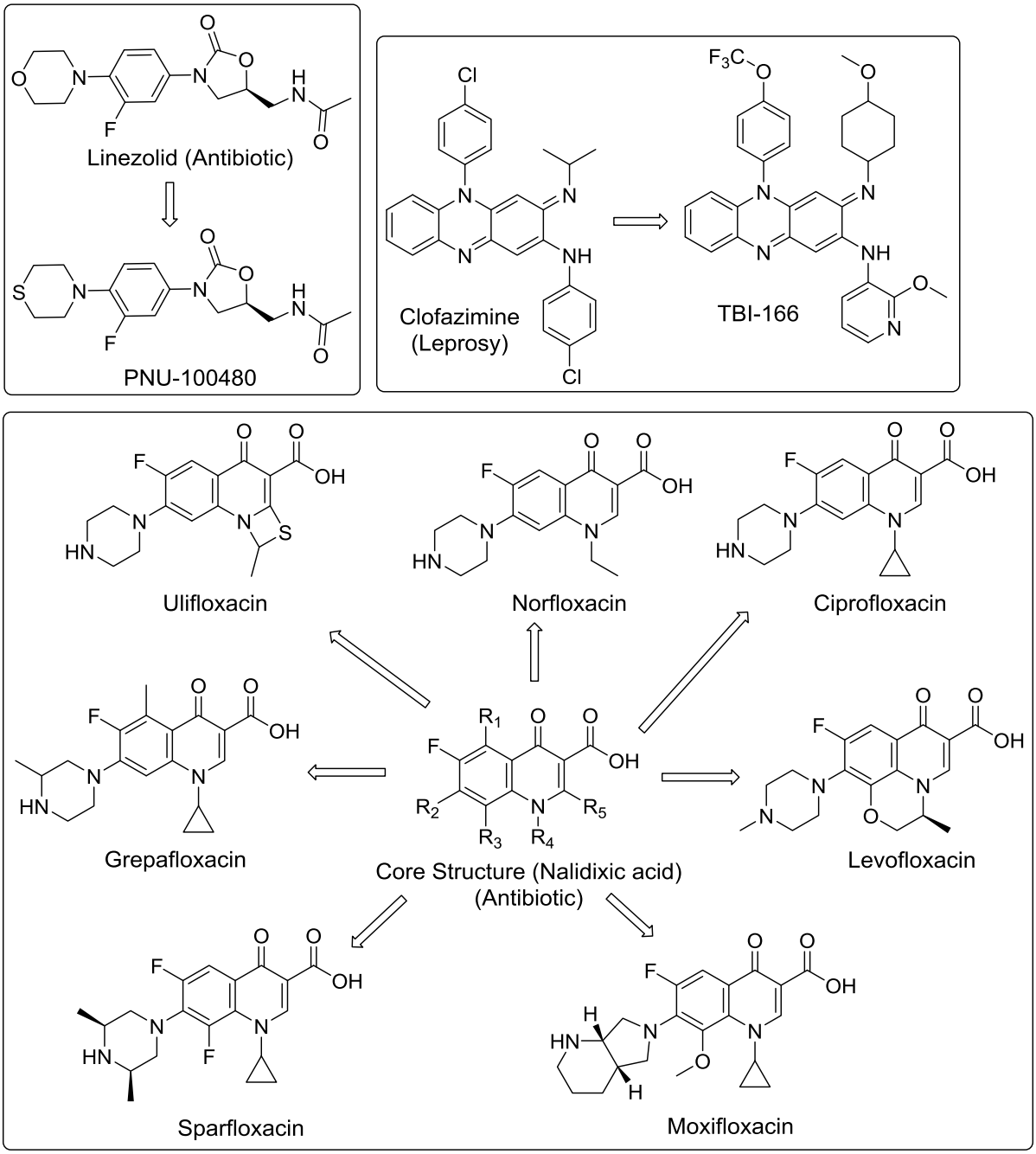

Figure 15: Repositioned drugs for TB.[76–79]

The drug repositioning approach is advantageous since it is less expensive, reduces risks associated with drug discovery and it provides a shorter time period for drug development.[74,80] On the other hand, drug repurposing, a closely related strategy, is the use of an existing drug in a different disease indication without any chemical modification.[74,75] Examples of drugs that have been repurposed for TB are shown in **Figure 16**.

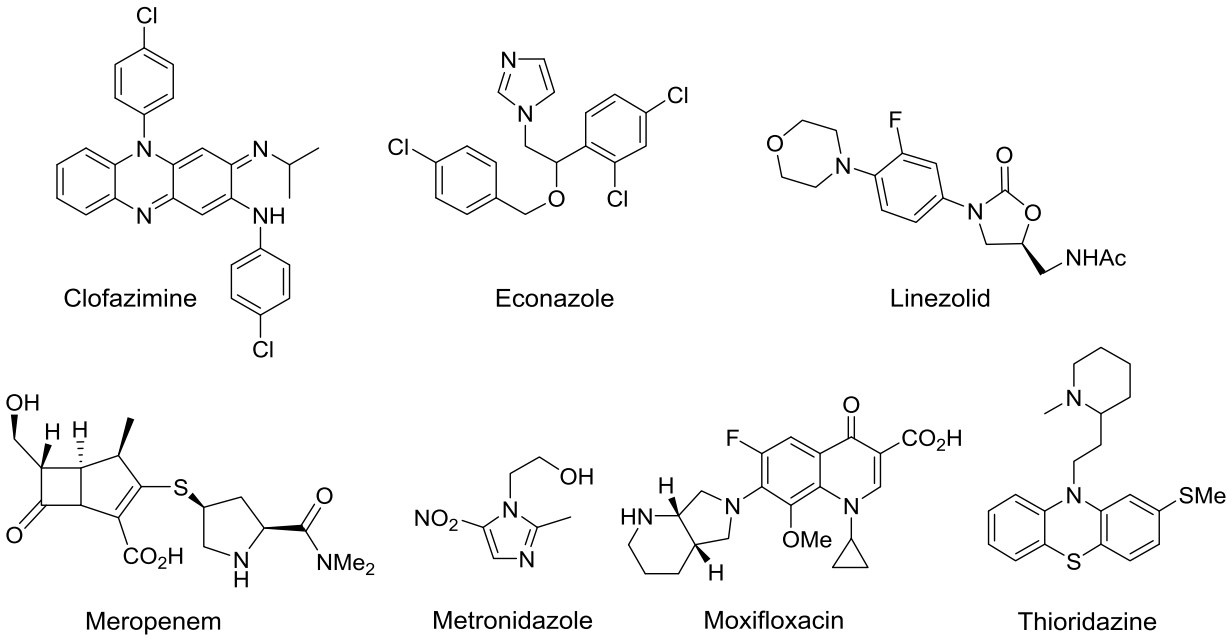

Figure 16: Repurposed drug for TB treatment.[81]

In view of the above mentioned advantages associated with drug repositioning, this project aims to reposition the natural product fusidic acid through the design and synthesis of potential novel antimycobacterial agents.

2.5 Aims and Objectives

2.5.1 Objective

The objective of this project is to investigate antimycobacterial SAR of the natural product fusidic acid through semi-synthesis.

2.5.2 Research question

Can fusidic acid be repositioned for TB through medicinal chemistry SAR exploration?

2.5.3 Specific aims

Synthesis, characterization, *in vitro* antimycobacterial evaluation and SAR studies of fusidic acid analogues.

CHAPTER 3

Design, synthesis and biological evaluation of fusidic acid derivatives

3.1 Introduction

This chapter describes the design, synthesis and characterization of fusidic acid derivatives. All the synthesized analogues were evaluated for their *in vitro* antimycobacterial activity against the virulent H37Rv strain of *Mtb*.

3.2 Rationale

An initial study conducted by Cicek-Saydam and co-workers on the *in vitro* susceptibility of 170 clinical isolates of *Mtb* to fusidic acid and other drugs revealed that 19 isolates were resistant to one or more first-line anti-TB drugs. Three of the isolates were resistant to fusidic acid and the remaining 151 isolates were susceptible to first-line anti-TB drugs. Fusidic acid was also found to have no cross-resistance with first line anti-TB drugs.[72] Furthermore, a High-Throughput Screen (HTS) conducted by the Tuberculosis Antimicrobial Acquisition Coordinating Facility (TAACF) revealed that fusidic acid has an IC_{90} of 1.20 µM against the H37Rv strain of *Mtb*.[73]

In another study that was conducted by the Global Alliance for TB Drug Development in collaboration with Prof. Anne Leanerts of Colorado State University, fusidic acid was found to lack *in vivo* efficacy in a tuberculosis mouse model up to a dosage of 200 mg/kg. This finding is in agreement with that of Payne *et al.*,[68] who found fusidic acid to have *in vitro* inhibitory activity against *Toxoplasma gondii* and *Listeria monocytogenes* but no *in vivo* efficacy in the corresponding mouse model.[68] This lack of *in vivo* efficacy has been attributed to fusidic acid's poor absorption in rodents, leading to a low serum concentration.[82]

Within this context, our research group has embarked on a multi-disciplinary approach to reposition fusidic acid for tuberculosis. This has involved medicinal chemistry, biology as well as drug metabolism and pharmacokinetic (DMPK) studies as follows;

An *in vitro* drug-drug interaction analysis of fusidic acid against various current anti-TB drugs exhibited synergistic interaction, resulting into a 4-16 fold reduction in MIC values against *M. smegmatis* as determined by the Fractional inhibitory concentration (FIC) index (FICI).[83]

The drugs used in this study included; rifampicin, streptomycin, spectinomycin, linezolid, roxithromycin, erythromycin, clarithromycin and tetracycline.[84] This synergistic interaction against various antibiotics makes fusidic acid a promising lead to be repositioned as a potential anti-TB drug.

Alongside this study, various fusidic acid analogues with different substituents at the C-3, C-16 and C-21 were designed and synthesized by Dr. Gurminder Kaur, Dr. Kawaljit Singh and Ms. Antonina Wasuna from the Department of Chemistry, University of Cape Town (South Africa, Figure 17). This set of compounds were then evaluated for their antimycobacterial activity against the H37Rv strain of *Mtb*.

An example of some of these compounds with promising *in vitro* antimycobacterial activity (MIC_{99} values 1.25-20 µM) is shown in **Figure 17**. These compounds were further tested for their *in vitro* antiplasmodial activity against the chloroquine (CQ)-sensitive NF54 strain of *P. falciparum* with IC_{50} values of 1.2-48.1 µM.[85,86]

The design of these various fusidic acid derivatives was based on the initial hypothesis that the lack of *in vivo* efficacy was a result of poor cell wall permeation due to the carboxylic acid moiety. To circumvent this problem and potentially increase penetration, various ester

and amide analogues were synthesized as hybrids and bioisosteres of the carboxylic acid group, and as prodrugs of the C-3 hydroxyl.[85,86]

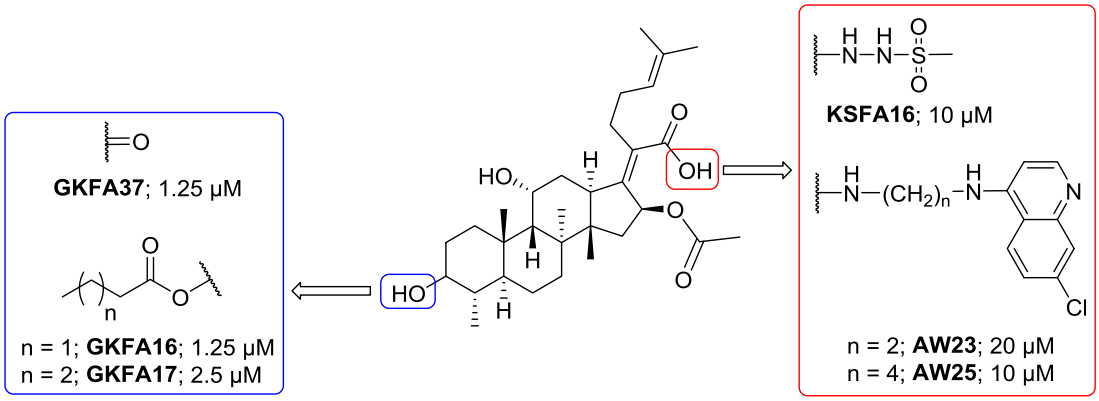

Figure 17: Examples of fusidic acid derivatives at the C-3 and C-21 position with their respective MIC_{99} values against H37Rv strain of *Mtb*.[85,86]

The *in vitro* assay results revealed that the amides and esters were found to be less potent than fusidic acid with MIC_{99} values ranging from 2-8 folds lower than that of fusidic acid. These hybrid analogues were also found to be cytotoxic against two mammalian cell lines [Chinese Hamster ovarian (CHO) and THP-1 cell].[85,86]

Compounds **GKFA16**, **GKFA17** and **GKFA37** (Figure 17), which displayed better extracellular antimycobacterial and toxicity profiles, were progressed to macrophage (intracellular) efficacy studies. These compounds were found to reduce the bacterial burden in infected human monocytic cells (THP-1) at concentrations two or five times higher than their inhibitory concentrations in broth cultures.[86] The intracellular efficacy observed for fusidic acid and the analogues point to their ability to accumulate within phagocytic cells. This is consistent with existing literature reports of the intracellular efficacy of fusidic acid against several strains of *S.aureus*.[86,87]

In an attempt to understand the disconnect between *in vitro* activity and *in vivo* efficacy of fusidic acid, the drug and its analogues (**GKFA16**, **GKFA17**, **KSFA16**, **AW23** and **AW25**)

were screened for their metabolic stability in rodent and human liver microsomes and their resulting metabolites identified. The metabolism of fusidic acid has been shown to be species specific between rodents and humans, with the acyl glucuronide, 3-keto-, 27-carboxy- and hydroxylate being the main metabolites in man (Figure 18). These metabolites were shown to be less active than fusidic acid.[88]

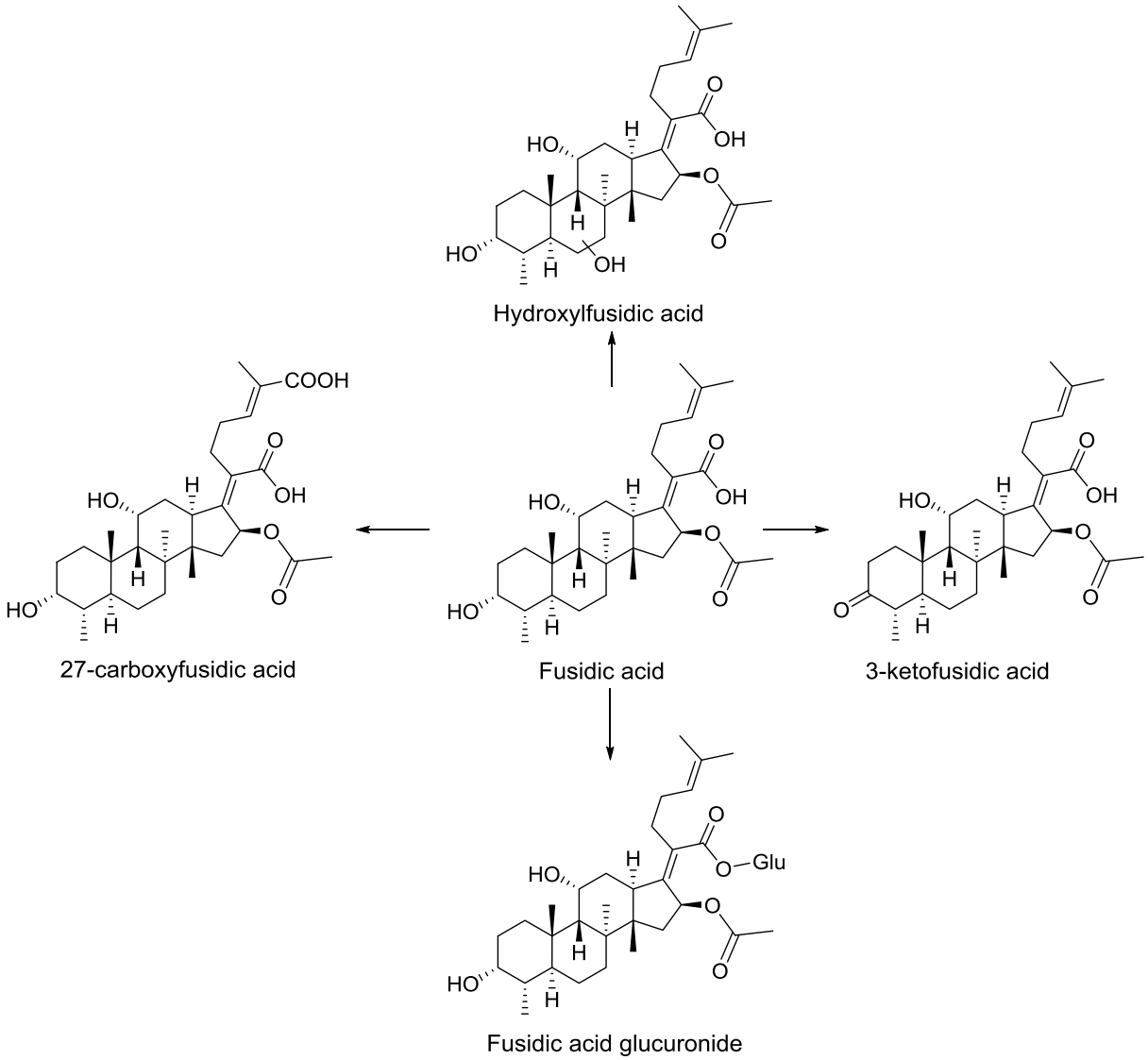

Figure 18: Fusidic acid metabolites in man.[88]

However, fusidic acid is metabolized to 3-ketofusidic acid and 3-epifusidic acid in mouse liver microsomes (MLM, Figure 19). The main metabolite in MLM being the inactive 3-

epifusidic acid, which is not observed in human liver microsomes (HLM).[89] These metabolites have been found to have lower antibacterial activity than fusidic acid.[55]

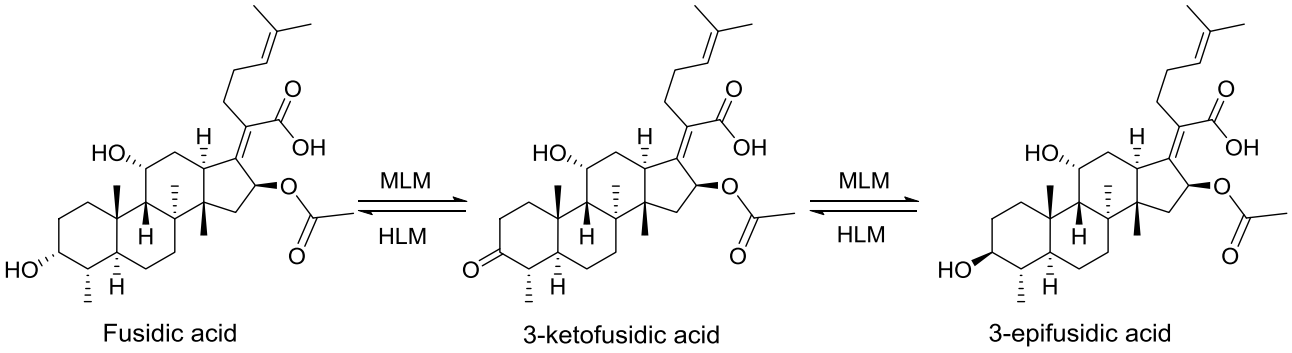

Figure 19: Fusidic acid metabolites in mouse liver microsomes (MLM) and human liver microsomes (HLM).[89]

In rodent plasma, the fusidic acid is slowly hydrolysed at C-16 to a free alcohol, followed by lactonization with the acid moiety at C-21, to form a metabolite that is not observed in human plasma (Figure 20).[90]

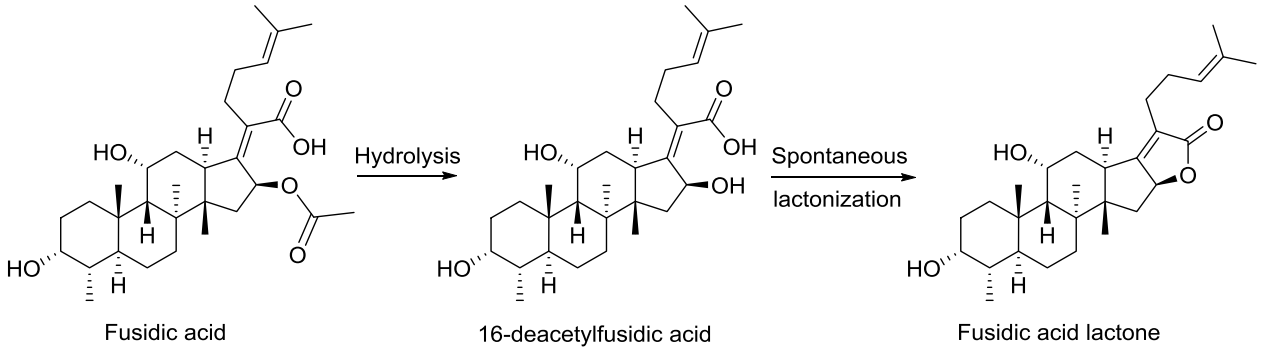

Figure 20: C-16 hydrolysis and lactonization of fusidic acid in rodent plasma.[90]

Overall, the microsomal stability of these compounds was comparable across the three species (65% ± 5% remaining).[89] It was observed that the C-3 esters, **GKFA16** and **GKFA17**, were metabolized to fusidic acid in rat liver microsomes (RLM), suggesting that they act as prodrugs. The stability in plasma varied in the order of mouse >> rat > man, which is in agreement with literature reports.[89,91] Moreover, both these C-3 esters were observed to be very stable in human plasma.[89]

As for the C-21 derivatives, only compound **KSFA16** was metabolized to fusidic acid.[89] The release of the sulfonyl hydrazide can be considered as a structural alert, since it is associated with organ toxicity.[92,93] The C-21 amides **AW23** and **AW25** were not metabolized to fusidic acid, which may have contributed to their low *in vitro* activity.[86]

The two prodrugs, **GKFA16** and **GKFA17**, were then considered for further pharmacokinetic studies in a mouse model with the hypothesis that the lack of fusidic acid efficacy in mouse could be due to poor exposure of fusidic acid at the site of infection.

Intravenous and oral administration of fusidic acid in mouse showed a higher level of the 3-epifusidic acid metabolite than fusidic acid, suggesting that the low bioavailability was due to the inactive 3-epifusidic acid as opposed to low absorption. The metabolism of fusidic acid to the 3-epifusidic acid was observed to be gender specific, with a higher rate of metabolism in females rats compared to males.[94]

Examination of the pharmacokinetic properties of selected compounds revealed that both **GKFA16** and **GKFA17** were metabolized to fusidic acid, with **GKFA17** having a higher rate of clearance than **GKFA16** and exposed the fusidic acid 3-hydroxy group to be further metabolized to 3-epifusidic acid (Table 3). Compound **GKFA16** therefore sustained the concentrations of fusidic acid longer and acted as a slow metabolic activation compound. However, the final concentrations of fusidic acid remained low and unlikely to have any impact in the tuberculosis mouse model at a 20 mg/kg dosage.[94]

Table 3: *In vivo* pharmacokinetic results of C-3 esters in mouse model at 20 mg/kg dose.[94]

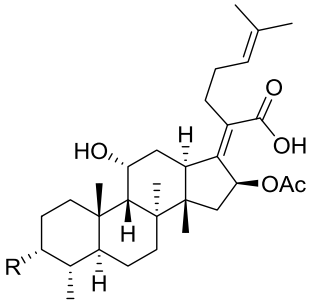

R	Fusidic acid 	**GKFA16** 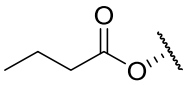	**GKFA17** 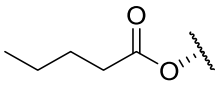
Cl (*ml/min/kg*)	58.0	40.3	134
$t_{1/2}$ (*hr*)	1.80	1.19	1.63
F (%)	12.4	43.5	44.5
Fusidic acid AUC (*min.uM/L*)	116	134	165
Increase in fusidic acid *AUC*	-	15.5 %	42.2 %

Cl, clearance; $t_{1/2}$, half-life; F, bioavailability; AUC, area-under-the curve

In addition, it was observed that the 3-ketofusidic acid (**GKFA37**) had a higher rate of metabolism to 3-epifusidic acid when administered intravenously compared to oral administration. The metabolism from 3-ketofusidic acid to fusidic acid, on the other hand, was negligible.[94]

Furthermore, compounds **GKFA16** and **GKFA17** were evaluated for their organ distribution as follows (i) in the lungs and spleen due to the high bacterial burden at these sites, (ii) liver and kidneys due to their role as elimination sites, and (iii) the heart and brain due to pericarditis and meningitis tuberculosis complications as well as the fact that fusidic acid is known to cross the blood brain barrier.[94,95]

Generally, the prodrug analogues showed improved organ distribution when compared to fusidic acid administration, resulting in a higher ratio of fusidic acid being observed in tissues than in blood.

It is important to note that the presence of 3-epifusidic acid metabolite highlights the inappropriateness of the rodent models for fusidic acid *in vivo* evaluation.

Further examples of fusidic acid derivatives that were synthesized in our research group include; C-21 bioisosteres which led to loss of antimycobacterial activity compared to fusidic acid, with most of the derivatives displaying MIC_{99} values $\geq$ 20 μM. However, a fusidic acid-isoniazid conjugate showed respectable activity with MIC_{99} value of 10 μM. The decrease in antimycobacterial activity of C-21 derivatives suggests that the free carboxyl group is essential for activity (Figure 21).[85]

The introduction of 3-epifusidic acid, carboxylic and silicate esters as well as oxime and keto functionalities at the C-3 position decreased the antimycobacterial activity (Figure 21). The *in vitro* antimycobacterial activity of 3-epifusidic acid suggests that the inversion of configuration at the C-3 position significantly reduces the antimycobacterial activity of fusidic acid derivatives.[85]

Furthermore, C-16 derivatives were obtained by replacing the C-16 acetoxy group with methoxy and ethoxy groups, respectively, with the ethoxy derivative showing antimycobacterial activity comparable to fusidic acid.[85] A summary of the results obtained by the SAR performed in our laboratory is shown in **Figure 21**.

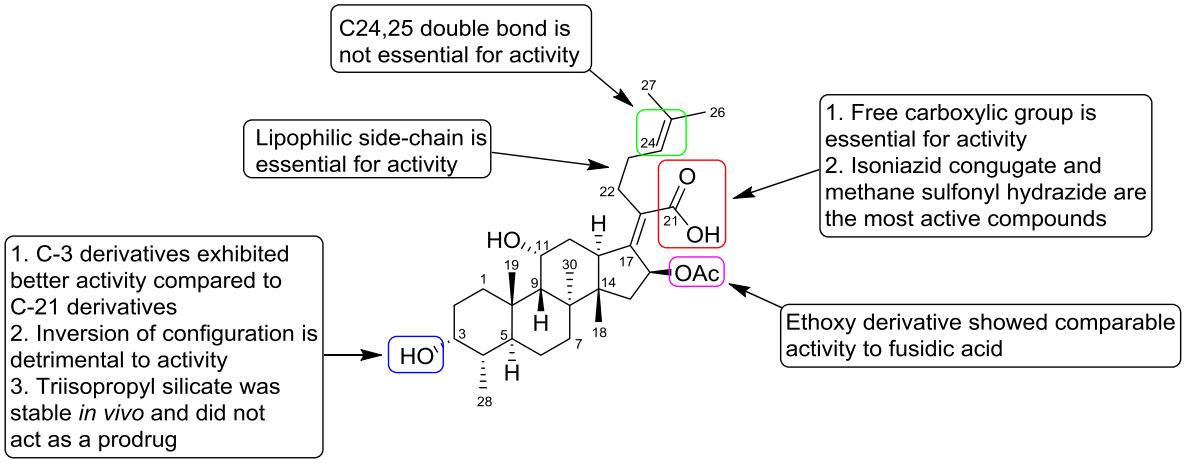

Figure 21: SAR summary of fusidic acid derivatives from our laboratory.[85]

Inspired by the above information; this project has therefore focused on expanding the SAR studies previously explored, using bioisosterism and prodrug approaches.

3.3 Design of fusidic acid derivatives

3.3.1 Bioisosterism approach

Bioisosteres are defined as atoms or group of atoms or molecules which may or may not have similar chemical and physical properties but their replacement produce broadly similar biological activity.[96] Carboxylic acid groups are known to be responsible for a significant number of pharmacological drawbacks such as metabolic instability, toxicity and limited passive diffusion across biological membranes.[97] Therefore, bioisosterism is used as an approach to optimize the biological activity of carboxylic acid containing drugs. Examples of carboxylic acid bioisosteres includes acyclic bioisosteres such as hydroxamic acid, acylsulfonamides, sulfonylureas, sulfonamides, sulphonic acid and cyclic bioisosteres such as tetrazole and oxadiazoles (Figure 22).[97]

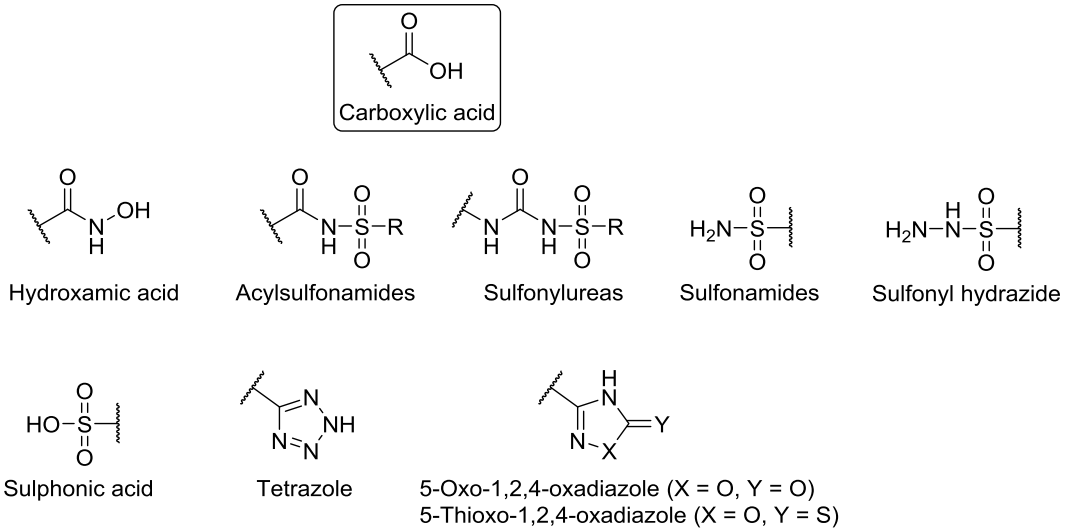

Figure 22: Example of carboxylic acid bioisosteres

Within the context of the bioisosterism approach, this study envisions introducing sulfonamide derivatives and sulfonyl hydrazide as bioisosteres of the carboxylic acid group of fusidic (Figure 23).

3.3.2 Prodrug approach

A prodrug is an inactive, bio-reversible derivative of an active drug molecule that can undergo *in vivo* enzymatic and/or chemical transformation to enable the bioactivation of the pharmacologically active parent drug at efficacious levels. The main objective of a prodrug design is to mask undesirable drug properties, such as low solubility, low target selectivity, metabolic instability, undesirable taste, irritation or pain after local administration, pre-systemic metabolism and toxicity.[98–100]

A prodrug approach is widely used in drug development programmes to improve on the physicochemical and/or pharmacokinetic properties of pharmacologically active compounds, through the optimization of ***a***bsorption, ***d***istribution, ***m***etabolism, ***e***xcretion, and ***t***oxicity (ADMET) properties.[98,100]

Therefore, the prodrug approach at the C-3 hydroxyl position was chosen to synthesize various fusidic acid ester derivatives based on the hypothesis that they will be metabolized to fusidic acid *in vivo*. The two C-3 open chain esters were resynthesized for comparison purposes, and to be used as a control in the screening of other test compounds (Figure 23).[85]

Lastly, in an attempt to expand on the SAR exploration an amine derivative was included in the SAR strategy of this dissertation (Figure 23).

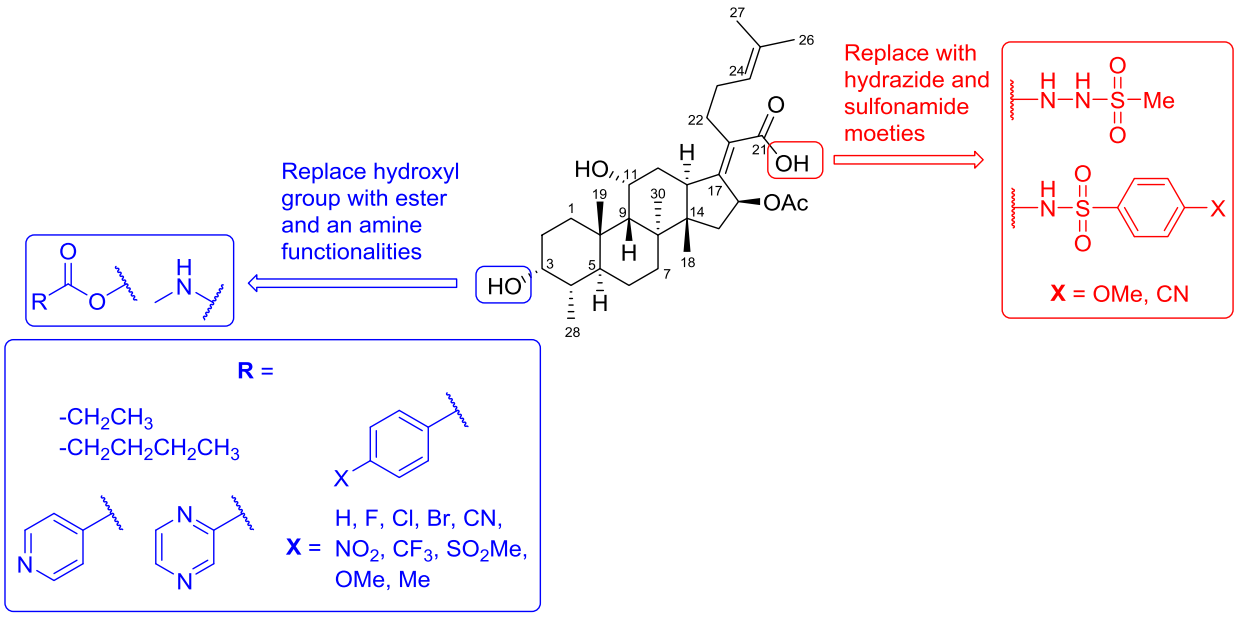

Figure 23: Proposed antimycobacterial SAR study.

To increase structural diversity and expand on the SAR of any lead compound, desired chemical and biological properties can be achieved by manipulating its physicochemical properties through the use of a Craig plot (Figure 24).[101] A Craig plot predicts the correlation between physicochemical properties of a drug and its biological activity through a graph of hydrophobic character (π) of a substituent versus its electronic effect (Hammett substitution constant, σ).[101] Therefore, to create structural diversity, the different substituents used in this study were selected from the Craig plot covering all four quadrants.[101]

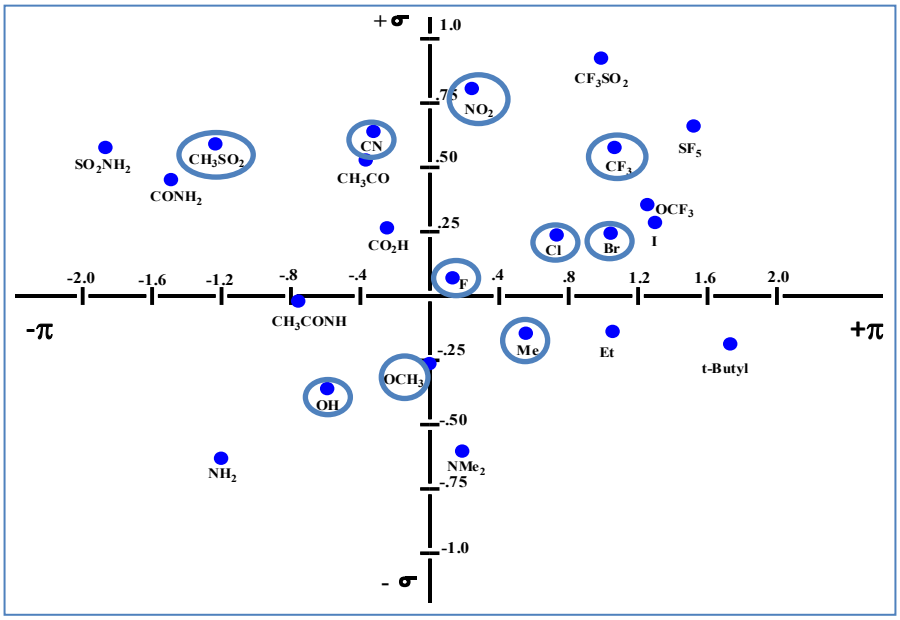

Figure 24: Craig Plot.[101]

3.4 Synthesis and characterization of fusidic acid derivatives

3.4.1 Synthesis of C-21 derivatives (SAR 1)

Scheme 1 shows the synthetic scheme for C-21 (SAR 1) derivatives of fusidic acid, using a procedure reported by Espinoza-Moraga, *et. al*.[102] These target compounds were obtained via the coupling of fusidic acid (**3.1**) with the corresponding sulfonamide in the presence of 1-ethyl-3-(3-dimethylaminopropyl)carbodiimide (EDCI) as an activating agent and a catalytic amount of 4-dimethylaminopyridine (DMAP).[103] The detailed synthetic procedure is described in Chapter 5.

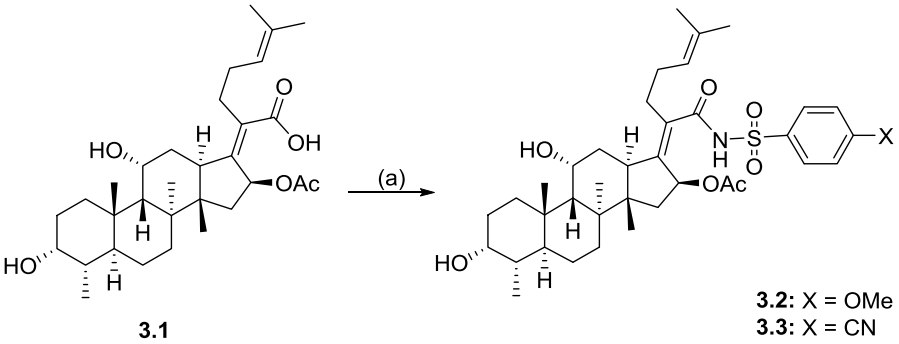

Scheme 1: General synthetic protocol towards compound **3.2** and **3.3** (SAR 1). *Reagents and conditions:* (a) *p*-X-$C_6H_4SO_2NH_2$, EDCI, DMAP, DCM, 25 °C, 3 days (**3.2**), 7 days (**3.3**).

The C-21 target compounds were obtained in extremely poor yields, summarized in **Table 4**, along with melting points. The poor yields can be attributed to the poor nucleophilicity of the sulfonamide reagent, as a result of the delocalization of the nitrogen non-bonding electron pair by the sulfone group. Starting material was largely recovered in these reactions, which did not go to completion.

Table 4: Isolated yields and melting points of C-21 (SAR 1) derivatives and fusidic acid

Compound	Yield (%)	Mp. (°C)
3.1	-	187 – 189
3.2	5	198 – 200
3.3	3	219 – 221

3.4.2 EDCI/DMAP-mediated amide coupling reaction mechanism

The amide coupling reaction using EDCI and a catalytic amount of DMAP is believed to proceed through the formation of a reactive *O*-acylisourea intermediate, a product of a nucleophilic addition of the carboxylate ion to EDCI. DMAP is used to prevent rearrangement of the unstable *O*-acylisourea to *N*-acylurea via acyl transfer. The resulting acid-DMAP intermediate undergoes a nucleophilic attack by the amine to furnish the desired amide (Figure 25). This reaction is driven forward by the formation of a stable urea by-product.[104,105]

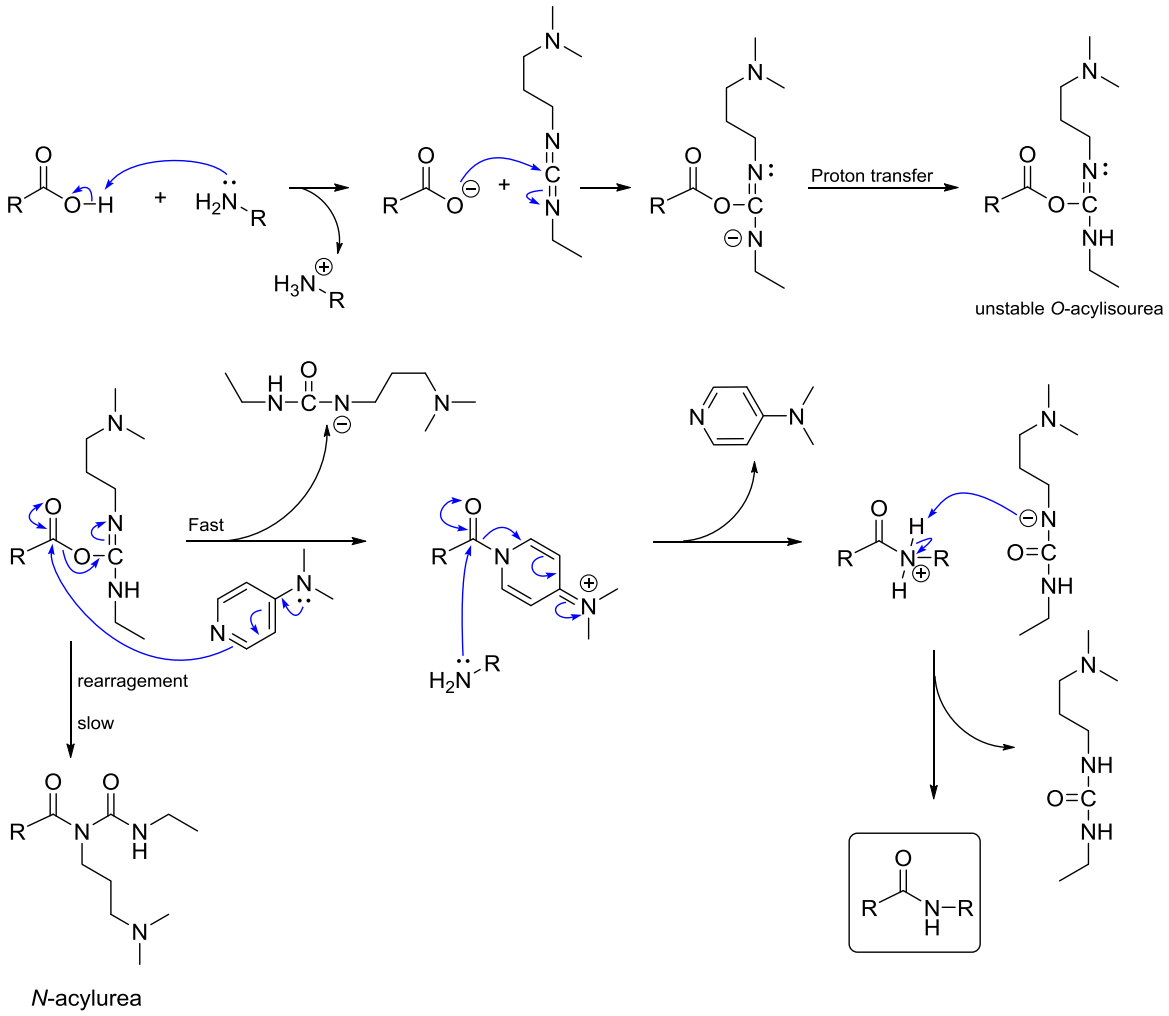

Figure 25: Proposed reaction mechanism of EDCI/DMAP mediated amide coupling.[104,105]

3.2.3 Characterization of target compounds

All the fusidic acid analogues were characterized using ^{1}H-NMR, ^{13}C-NMR and mass spectroscopy (MS). For some of the synthesized compounds, 2D homonuclear correlation spectroscopy (COSY), heteronuclear single quantum correlation (HSQC), heteronuclear multiple bond correlation (HMBC) NMR experiments were acquired to aid in ^{1}H-NMR and ^{13}C-NMR assignments. The purity of all target compounds was checked using liquid chromatography-mass spectroscopy (LC-MS).

3.2.3.1 Characterization of fusidic acid (3.1) in $CDCl_3$

The ^{1}H-NMR spectra of fusidic acid and its derivatives are complex, especially in the aliphatic region, due to the unsaturated ring systems. However, the characteristic ^{1}H-NMR signals of fusidic acid (**3.1**, in $CDCl_3$ at 400 MHz) appear at δ 5.87 (d, *J* = 8.4 Hz, H-16), 5.08 (m, H-24), 4.33 (m, H-11), 3.75 (m, H-3), 3.04 (m, H-13), 1.95 (s, H-31), 1.66 (s, H-27), 1.58 (s, H-26), 1.36 (s, H-30), 0.96 (s, H-19), 0.91 (d, *J* = 5.9 Hz, H-28) and 0.90 (s, H-18) ppm. The remaining proton signals appear in the aliphatic region δ 2.53-0.80 ppm (Figure 26). Key ^{1}H-^{1}H COSY correlations are shown in appendix 1.

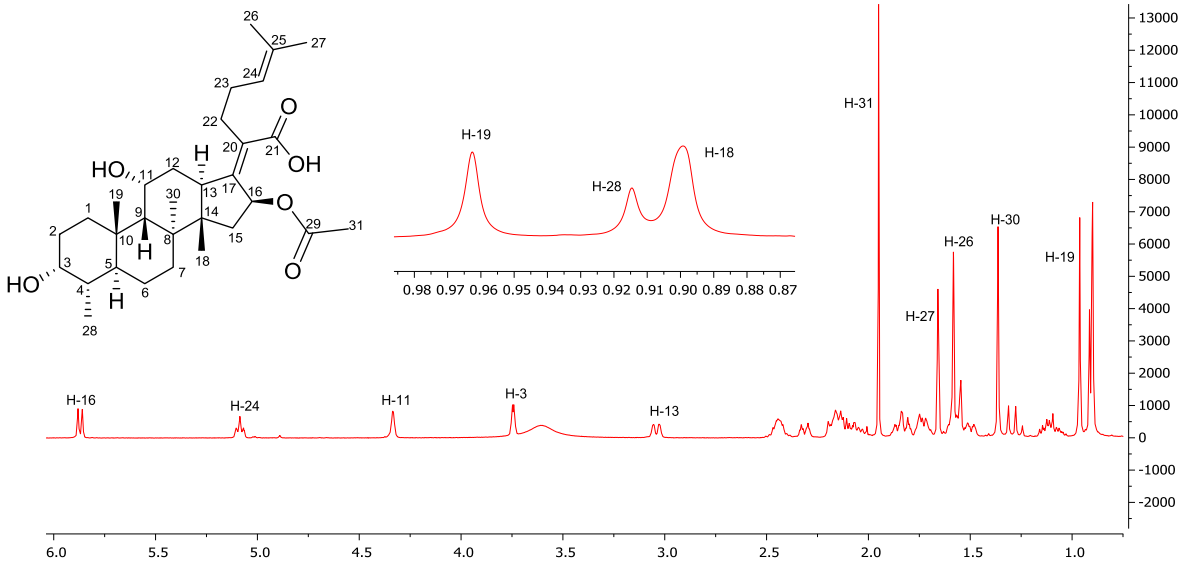

Figure 26: ^{1}H-NMR spectrum ($CDCl_3$, 400 MHz) of fusidic acid (**3.1**)

The ^{13}C-NMR spectrum of fusidic acid (**3.1**) indicates 31 non-equivalent carbon signals. Six of these signals correspond to the two carbonyl carbons, C-21 at δ 174.0 ppm and C-29 at δ 170.6 ppm and the other four carbon signals correspond to C-17, C-25, C-20 and C-24 appearing at δ 150.8, 132.6, 129.6 and 123.0 ppm, respectively. The rest of the carbon signals appear in the aliphatic region δ 75-15 ppm, with the characteristic signals C-16, C-3 and C-11, appearing at δ 74.4, 71.5, 68.3 ppm, respectively (Figure 27). This assignment of ^{1}H- and ^{13}C-NMR signals corresponds to those reported in literature.[106] In addition, the mass

spectroscopy (MS) of fusidic acid (**3.1**) displays a mass peak of *m/z* 457.3 corresponding to $[M\text{-}OAc]^+$ and *m/z* 515.3 for $[M\text{-}H]^-$.

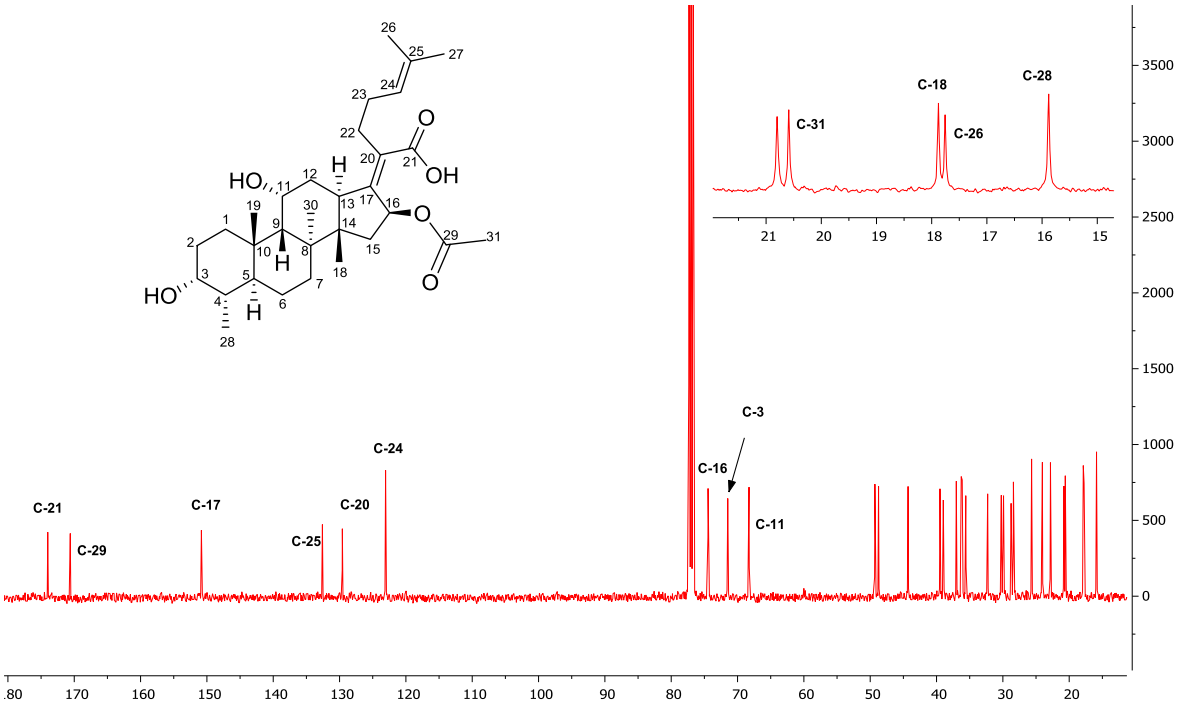

Figure 27: ^{13}C-NMR spectrum ($CDCl_3$, 100 MHz) of fusidic acid (**3.1**)

3.2.3.2 Characterization of C-21 analogues

The ^{1}H-NMR and ^{13}C-NMR spectra of the C-21 synthesized derivatives exhibit similar chemical shifts to those of fusidic acid (**3.1**), with additional signals corresponding to the respective attached sulfonamide moiety. Compound **3.2** is used here as a representative example for this set of target compounds.

The ^{1}H-NMR spectrum of compound **3.2** was recorded in DMSO-d_6 at 400 MHz. The characteristic signals are the symmetrical aromatic signals appearing as doublets at δ 7.84 (d, *J* = 9.0 Hz, H-33/37) and 7.11 (d, *J* = 9.0 Hz, H-34/36) ppm. The appearance of two singlets at δ 11.75 (s, 1H, H-N*H*) and 3.83 (s, 3H, H-38) ppm corresponding to -CON*H* and H-38 respectively, confirm the formation of an amide bond and therefore, the successful incorporation of the sulfonamide moiety into the fusidic acid structure (Figure 28). The

remaining proton signals appear in the region similar to that of fusidic acid. Stacked ^{1}H-NMR spectra of compounds **3.1** and **3.2** are shown in appendix 2.

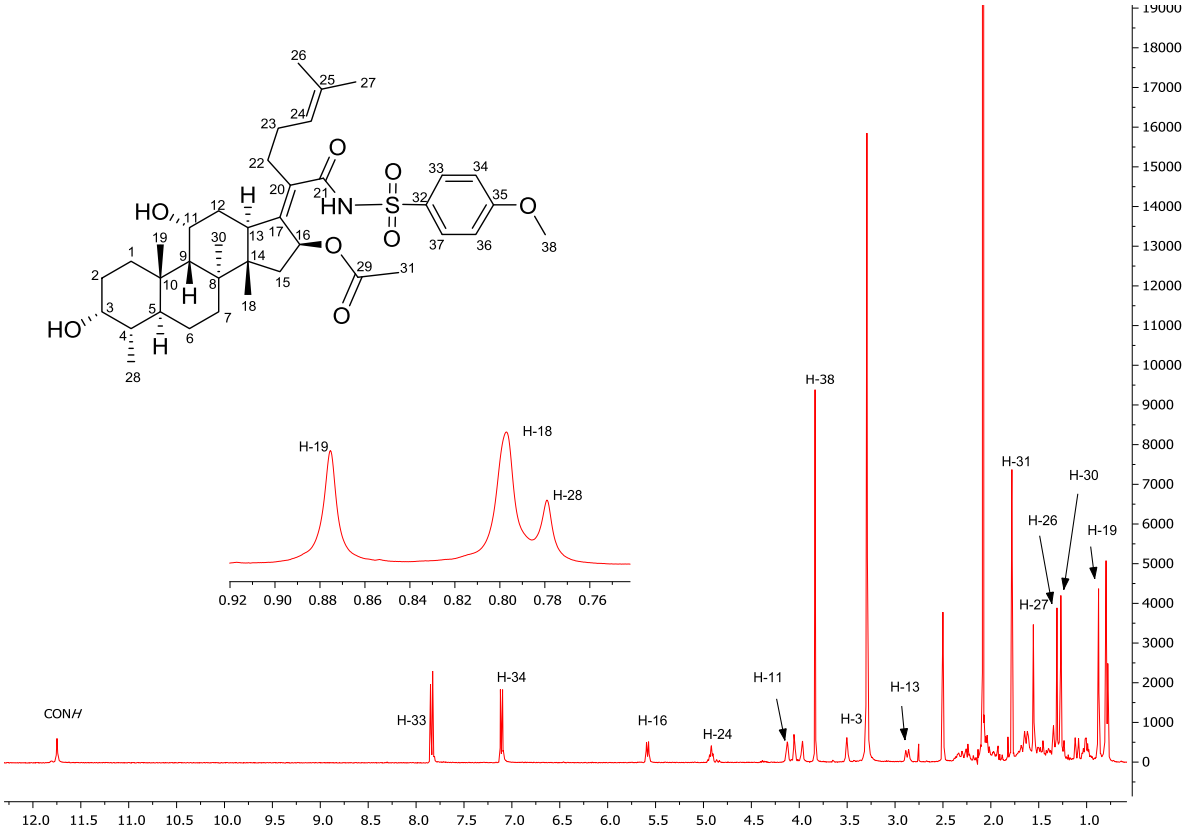

Figure 28: ^{1}H-NMR spectrum (DMSO-d_6, 400 MHz) of compound **3.2**

The ^{13}C-NMR spectrum of compound **3.2** revealed 35 carbon signals, with three of the signals accounting for two carbons each. The five additional signals correspond to the sulfonamide moiety, that is, C-32, C-33, C-34, C-35 and C-38, appearing at δ 163.0, 131.1, 130.9, 114.2 and 55.7 ppm respectively. The defining carbon signal is the C-29 signal at δ 169.7 ppm that has shifted downfield of the C-21 signal at δ 168.7 ppm (Figure 29). The remaining carbon signals appear in similar regions as those of fusidic acid. Moreover, a mass peak of *m/z* 626.2, corresponding to $[M\text{-}OAc]^{+}$ is observed for this compound, as expected. Thus, structure **3.2** was assigned to this compound.

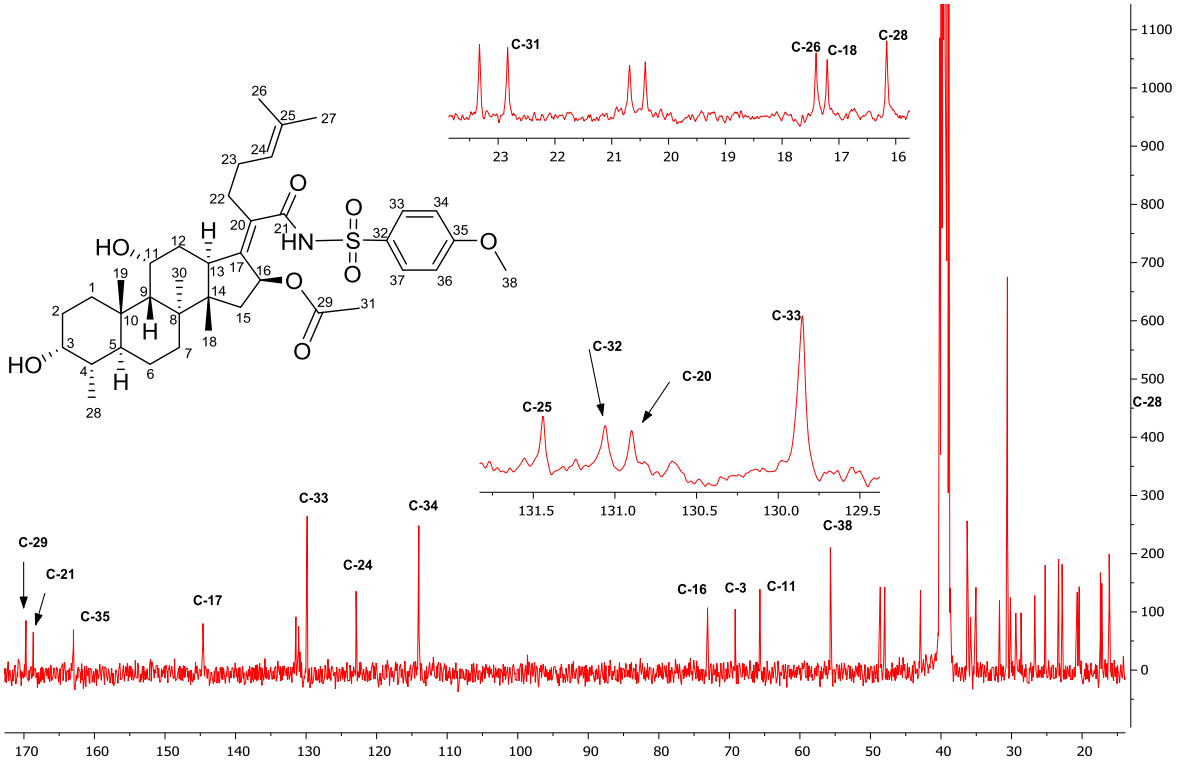

Figure 29: ^{13}C-NMR spectrum (DMSO-d_6, 100 MHz) of compound **3.2**

3.2.4 Synthesis of C-3 fusidic acid derivatives (SAR 2)

3.2.4.1 Synthesis of C-3 aliphatic esters and hydrazides

The synthesis of target compounds **3.8** and **3.9** was achieved following the literature procedure reported by Kaur *et al.*,[103] and Duvold *et al.*,[107] (Scheme 2). The aliphatic ester intermediates **3.4** and **3.5** were synthesized via esterification of **3.1** with the respective acid or acid anhydride in pyridine. Compound **3.4** was obtained by the reaction of **3.1** with propanoic acid in pyridine in the presence of n-Propanephosphoric acid anhydride (T3P) as a coupling reagent. Compound **3.5** was obtained from the reaction of **3.1** with valeric acid anhydride in pyridine acting as a base and solvent (Scheme 2).

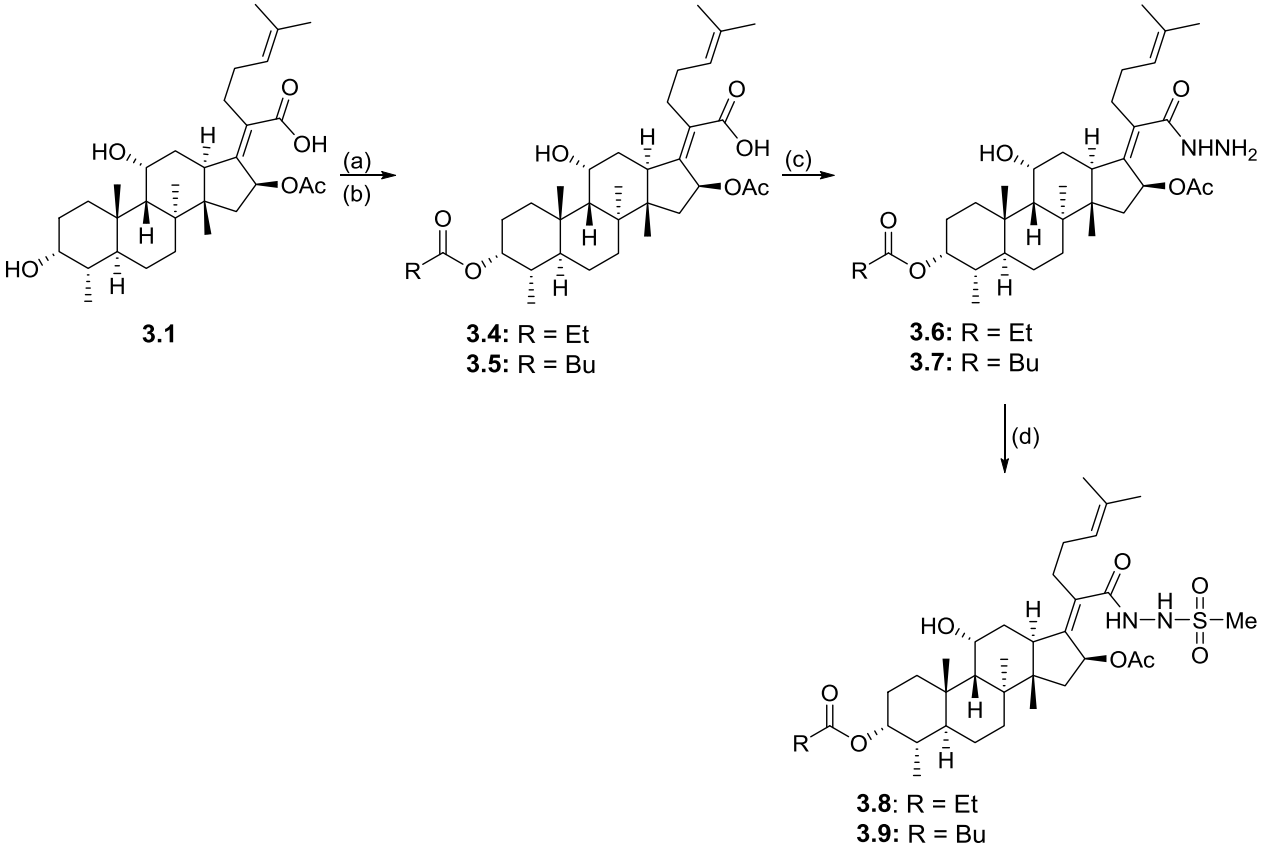

Scheme 2: General synthetic protocol towards compound **3.4** to **3.9** (SAR 2). *Reagents and conditions:* (a) valeric acid anhydride, pyridine, 25 ^{o}C, 3 h; (b) propanoic acid, T3P (50% w/v solution in DMF), pyridine, 0 ^{o}C – 25 ^{o}C, 17 h; (c) (i) EDCI, HOBt, CH_3CN, 25 ^{o}C, 3 h, (ii) $NH_2NH_2.H_2O$, 25 ^{o}C, 19 h (**3.6**) and 24 h (**3.7**); (d) MsCl, pyridine, 25 ^{o}C, 1 h (**3.8**) and 2 h (**3.9**).

The fusidic acid hydrazides **3.6** and **3.7** were prepared by reacting 3-ester fusidic acid **3.4** or **3.5** with hydrazine monohydrate in the presence of EDCI and HOBt in acetonitrile. The target compounds **3.8** and **3.9** were then obtained via a mesylation of the fusidic acid hydrazides with methanesulfonyl chloride (MsCl) in the presence of pyridine. Low to high isolated yields were obtained for these reactions as summarized in **Table 5**.

Table 5: Isolated yields and melting points of C-3 (SAR 2) aliphatic ester

Compound	Yield (%)	Mp (°C)
3.4	32	176 – 178
3.5	45	155 – 157
3.6	78	102 – 104
3.7	58	86 – 88
3.8	44	102 – 104
3.9	54	103 – 105

In these reactions, the C-3 hydroxyl was preferentially esterified, as the hydroxyl at C-11 is sterically hindered due to the chair-boat-chair conformation of fusidic acid (Figure 30).

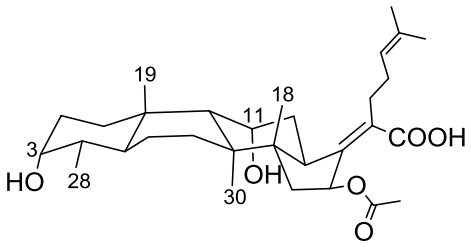

Figure 30: Chair-boat-chair conformation of fusidic acid.

3.2.4.2 T3P-mediated reaction mechanism

The reaction occurs via carboxylic acid activation through an attack of the carboxylate ion on the phosphorous atom of T3P. A nucleophilic attack on the activated acid intermediate and a proton transfer leads to the formation of the desired ester (Figure 31).[108,109]

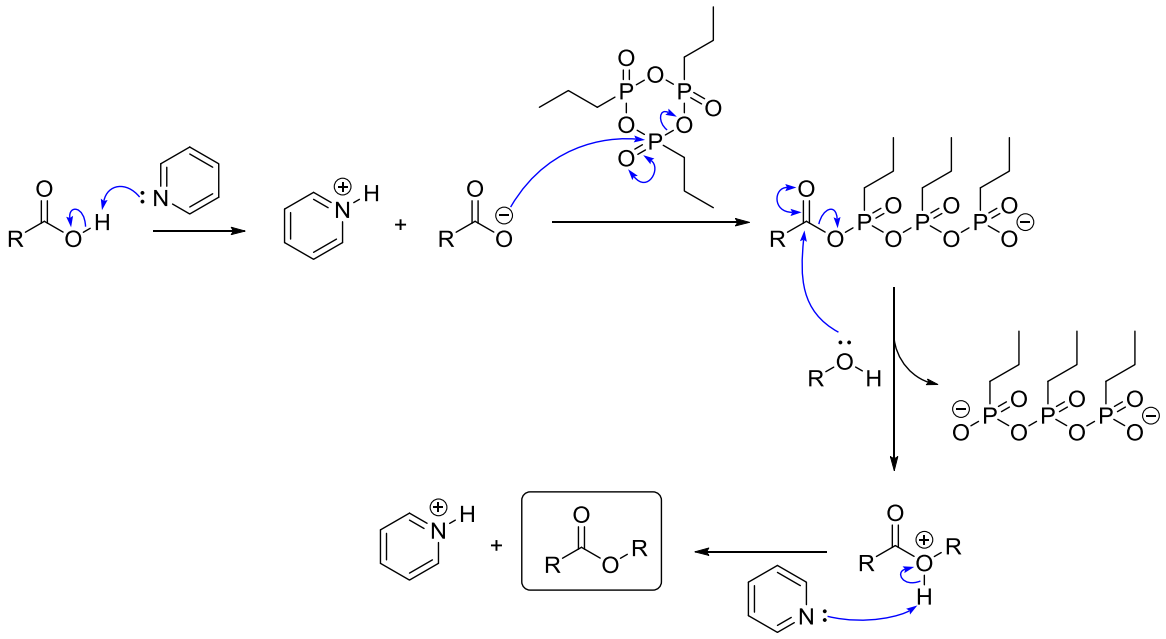

Figure 31: Proposed reaction mechanism for T3P-mediated coupling reaction.[108,109]

3.2.4.3 Characterization of C-3 aliphatic ester analogues

The ^{1}H- and ^{13}C-NMR spectra of these C-3 aliphatic esters can be described using intermediates **3.4**, **3.6** and target compound **3.8** as illustrative examples. Stacked ^{1}H-NMR spectra of compounds **3.1**, **3.4**, **3.6** and **3.8** are shown in appendix 3.

3.2.4.3.1 Characterization of intermediate 3.4

The ^{1}H-NMR spectrum of intermediate **3.4** was recorded in $CDCl_3$ at 400 MHz, with the distinct ^{1}H-NMR spectral feature being the deshielded H-3 signal at δ 4.94 ppm from δ 3.75 ppm (in **3.1**). In addition, the structure is confirmed by the appearance of two new proton signals of H-2' and H-3', corresponding to the aliphatic chain at δ 2.35 ppm (q, J = 7.6 Hz) and δ 1.15 ppm (t, J = 7.6 Hz) respectively. The remaining proton signals appear in the similar region as that of **3.1** (Figure 32).

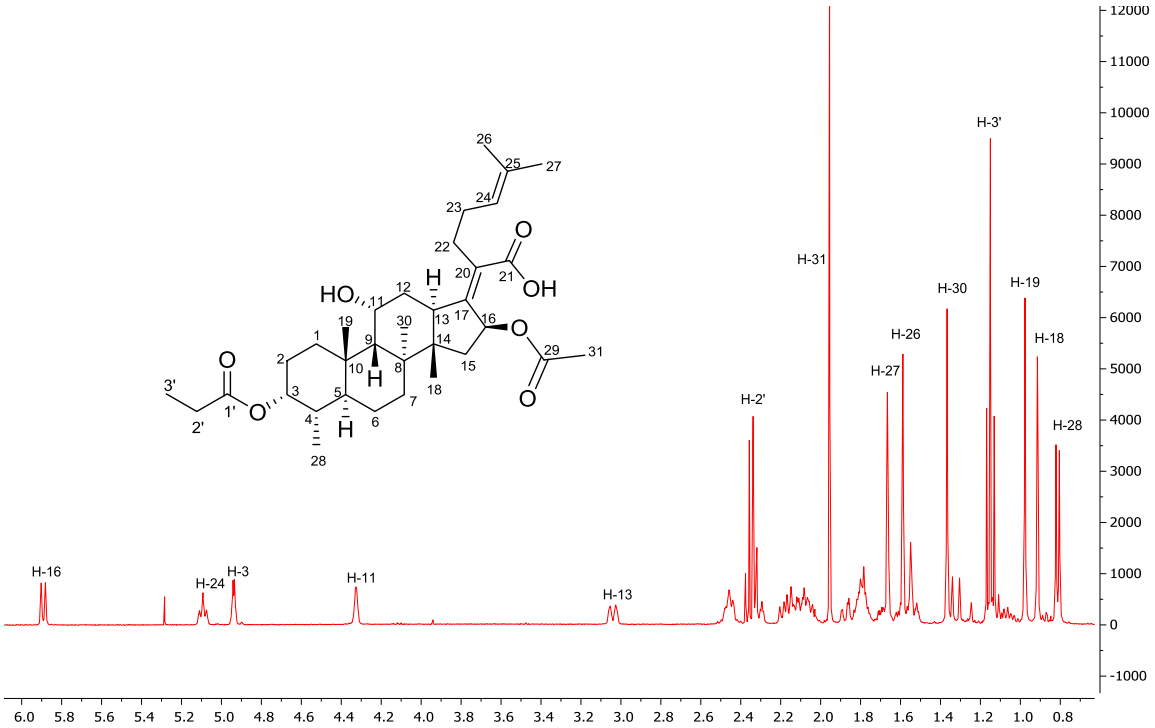

Figure 32: ^{1}H-NMR spectrum ($CDCl_3$, 400 MHz) of compound **3.4**

The ^{13}C-NMR spectrum for compound **3.4** indicates the presence of characteristic signals which supports the presence of an ester group at δ 174.1 (C-1') ppm. Furthermore, the downfield shift of the C-3 signal from δ 71.5 ppm in **3.1** to δ 74.0 ppm in **3.4** along with the appearance of the two ester side chain signals at δ 28.3 ppm (C-2') and δ 9.6 ppm (C-3'), indicate a successful esterification reaction (Figure 33). A MS peak of *m/z* 513.3, corresponding to $[M\text{-}OAc]^+$ further confirms the formation of intermediate **3.4**.

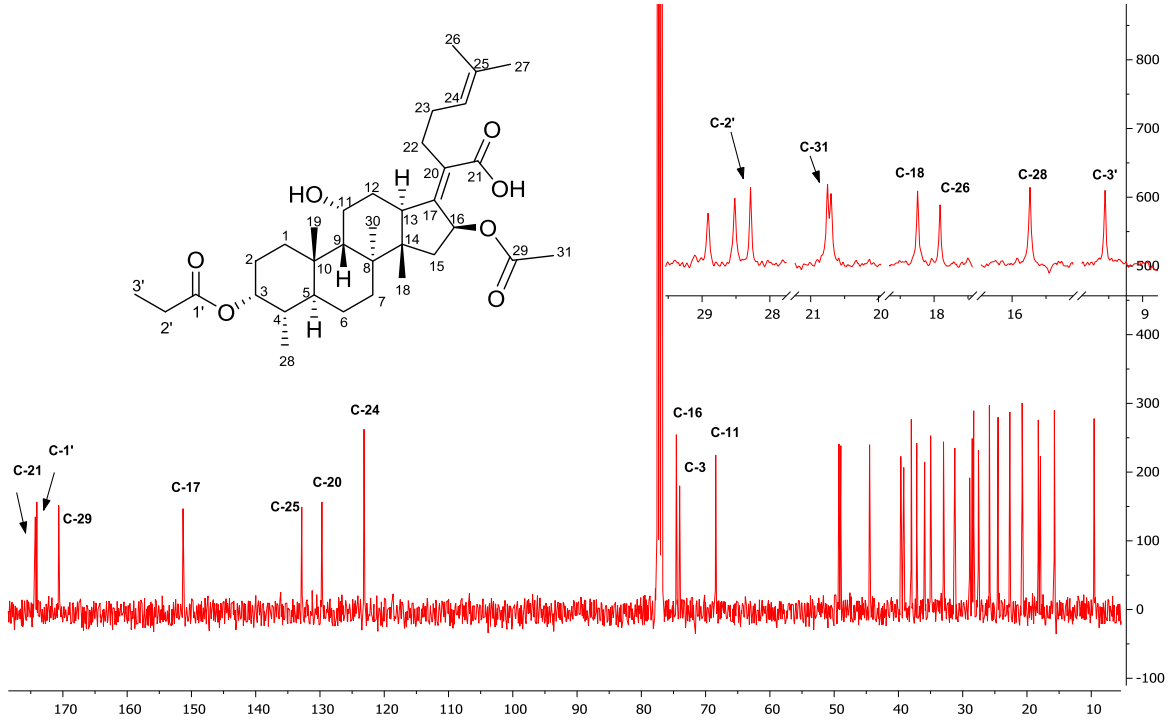

Figure 33: ^{13}C-NMR spectrum ($CDCl_3$, 100 MHz) of compound **3.4**

3.2.4.3.2 Characterization of intermediate 3.6

Intermediate **3.6** was obtained from the coupling of hydrazine monohydrate to intermediate **3.4** with the ^{1}H-NMR spectrum being recorded in $CDCl_3$ at 400 MHz. In the ^{1}H-NMR spectrum of **3.6**, no evident change in chemical shifts is observed when compared to **3.4**. For this reason, ^{13}C-NMR and MS were used to confirm the success of the synthesis.

In the ^{13}C-NMR spectrum (Figure 34), the C-21 signal has shifted upfield from δ 174.3 ppm (in **3.4**) to δ 171.9 ppm (in **3.6**). The rest of the carbon signals appear in similar regions as in compound **3.4**. The MS analysis of **3.6** reveals a *m/z* of 527.4 corresponding to $[M\text{-}OAc]^+$, as expected.

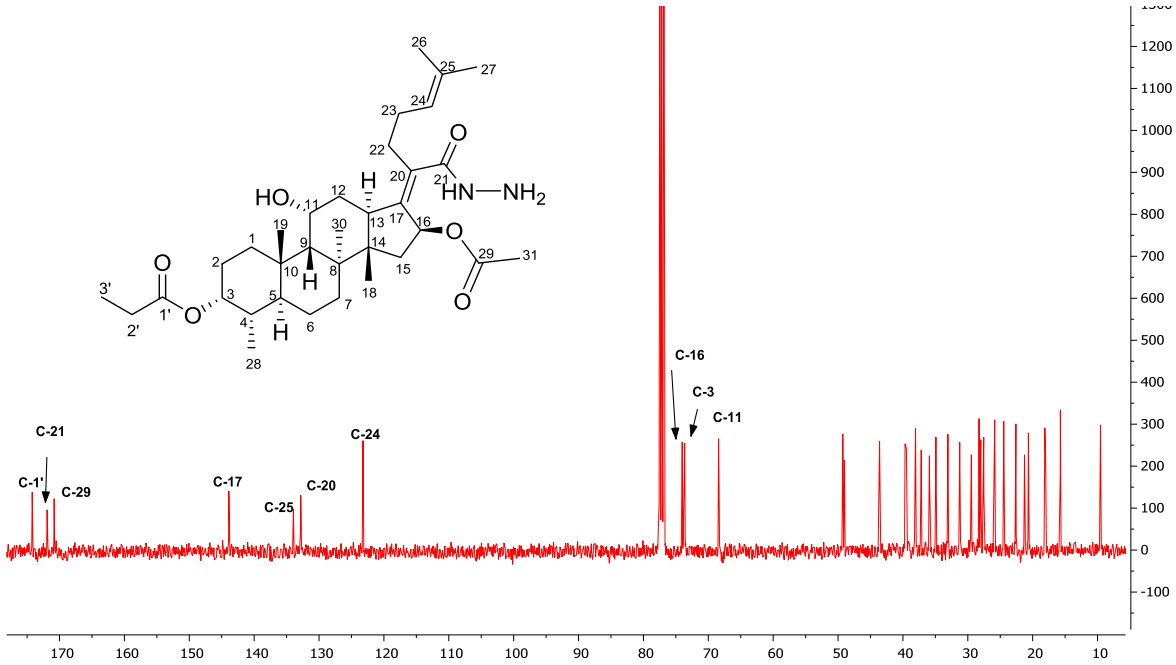

Figure 34: ^{13}C-NMR spectrum ($CDCl_3$, 100 MHz) of compound **3.6**

3.2.4.3.3 Characterization of target compound 3.8

Target compound **3.8** was obtained via mesylation of **3.6** with MsCl in pyridine. The characteristic features in the ^{1}H-NMR spectrum of **3.8** (Figure 35) are the appearance of doublets in the aromatic region resonating at δ 7.82 ppm (J = 4.4 Hz) and 6.96 ppm (J = 4.5 Hz) corresponding to –CON*H* and –SO_2N*H* groups respectively. In addition, a H-32 signal at δ 2.97 ppm confirms the presence of the methyl group. The remaining proton signals appear in similar regions as in **3.6**.

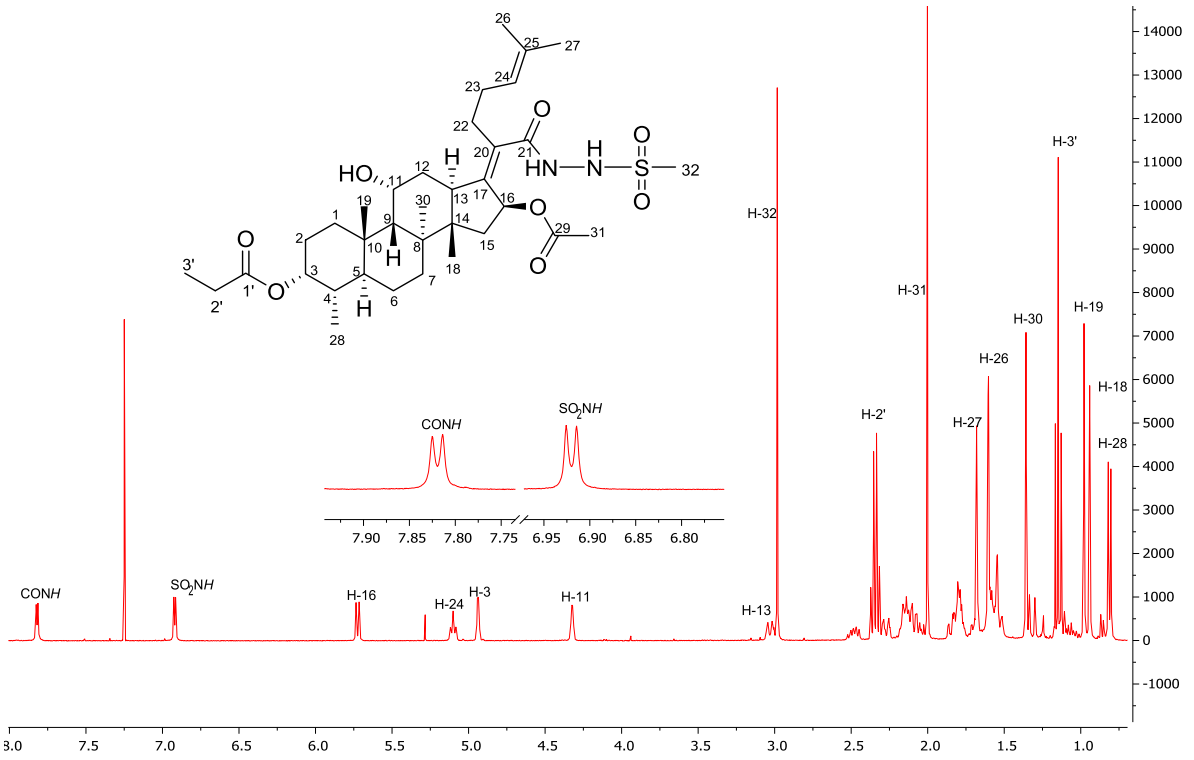

Figure 35: ^{1}H-NMR spectrum ($CDCl_3$, 400 MHz) of compound **3.8**

The ^{13}C-NMR spectrum of **3.8** indicates 36 non-equivalent carbon signals (Figure 36). The presence of an additional carbon signal at δ 39.2 ppm (C-32) and the upfield shift of the C-21 carbonyl carbon from δ 171.9 ppm (in **3.6**) to δ 170.6 ppm (in **3.8**) confirms the structure of target compound **3.8**. Furthermore, a MS spectrum indicate a mass peak of *m/z* 605.3 corresponding to $[M\text{-}OAc]^+$ for this compound.

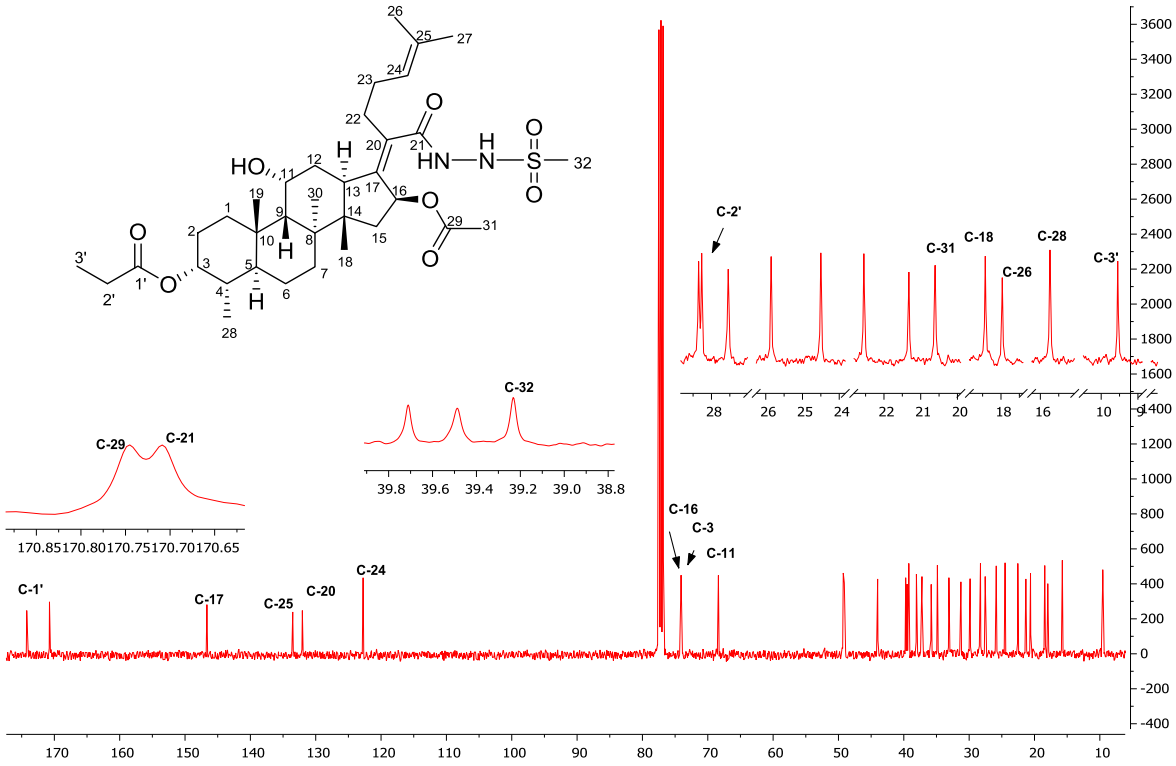

Figure 36: ^{13}C-NMR spectrum ($CDCl_3$, 100 MHz) of compound **3.8**

3.2.4.4 Synthesis of C-3 aromatic esters

3.2.4.4.1 Synthesis of C-3 *para* substituted aromatic esters

The synthesis of C-3 *para* substituted aromatic esters was performed according to a procedure reported by Xu *et al*.,[110] via a Steglich esterification without any modification. This involved the addition of the respective aromatic acid to a mixture of compound **3.1**, *N*,*N*-dicyclohexylcarbodiimide (DCC) and DMAP in dry DCM (Scheme 3). The reactions were performed at 25 ^{o}C between 2–12 h. These C-3 esters were obtained in very low isolated yields (Table 6).

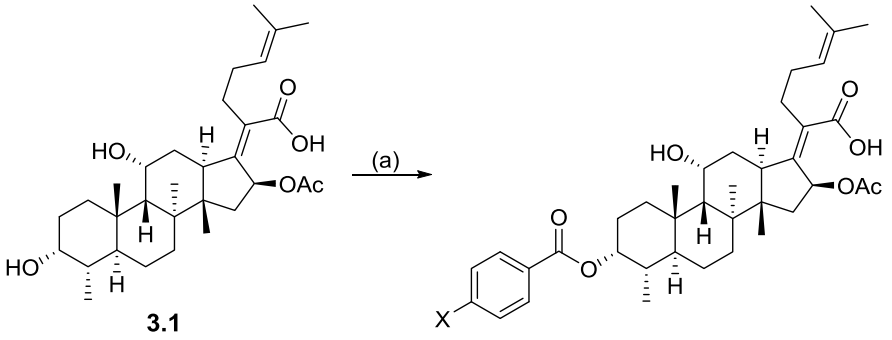

3.1

3.10: X = H
3.11: X = F
3.12: X = Cl
3.13: X = Br
3.14: X = CN
3.15: X = NO_2
3.16: X = CF_3
3.17: X = SO_2Me
3.18: X = OMe
3.19: X = Me

Scheme 3: General synthetic protocol towards compound **3.10** to **3.19** (SAR 2). *Reagents and conditions:* (a) *p*-X-C_6H_4COOH, DCC, DMAP, dry DCM, N_2, 25 ^oC, 2-12 h.

The very low yield is probably a result of the presence of both the carboxylic acid and alcohol functionalities in fusidic acid leading to an increase in competing side-reactions.

Table 6: Isolated yields and melting points of SAR 2 aromatic esters

Compound	Yield (%)	Mp (°C)	Compound	Yield (%)	Mp (°C)
3.10	10	172 – 174	**3.15**	14	135 – 137
3.11	6	76 – 78	**3.16**	35	171 – 173
3.12	13	118 – 120	**3.17**	39	177 – 179
3.13	24	179 – 181	**3.18**	6	162 – 164
3.14	13	161 – 163	**3.19**	12	166 – 168

The ^{1}H-NMR and ^{13}C-NMR spectra of the *para*-substituted aromatic esters shows similar chemical shifts. Therefore, compound **3.13** is used here as an illustrative example for the characterization of this series of compounds. Stacked ^{1}H-NMR spectra of compounds **3.1** and **3.13** are shown in appendix 4.

3.2.4.4.2 Characterization of target compound 3.13

The ^{1}H-NMR spectrum of **3.13** was recorded in CD_3OD at 400 MHz, with the characteristic signals being the new symmetric doublets resonating at δ 7.94 (*J* = 8.7 Hz, H-3'/7') and 7.65 (*J* = 8.7 Hz, H-4'/6') ppm and the downfield shift of the key H-3 signal from δ 3.66 ppm in **3.1** (in CD_3OD, spectrum not shown) to δ 5.15 ppm. The remaining proton signals appeared in similar regions as in the starting material **3.1** (Figure 37).

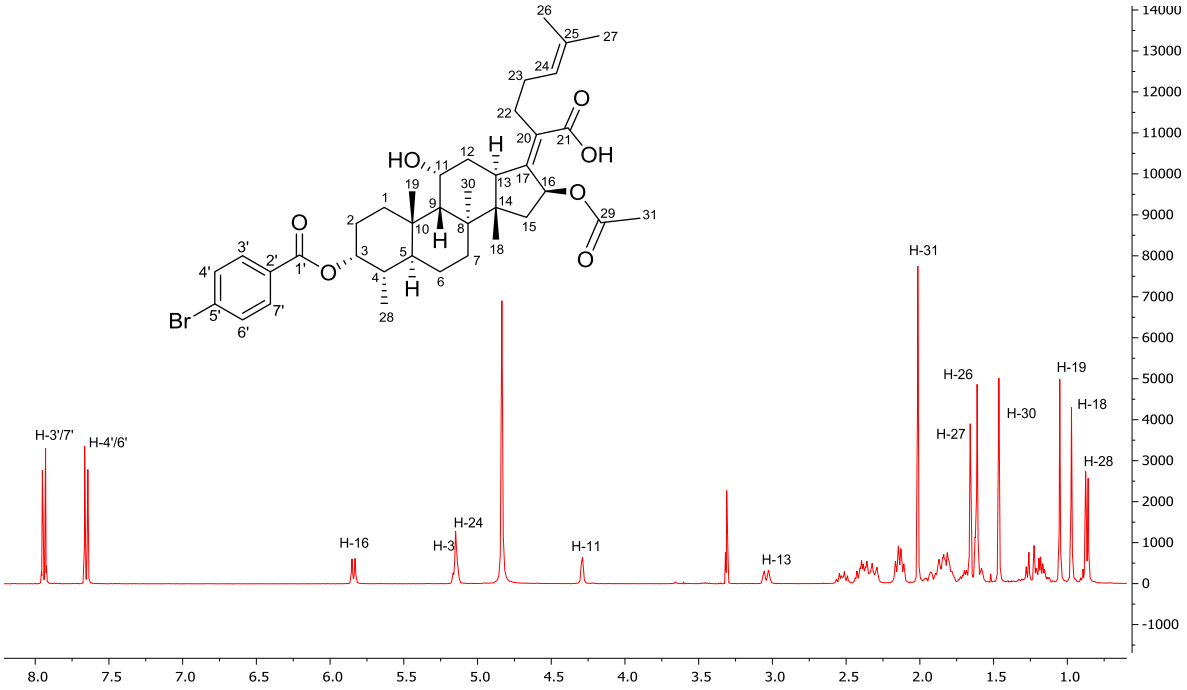

Figure 37: ^{1}H-NMR spectrum (CD_3OD, 400 MHz) of compound **3.13**

The ^{13}C-NMR spectrum indicates 36 carbon signals, with two of the signals accounting for four carbons. The characteristic feature is the downfield shift of the C-3 signal from δ 72.4 in **3.1** (in CD_3OD, spectrum not shown) to δ 77.3 ppm in **3.13**. In addition, the carbonyl carbon of the ester appears at δ 166.8 ppm (C-1') while the aromatic carbon signals appear at δ 138.9 (C-2'), 133.0 (C-3'), 132.1 (C-4') and 131.2 (C-5') ppm (Figure 38). The LC-MS of **3.13** indicates a clear presence of isotopic bromine signals (*m/z* 697.3, 699.3) for $[M-H]^-$.

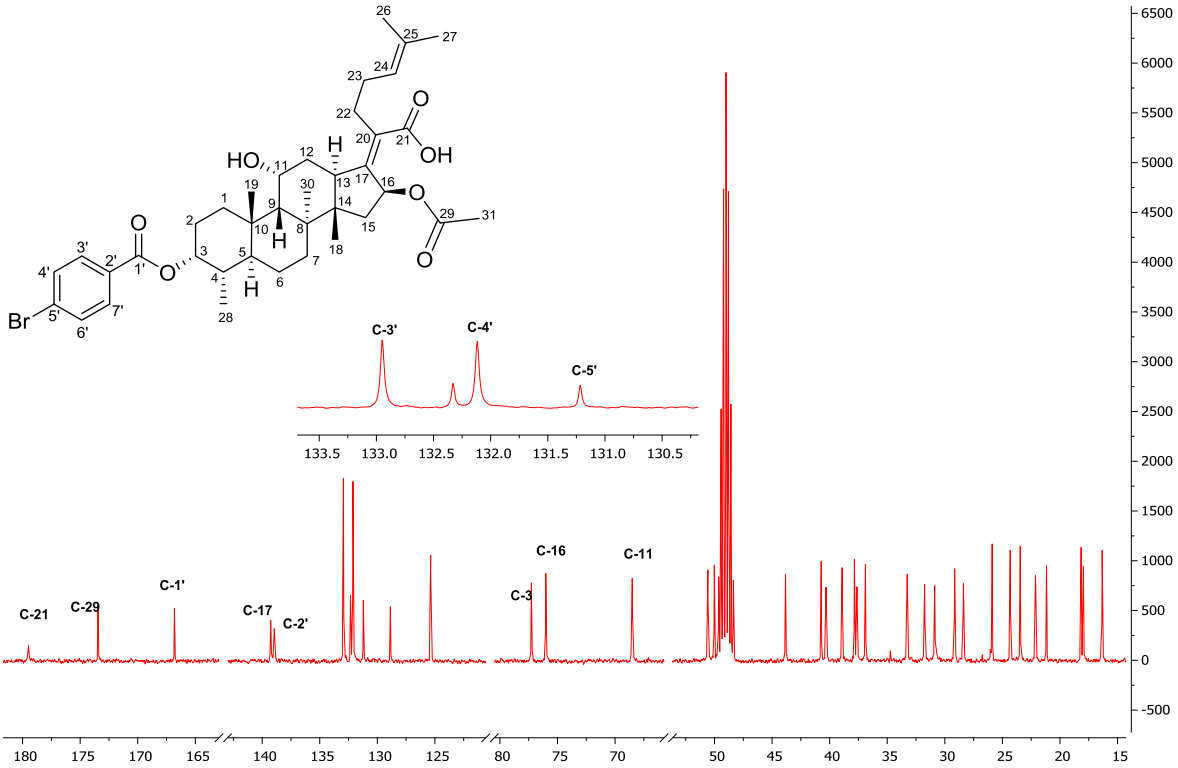

Figure 38: ^{13}C-NMR spectrum (CD_3OD, 400 MHz) of compound **3.13**

3.2.4.4.3 Synthesis of C-3 heterocyclic esters

The synthesis of C-3 heterocyclic esters was done similarly to *para*-substituted aromatic esters as reported by Xu *et. al.*,[110] (Scheme 4). The synthesis of compound **3.21** resulted into a mixture of a mono-esterification product (**3.21**) and di-substituted ester (**3.22**) (Scheme 4). These reactions results in very low isolated yields of the products as summarized in **Table 7**. The low yields of these compounds can be explained by the same reasons indicated early for compounds **3.10**-**3.19**.

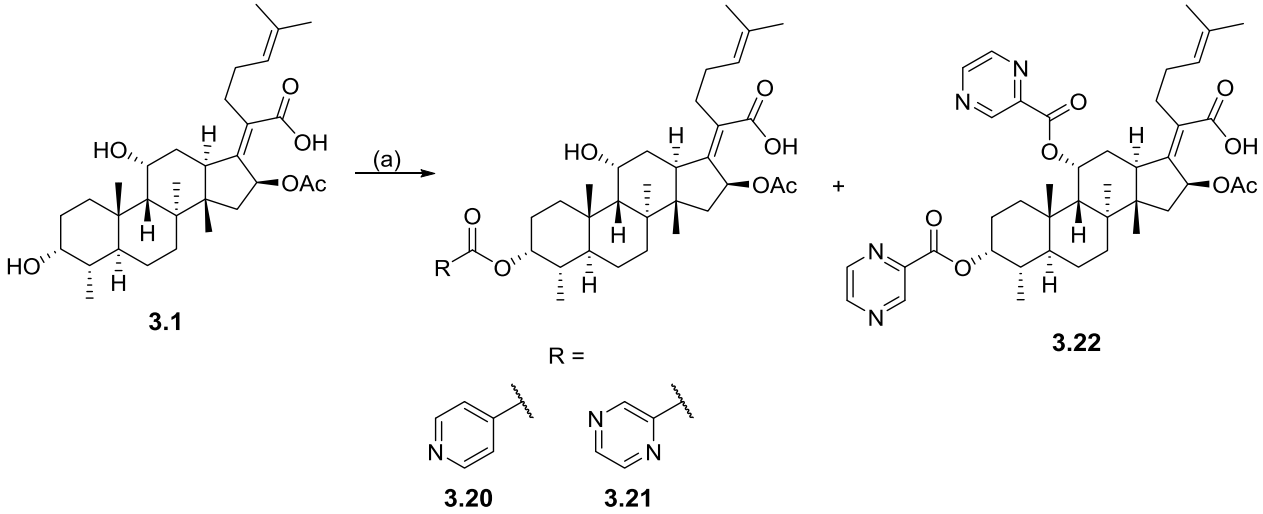

Scheme 4: General synthetic protocol towards compound **3.20** to **3.22** (SAR 2). *Reagents and conditions:* (a) RCOOH, DCC, DMAP, dry DCM, N_2, 25 ^oC, 2-12 h.

Table 7: Isolated yields and melting points of SAR 2 heterocyclic esters

Compound	Yield (%)	Mp (°C)
3.20	11	184 – 186
3.21	9	116 – 118
3.22	12	134 – 136

3.2.4.4.4 Characterization of C-3 heterocyclic aromatic esters

The heterocyclic esters display closely related spectroscopic data. Thus compound **3.21** and **3.22** are used as representative examples for this class of compounds. Stacked ^{1}H-NMR spectra of compounds **3.1**, **3.21** and **3.22** are shown in appendix 5.

3.2.4.4.4.1 Characterization of compound 3.21

The ^{1}H-NMR spectrum of compound **3.21** was recorded in CD_3OD at 400 MHz. The ^{1}H-NMR characteristic features of compound **3.21** include; a greatly deshielded signal of H-3 from δ 3.66 in **3.1** (in CD_3OD, spectrum not shown) to 5.30 ppm and the appearance of two new signals in the aromatic region at δ 9.30 (s, H-3') and 8.82 (m, H-4'/5') ppm (Figure 39). The rest of the proton signals appear in a similar region as in **3.1**.

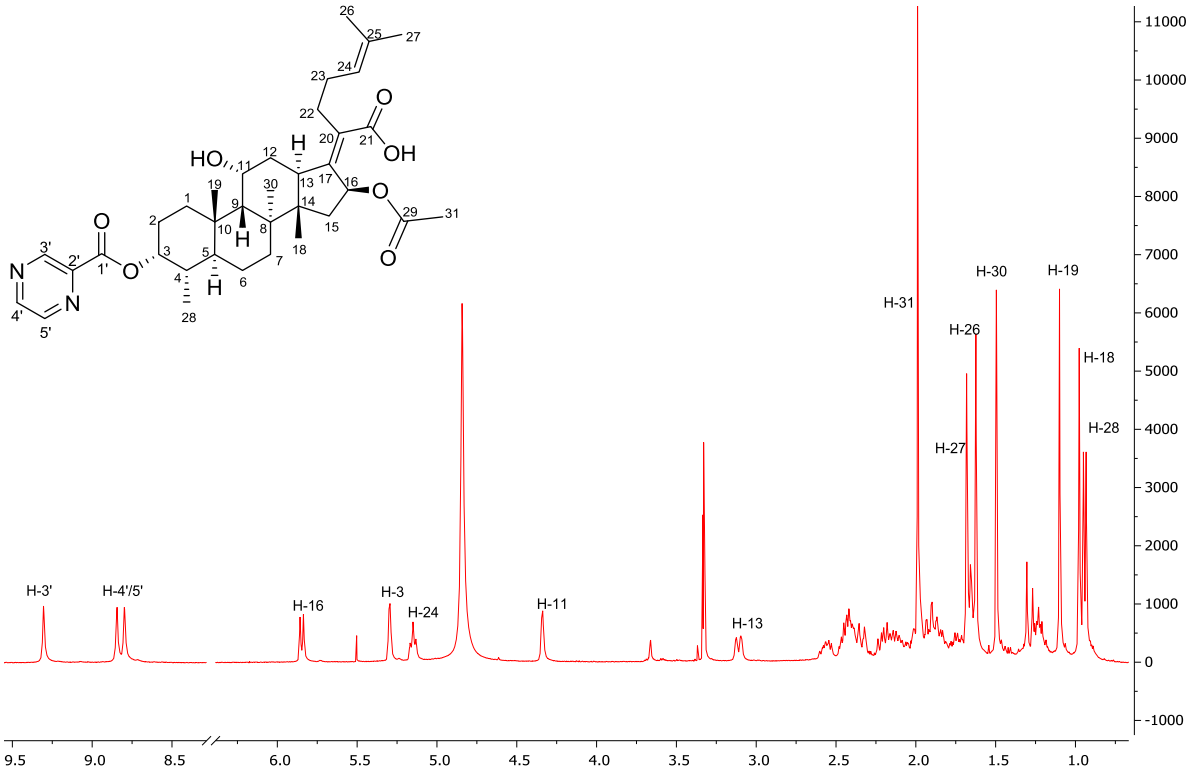

Figure 39: ^{1}H-NMR spectrum (CD_3OD, 400 MHz) of compound **3.21**

The characteristic signals from the ^{13}C-NMR spectrum include, the extra carbonyl carbon at δ 164.8 ppm corresponding to C-1' and the downfield shift of the C-3 signal from δ 72.4 ppm in **3.1** (in CD_3OD, spectrum not shown) to δ 78.8 ppm. Moreover, the carbon signals of the 2-pyrazinecarboxylic moiety appear at δ 149.1 (C-5'), 146.8 (C-4'), 146.1 (C-3') and 145.1 (C-2') ppm (Figure 40). A MS peak of *m/z* 621.4 for $[M-H]^-$ further confirms the authenticity of compound **3.21**.

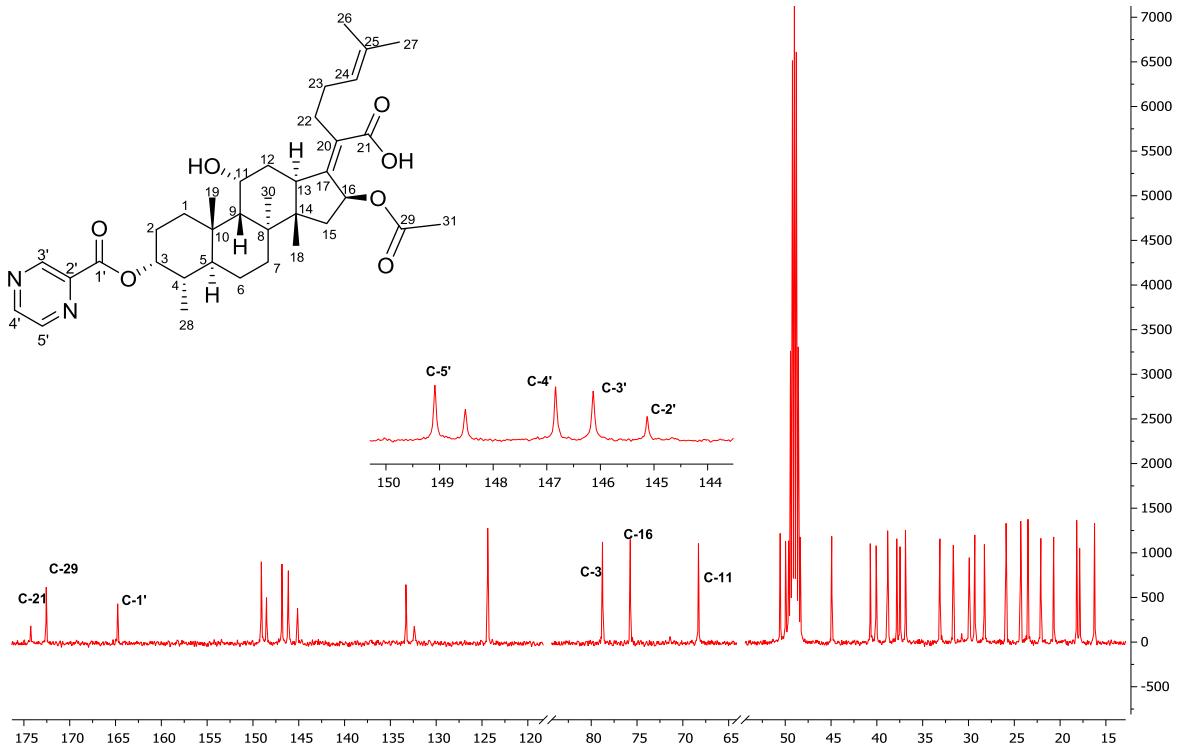

Figure 40: ^{13}C-NMR spectrum (CD_3OD, 100 MHz) of compound **3.21**

3.2.4.4.4.2 Characterization of compound 3.22

The ^{1}H-NMR spectrum of compound **3.22** was recorded in CD_3OD at 400 MHz. The characteristic features include the highly deshielded signals of H-3 resonating at δ 5.30 ppm from 3.66 (in **3.1**, in CD_3OD, spectrum not shown) and H-11 at δ 5.71 ppm from δ 4.32 in **3.1** (in CD_3OD, spectrum not shown). In addition, the aromatic proton signals are observed as follows; δ 9.18 (d, *J* = 1.2 Hz, H-3'), 9.06 (d, *J* = 1.4 Hz, H-8'), 8.80 (d, *J* = 2.4 Hz, H-5'), 8.73 (dd, *J* = 2.5, 1.4 Hz, H-4') and 8.70 (m, H-9'/10') ppm (Figure 41). The rest of the proton signals appear in a similar region as in **3.1** and **3.21**.

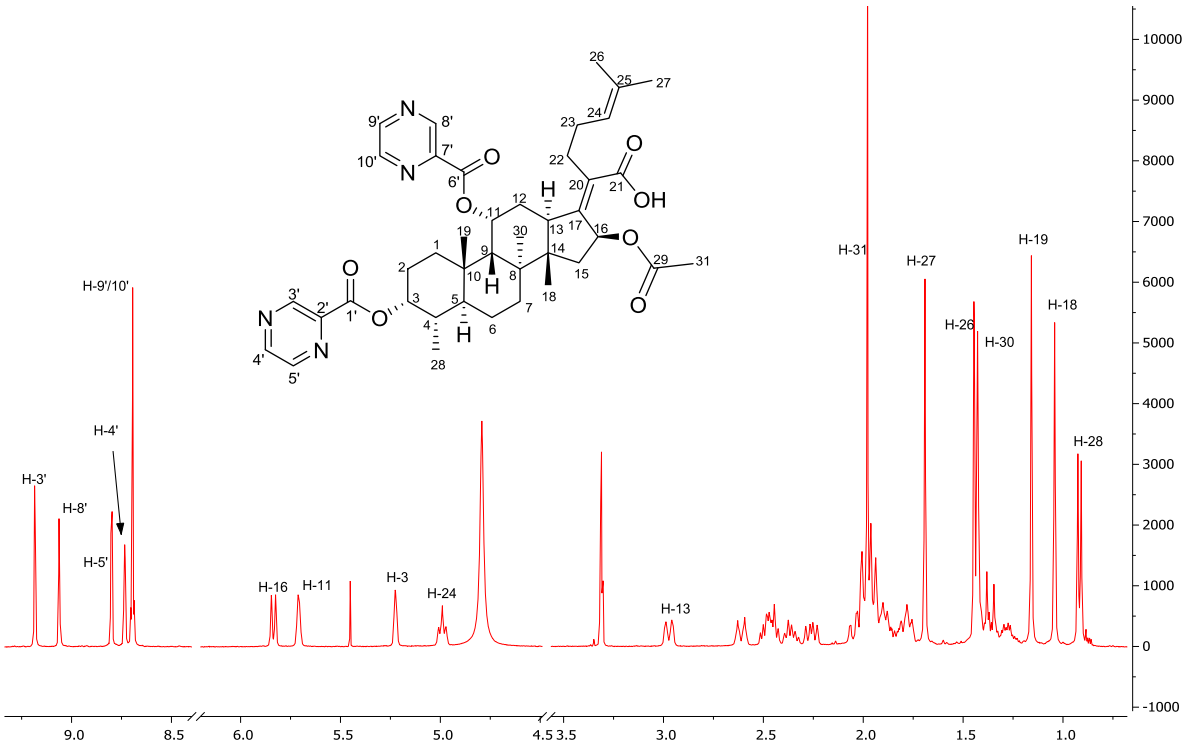

Figure 41: ^{1}H-NMR spectrum (CD_3OD, 400 MHz) of compound **3.22**

The ^{13}C-NMR spectrum of compound **3.22** exhibits 40 distinct carbon signals, with four characteristic carbonyl signals at δ 173.7 (C-21), 172.4 (C-29), 164.8 (C-1') and 164.5 (C-6') ppm (Figure 42). Moreover, there is a downfield shift of C-3 from δ 72.4 in **3.1** (in CD_3OD, spectrum not shown) to 78.1 ppm and C-11 from δ 68.6 in **3.1** (in CD_3OD, spectrum not shown) to 74.4 ppm. The carbon signals of the two 2-pyrazinecarboxylic moieties appear at δ 148.8 (C-5'), 147.23 (C-10'), 146.5 (C-4'), 146.3 (C-3'/8'), 146.2 (C-9'), 144.8 (C-2') and 144.7 (C-7') ppm. The authenticity of **3.22** is further confirmed by the molecular ion peak with *m/z* ratio of 727.3, corresponding to $[M-H]^-$. No significant change in chemical shifts for the rest of the carbon signals is observed.

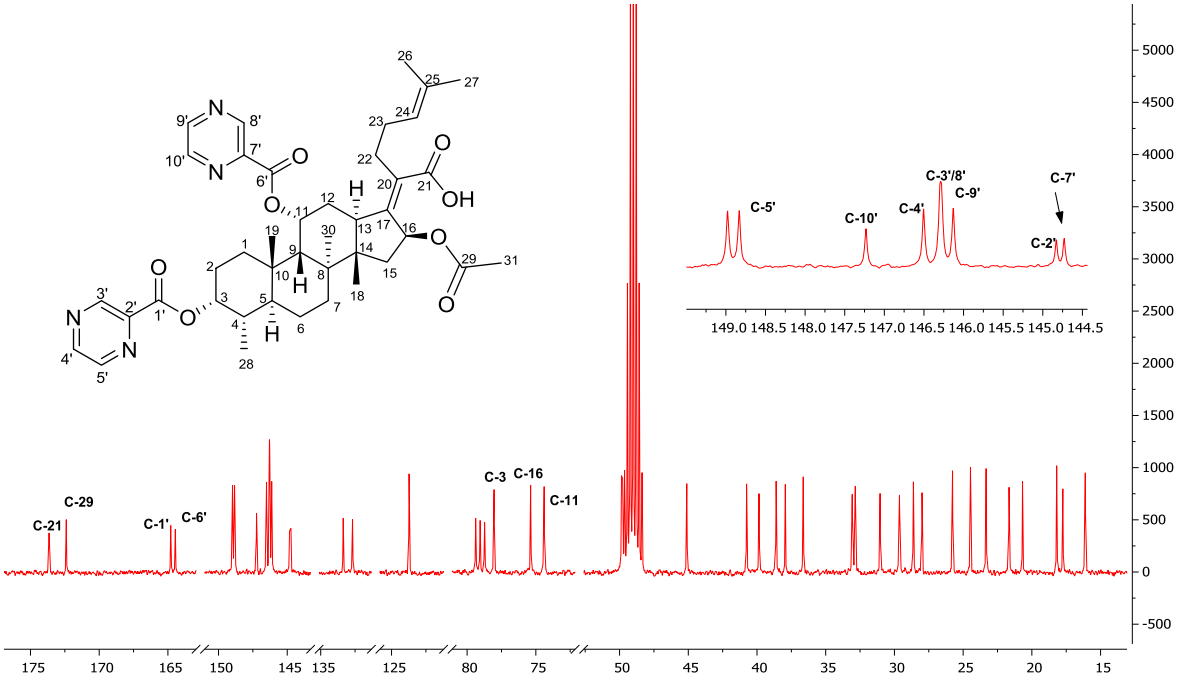

Figure 42: ^{13}C-NMR spectrum (CD_3OD, 100 MHz) of compound **3.22**

3.2.5 Synthesis of C-3 amine (SAR 3)

The synthetic route to intermediates **3.23** and **3.24** is similar to that used for intermediate **3.6** and **3.8** previously (Scheme 2) as reported by Kaur *et al.*[103] The synthesis of 3-ketofusidic acid (**3.25**) was accomplished via Jones oxidation as reported by Jursic *et al.*[111] The Jones reagent was used as the limiting reagent to avoid oxidation occurring at both C-3 and C-11 positions.

Target compound **3.26** was obtained via reductive amination of **3.25** in 1,2-dichloroethane (DCE) with acetic acid as a catalyst and sodium triacetoxyhydroborate ($Na(OAc)_3BH$) as a reducing agent (Scheme 5).[112,113] Compound **3.26** was obtained as a 1:1 diastereoisomeric mixture. The isolated yields of these SAR 3 derivatives ranged from 12 to 90% (Table 8). The proposed reaction mechanism for the Jones oxidation and reductive amination are shown in **Figures 43** and **44** respectively.

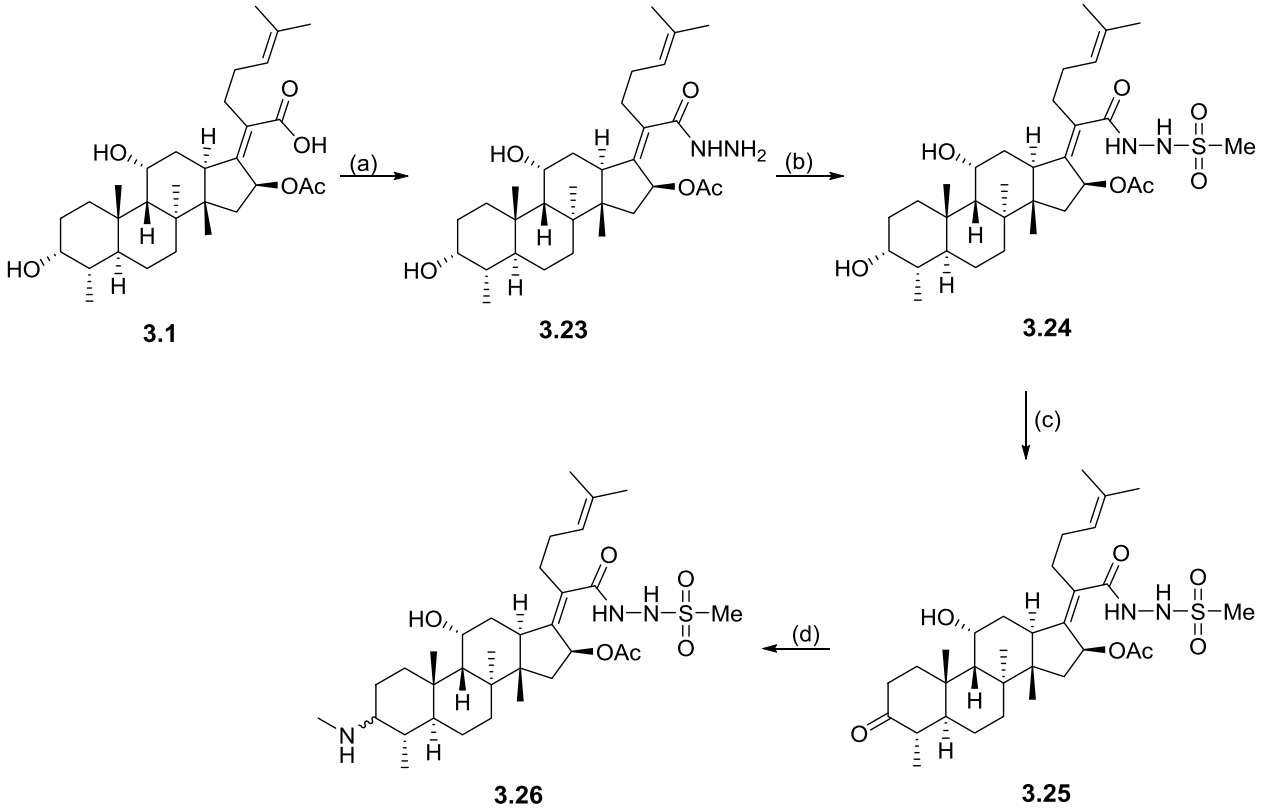

Scheme 5: General synthetic protocol towards compound **3.23** to **3.26** (SAR 3). *Reagents and conditions:* (a) (i) EDCI, HOBt, CH_3CN, 25 °C, 3 h; (ii) $NH_2NH_2.H_2O$, 25 °C, 24 h; (b) MsCl, pyridine, 25 °C, 3 h; (c) Jones Reagent, acetone, 0 °C, 40 min; (d) CH_3NH_2, $Na(OAc)_3BH$, AcOH, DCE, 60 °C, 48 h .

Table 8: Isolated yields and melting points of SAR 3 derivatives

Compound	Yield (%)	Mp (°C)
3.23	86	113 - 115
3.24	90	125 – 127
3.25	29	123 – 125
3.26	12	137 – 139

3.2.5.1 Mechanism of alcohol oxidation with chromic acid

The mechanism of Jones oxidation involves the formation of chromic acid in the first step followed by formation of a chromate ester, which proceeds through an E2 elimination to afford the desired ketone (Figure 43).[114,115]

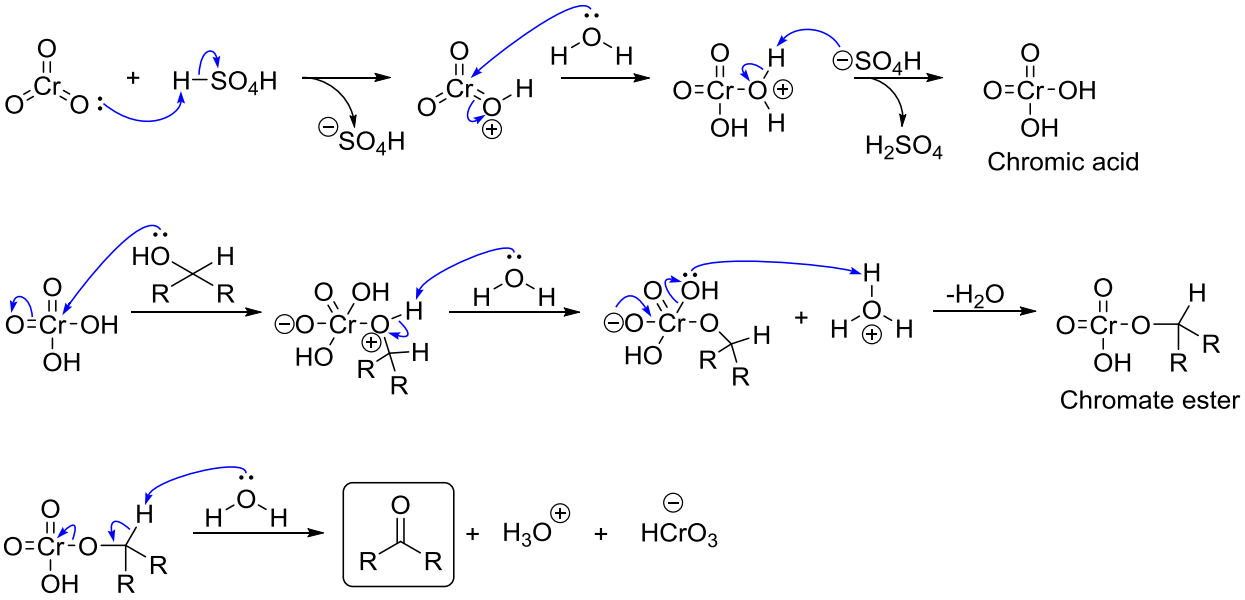

Figure 43: Proposed reaction mechanism for Jones oxidation.[114,115]

3.2.5.2 Mechanism of reductive amination

The first step of this reaction involves protonation and nucleophilic addition of the amine to the carbonyl carbon. This is followed by a proton transfer and elimination to produce an iminium ion. The iminium ion is then reduced by $Na(OAc)_3BH$ to afford the desired amine (Figure 44).[113,114,116]

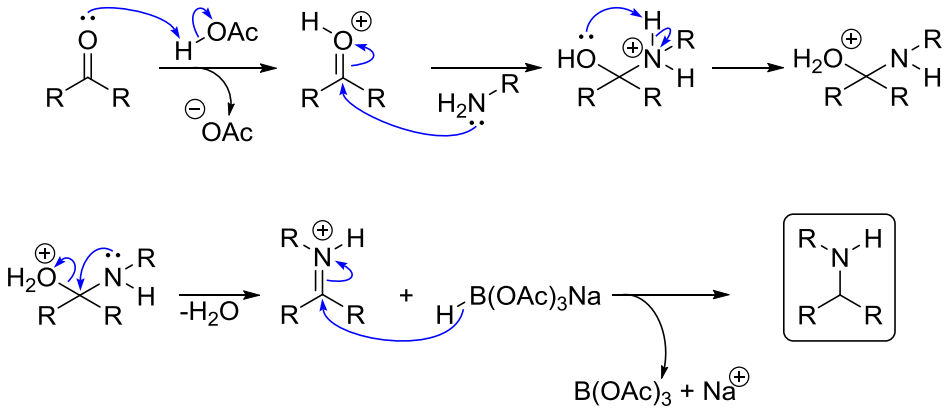

Figure 44: Proposed mechanism for reductive amination.[113,114,116]

3.2.5.3 Characterization of C-3 amine

3.2.5.3.1 Characterization of intermediate 3.23

The ^{1}H-NMR spectrum of **3.23** was obtained in CD_3OD at 400 MHz (Figure 45) and no significant change in proton chemical shifts is observed when compared to **3.1**, as was previously observed for **3.6**. Therefore, ^{13}C-NMR and MS were used for structural confirmation. Stacked ^{1}H-NMR spectra of compounds **3.1** and **3.24-26** are shown in appendix 6.

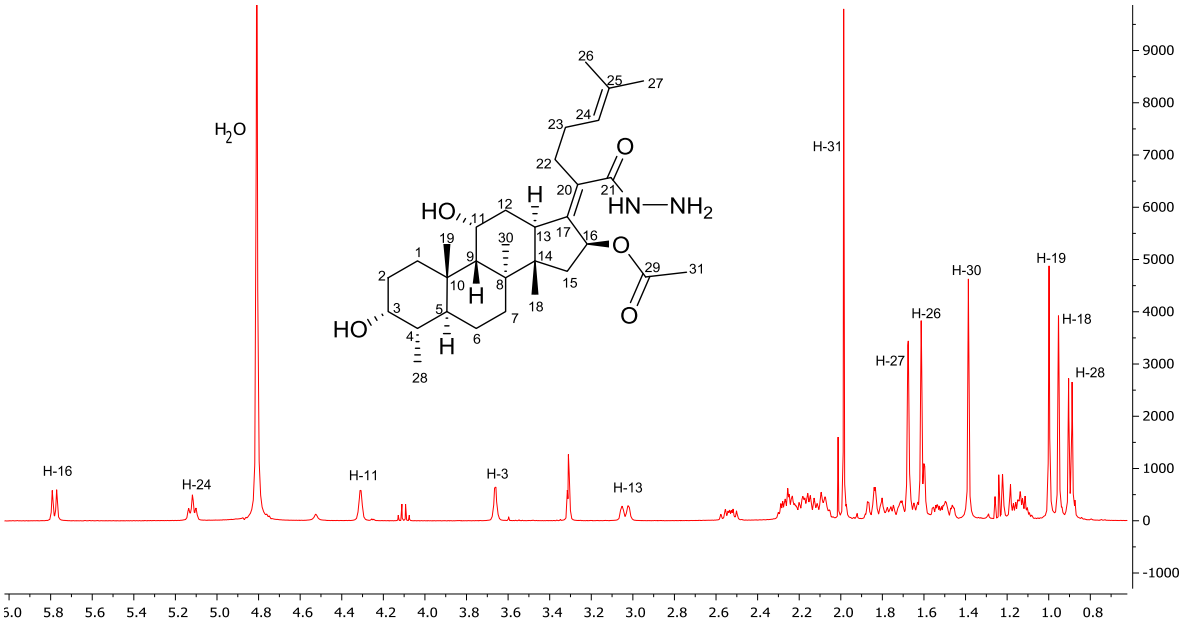

Figure 45: ^{1}H-NMR spectrum (CD_3OD, 400 MHz) of compound **3.23**

In the ^{13}C-NMR spectrum, an upfield shift of the C-21 signal from δ 174.1 ppm in **3.1** (in CD_3OD, spectrum not shown) to δ 173.1 ppm (in **3.23**) is observed (Figure 46). Furthermore, a MS peak of *m/z* 529.3, corresponding to $[M-H]^-$ is observed, as expected, which confirms the structure of **3.23**.

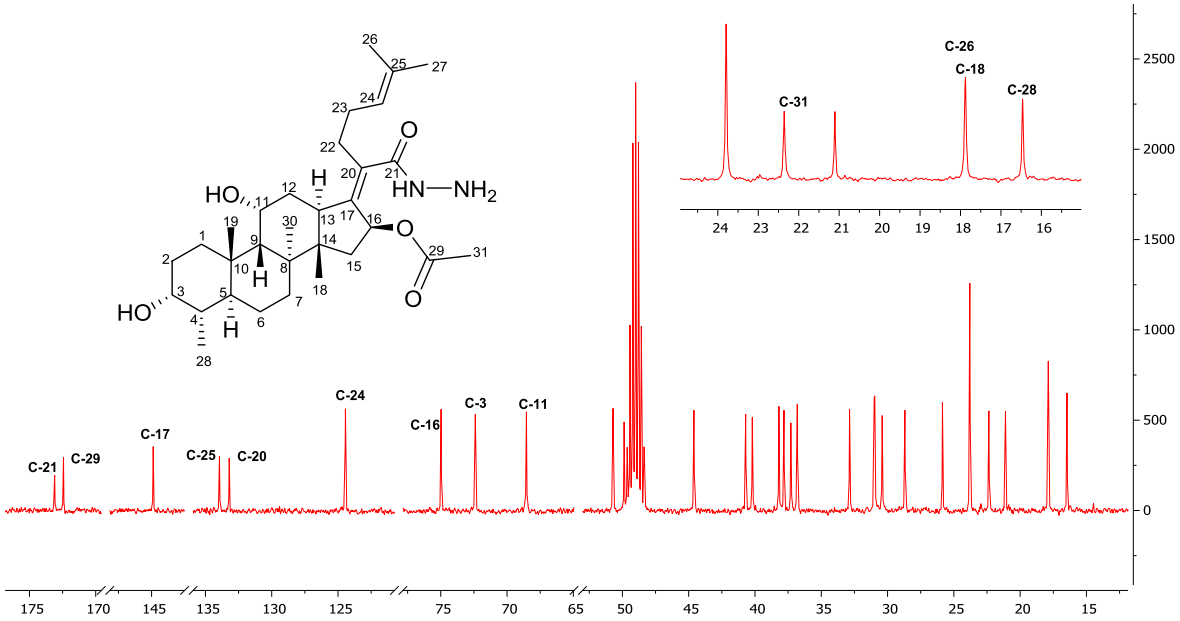

Figure 46: ^{13}C-NMR spectrum (CD_3OD, 100 MHz) of compound **3.23**

3.2.5.3.2 Characterization of intermediate 3.24

The ^{1}H-NMR spectrum of **3.24** was recorded in $CDCl_3$ at 400 MHz, with the characteristic features being the appearance of –CON*H* (δ 8.16 ppm, s) and –SO_2N*H* (δ 7.10 ppm, br s) signals in the aromatic region. In addition, a new singlet in the aliphatic region at δ 3.00 ppm corresponding to H-32, confirms the presence of a methyl group (Figure 47). The rest of the proton signals appear in similar regions as in **3.1**.

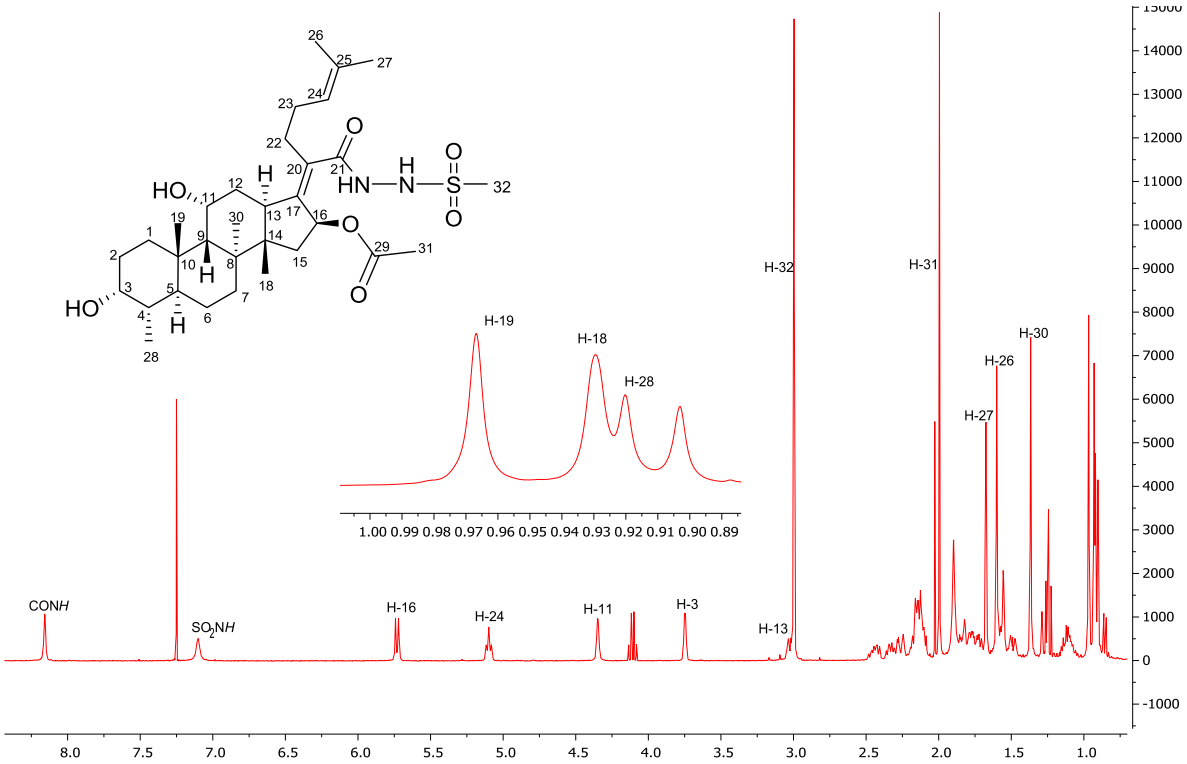

Figure 47: ^{1}H-NMR spectrum ($CDCl_3$, 400 MHz) of compound **3.24**

The ^{1}H-NMR spectrum is supported by the appearance of an additional carbon signal at δ 39.4 ppm, corresponding to C-32 (Figure 48). Furthermore, the MS spectrum displays a mass peak of *m/z* 549.3 corresponding to $[M\text{-}OAc]^{+}$, as expected. The remaining carbon signals remain in similar regions as in intermediate **3.23**.

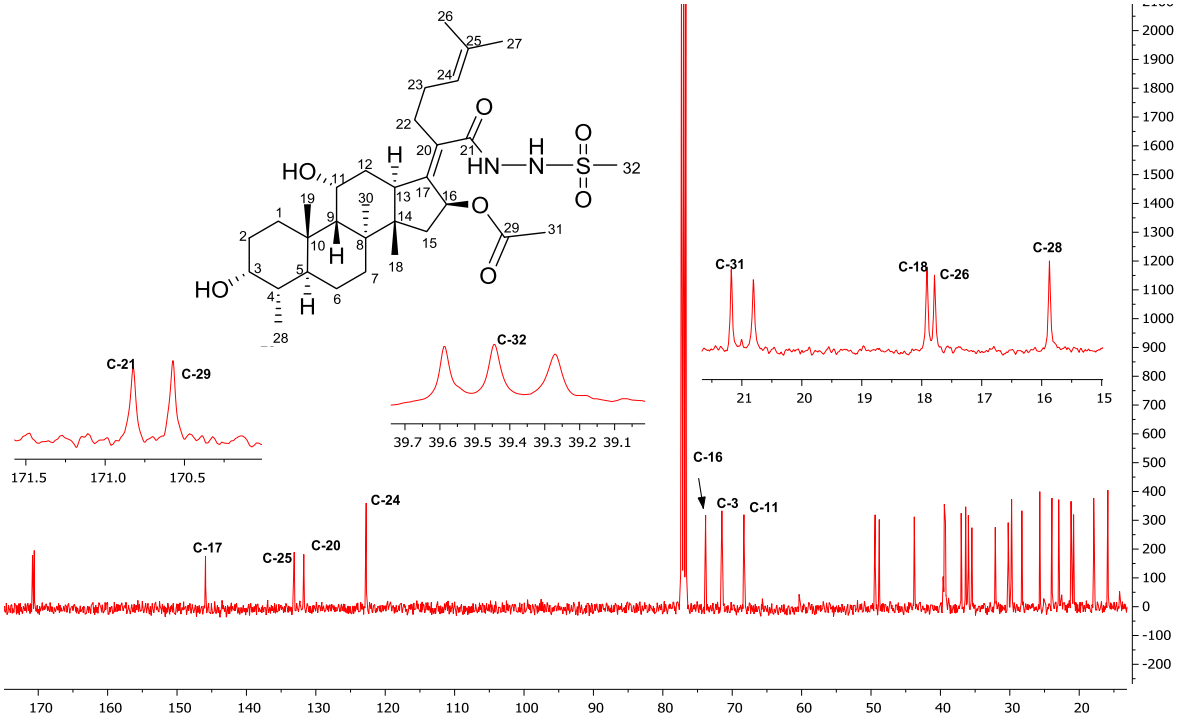

Figure 48: ^{13}C-NMR spectrum ($CDCl_3$, 100 MHz) of compound **3.24**

3.2.5.3.3 Characterization of intermediate 3.25

Intermediate **3.25** is a product of the Jones oxidation of **3.24** and the ^{1}H-NMR characteristic feature is the absence of the key H-3 signal (Figure 49) that was previously observed at δ 3.75 ppm in **3.24**. The other distinctive feature is the downfield shift of the H-28 signal from δ 0.91 ppm (in **3.24**) to δ 1.00 ppm in **3.25**. The rest of the signals remain in similar regions as compared to **3.24**.

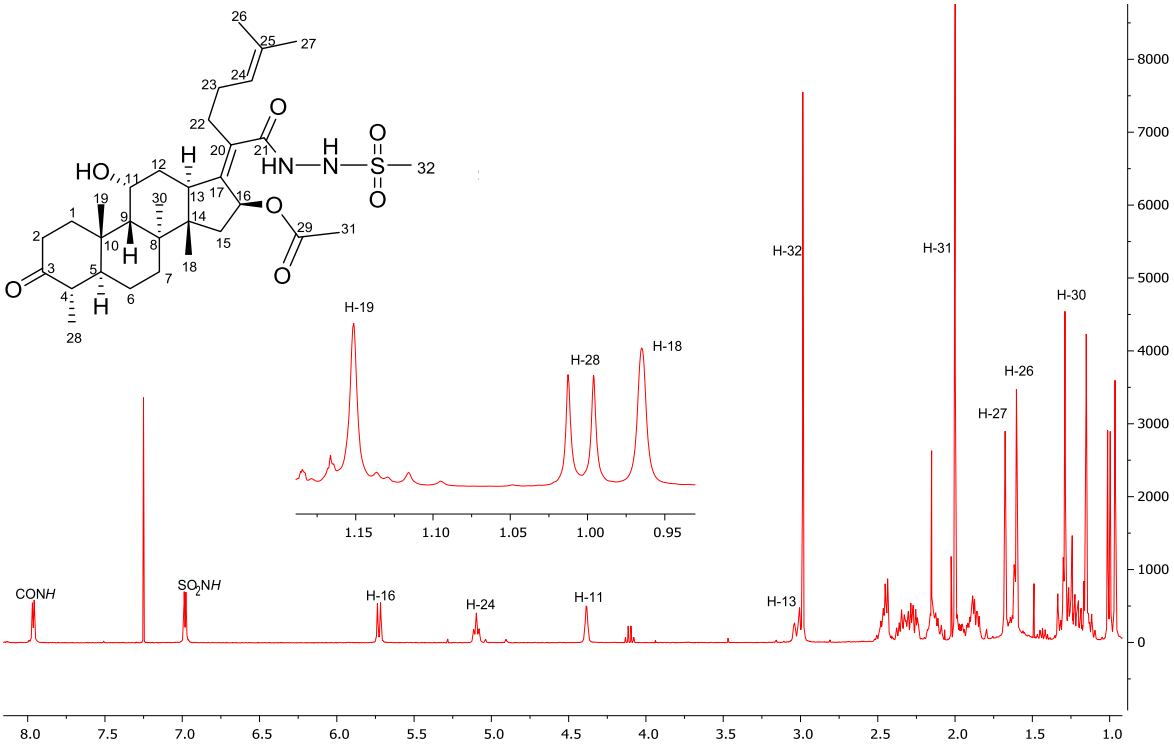

Figure 49: ^{1}H-NMR spectrum ($CDCl_3$, 400 MHz) of compound **3.25**

A carbonyl characteristic signal of a ketone at δ 213.5 ppm (C-3) in the ^{13}C-NMR spectrum and an upfield shift of the C-28 signal from δ 15.9 ppm (in **3.24**) to δ 12.3 ppm (in **3.25**) is evidence of the success of the Jones oxidation (Figure 50). Furthermore, a MS peak of *m/z* 605.3 for $[M-H]^-$ confirms the authenticity of intermediate **3.25**.

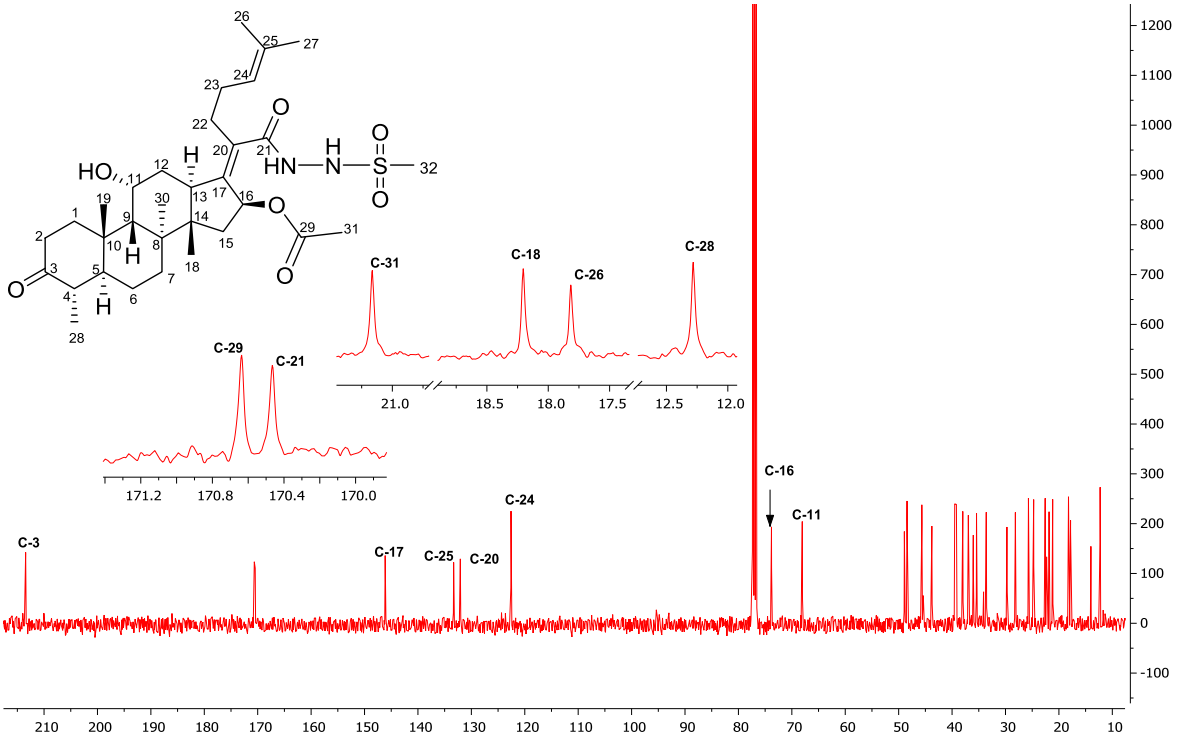

Figure 50: ^{13}C-NMR spectrum ($CDCl_3$, 100 MHz) of compound **3.25**

3.2.5.3.4 Characterization of target compound 3.26

The ^{1}H-NMR characteristic features are the appearance of the new H-3 signal resonating at δ 2.47 ppm and the H-1' singlet at δ 2.37 ppm (Figure 51).

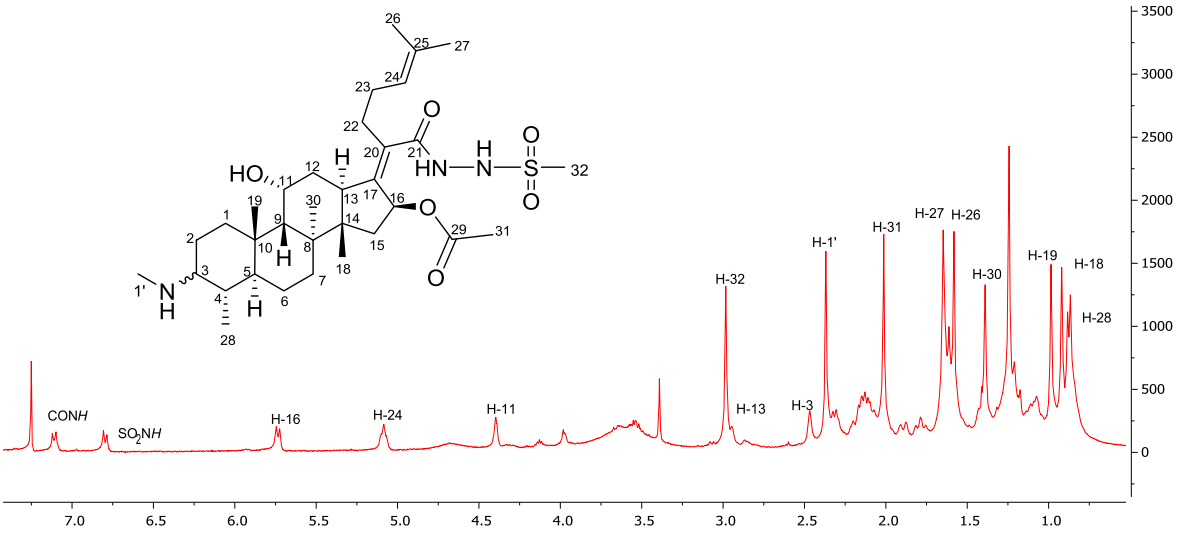

Figure 51: ^{1}H-NMR spectrum ($CDCl_3$, 400 MHz) of compound **3.26**.

The ^{13}C-NMR spectrum of **3.26** indicates the loss of a carbonyl carbon at δ 213.5 ppm in intermediate **3.25** and the appearance of a carbon signal at δ 61.5 ppm, corresponding to C-3. In addition, the carbon signal of C-1' at δ 35.0 ppm, confirms the success of the reductive amination reaction (Figure 52). A MS peak of *m/z* 620.3 for $[M-H]^-$ is observed as expected. The configuration at the C-3 chiral center was not determined as the compound was obtained as a mixture of diastereoisomers as indicated earlier.

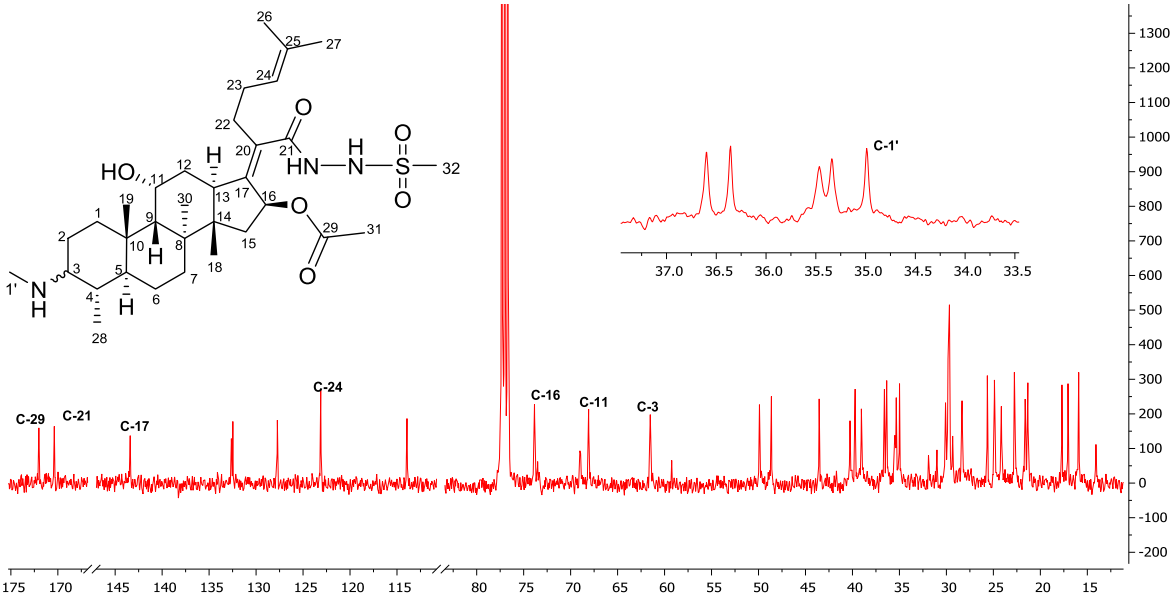

Figure 52: ^{13}C-NMR spectrum ($CDCl_3$, 100 MHz) of compound **3.26**

3.3 Biological evaluation of target compounds

All the synthesized target compounds and their intermediates were evaluated for their *in vitro* antimycobacterial activity against the human virulent H37Rv strain of *Mtb* using the microplate Alamar Blue assay (MABA) at the Institute of Infectious Disease and Molecular Medicine (IDM), University of Cape Town, South Africa. The reported MIC_{99} (minimum concentration that will inhibit 99% of the bacterial population) values at day 14, were performed in glycerol-alanine-salt with Tween-80 and iron (GAST/Fe) as well as in media comprising of bovine albumin, dextrose and catalase (7H9 GLU/ADC) with rifampicin as a control.

3.4.3 *In vitro* antimycobacterial activity

The *in vitro* antimycobacterial activities for these compounds are summarized in **Tables 9** and **10**. Upon observation of trends within different groups of compounds, neither of the four C-21 carboxylic acid bioisosteric analogues (**3.2**, **3.3**, **3.23** and **3.24**) exhibited comparable potency to fusidic acid (Table 9). This suggests that the carboxylic acid is essential for antimycobacterial activity, which is consistent with previous studies in our research group and the report by Duvold *et al*.[71] It is interesting to note that although derivatization of the carboxylic acid resulted in loss of activity, compounds **3.2**, **3.23** and **3.24** (MIC_{99} of 31.3 µM) displayed superior activity compared to analogue **3.3** (MIC_{99} of 125 µM). The *in vitro* antimycobacterial results indicate that almost all the tested compounds are inactive in the 7H9 GLU/ADC media, except compounds **3.4** (MIC_{99} of 7.81 µM) and **3.5** (MIC_{99} of 3.91 µM, Table 9). Due to the general lack of *in vitro* activity of the various derivatives in the 7H9 GLU/ADC media, the following SAR discussion will be based on data generated in the GAST/Fe media.

The two C-3 aliphatic esters **3.4** and **3.5** were previously synthesized in our research group[85] and were found to offer good activity, with both having MIC_{99} values of 2.5 µM in the same assays used at that time. Since good activity was observed with these two analogues, they were chosen as templates for further derivatization by incorporating carboxylic acid bioisosteres **3.6**-**3.9**. For this set of derivatives **3.4**-**3.9**, modification at both the C-3 and C-21 positions appear to be detrimental to activity. The exception was the long chain aliphatic ester **3.5**, which was found to be equipotent to fusidic acid with a MIC_{99} value of 0.49 µM. Interestingly, incorporation of a mesyl group resulted in a 2-fold increase in antimycobacterial activity for **3.8** (MIC_{99} of 7.81 µM) compared to the **3.6** (MIC_{99} of 15.6 µM). The rest of the tested compounds were deemed to have moderate to weak activity, with MIC_{99} values ranging between 15.6-62.5 µM.

The analogue aminated at C-3, which has a carboxylic acid bioisostere incorporated at the R_1 position (**3.26**), and its precursor intermediates (**3.23-3.25**) exhibited loss of antimycobacterial activity with moderate MIC_{99} values ranging between 31.3 to 62.5 µM (Table 9). In view of the good antimycobacterial activity of the 3-ketofusidic acid (MIC_{99} of 1.25 µM, H37Rv),[85] the activity displayed by compound **3.25** (MIC_{99} of 62.5 µM) in this study represents a significant loss in activity. This further supports the earlier observation that the carboxylic acid group at C-21 is essential for activity.[71,85]

Table 9: *In vitro* antimycobacterial activity at C-3 alkyl esters and C-21 bioisosteres of fusidic acid at day 14

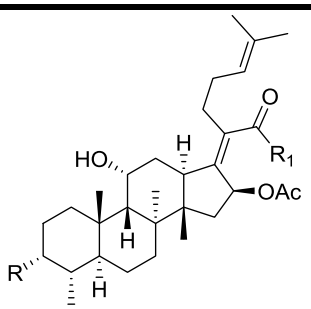

Compound	R	R_1	MIC_{99} (µM)	
			GAST/Fe	7H9 GLU/ADC
Fusidic acid	OH	OH	0.49	3.91
3.2	OH	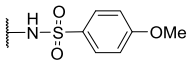	31.3	> 125
3.3	OH	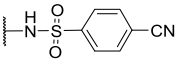	125	> 125
3.4	OCOEt	OH	3.91	7.81
3.5	OCOBu	OH	0.49	3.91
3.6	OCOEt	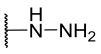	15.6	125
3.7	OCOBu	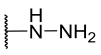	62.5	> 125
3.8	OCOEt	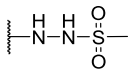	7.81	62.5
3.9	OCOBu	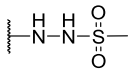	62.5	62.5
3.23	OH	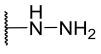	31.3	> 125
3.24	OH	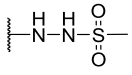	31.3	> 125
3.25	O	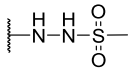	62.5	> 125
3.26		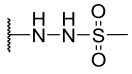	31.3	> 125
Rifampicin	-	-	0.01	0.01

On the other hand, the C-3 aromatic esters **3.10**-**3.22** were generally inactive (Table 10). However, introduction of substituents at the *para* position of the phenyl ring with groups such as methyl sulfonyl (**3.17**, MIC_{99} of 31.3 µM), methoxy (**3.18**, MIC_{99} of 62.5 µM) and methyl (**3.19**, MIC_{99} of 31.3 µM) groups led to a significant (2-4 fold) increase in antimycobacterial activity compared to the unsubstituted compound **3.10** (MIC_{99} of >125

µM). The rest of the other *para* substituted phenyl derivatives **3.11-3.16** exhibited poor activity against *Mtb* H_{37}Rv with MIC values of >125 µM.

Heterocyclic-containing esters **3.20** and **3.21** (Table 10) showed superior activity compared to aromatic esters with pyrazinoic acid-based ester **3.21** showing activity in both media. It is hypothesized that this compound and its bis derivative **3.22** could release both fusidic acid and pyrazinoic acid upon hydrolysis by mycobacterial esterases. This would be a potential way of delivering pyrazinoic acid (POA), the active form of pyrazinamide, which requires the pyrazinamidase enzyme to release POA.

Table 10: *In vitro* antimycobacterial activity of C-3 aromatic ester derivatives of fusidic acid at day 14

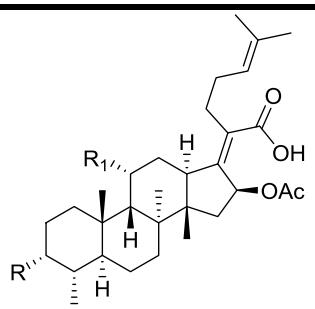

Compound	R	R_1	MIC_{99} (µM)	
			GAST/Fe	7H9 GLU/ADC
Fusidic acid			0.49	3.91
3.10	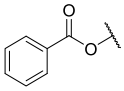		> 125	> 125
3.11	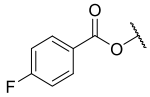		> 125	> 125
3.12	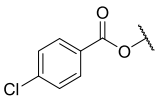		> 125	> 125
3.13	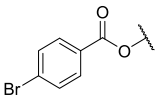		> 125	> 125
3.14	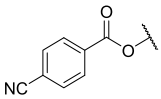		> 125	> 125
3.15	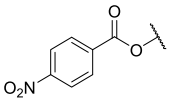		> 125	> 125
3.16	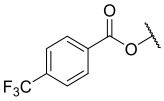		> 125	125
3.17	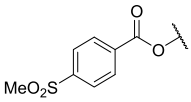		31.3	125
3.18	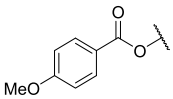		62.5	> 125
3.19	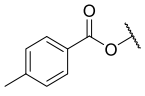		31.3	> 125
3.20	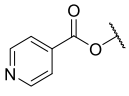		31.3	> 125
3.21	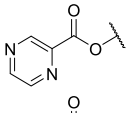		7.81	31.3
3.22	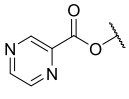	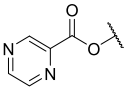	> 125	125
Rifampicin	-	-	0.01	0.01

3.5 Conclusion

Based on prior SAR exploration executed in our research group, this dissertation has broadened the SAR study around fusidic acid at the C-3, C-11 and C-21 positions. To this end, 25 fusidic acid derivatives were successfully synthesized, characterized and evaluated for their *in vitro* antimycobacterial activity. None of these derivatives was found to possess superior *in vitro* antimycobacterial activity compared to fusidic acid although analogues **3.4**, **3.5**, **3.8** and **3.21** were found to display good activity with MIC_{99} values ranging between 0.49-7.81 µM in the GAST/Fe media.

CHAPTER 4

Summary, conclusion and future work

4.1 Summary and conclusion

The broad aim of this project was to contribute to the repositioning of the antibacterial drug fusidic acid as a potential new antimycobacterial agent through a medicinal chemistry approach. The study was undertaken by executing various structural modifications on the fusidic acid scaffold at the C-3, C-11 and C-21 positions to broaden the SAR study. Standard organic synthetic routes such as amide coupling, esterification, Jones oxidation and reductive amination reactions were employed. Compounds were characterized by ^{1}H-NMR, ^{13}C-NMR, melting point and LC-MS. The synthesized target compounds and their respective intermediates were evaluated for their *in vitro* antimycobacterial activity against the H37Rv strain of *Mtb*.

All the synthesized analogues were obtained in poor to good yields (3 – 90%), with the poor yields of some of the analogues possibly due to the difficulty in their chromatographic purification and competing side reactions.

The antimycobacterial screening of fusidic acid analogues synthesized revealed a drop in activity with most analogues exhibiting MIC_{99} values of > 20 µM, except for compounds **3.4-3.6**, **3.8** and **3.21** (Figure 53). The new compounds **3.8** and **3.21** were the most potent compounds from this study with MIC_{99} values of 7.81 µM. The antimycobacterial activity data obtained suggests that the C-3 and C-11 hydroxyls, and C-21 carboxylic acid are essential for activity.

Lastly, the lack of *in vitro* activity displayed by these analogues, except **3.4** (MIC_{99} of 7.81 µM) and **3.5** (MIC_{99} of 3.91 µM), in the 7H9 GLU/ADC media suggests media-dependent activity.

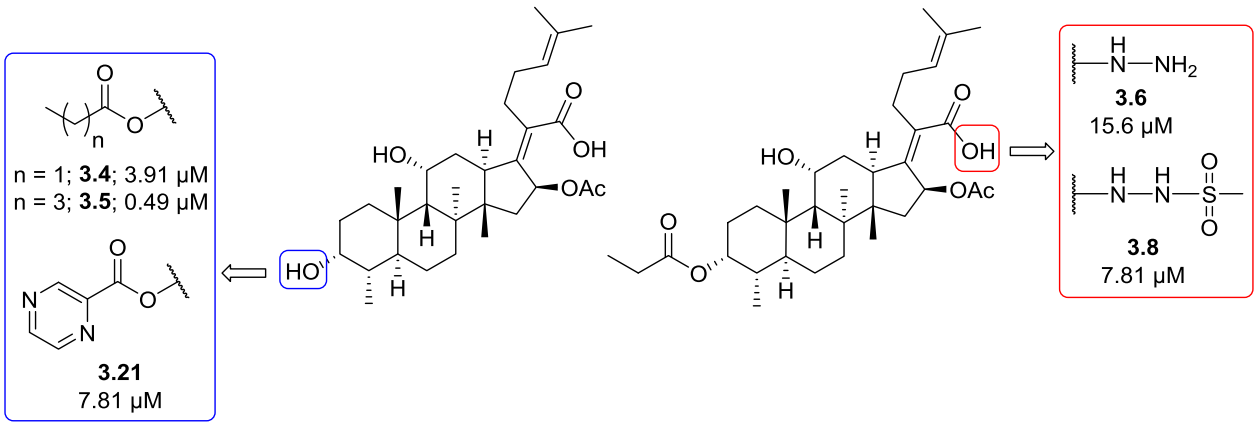

Figure 53: Summary of fusidic acid derivatives with MIC_{99} < 20 µM in GAST/Fe media

4.2 Future prospects

The *in vitro* antimycobacterial data shown by compounds **3.4-3.6**, **3.8** and **3.21** are encouraging. These compounds can be further explored for their cytotoxicity, microsomal metabolic stability and *in vivo* efficacy. To eradicate *Mtb* requires drug regimens that can penetrate multiple layers of complex pulmonary lesions; therefore, both intracellular and extracellular *in vitro* inhibition assays should be in the forefront of drug discovery and development for TB.

The lack of *in vitro* activity displayed by **3.20-3.22** is not entirely clear but may be attributed to factors such as (i) poor penetration inside the bacteria; (ii) lack of *Mtb*-mediated hydrolysis of the prodrugs to their respective active metabolites under the assay conditions or (iii) high rate of efflux mechanisms. Therefore, it would be interesting to study the stability of these compounds when incubated with mycobacteria lysate in order to ascertain whether or not they are hydrolyzed.

In addition, drugs like rifampicin and pyrazinamide have been shown to penetrate the cell well into necrotic caseum, the site of persisting tolerant mycobacteria that are responsible for drug resistance.[117] As a result, **3.21** and **3.22** could potentially be evaluated as alternative prodrugs of pyrazinoic acid to circumvent PZA-resistant isolates of *Mtb*.

Moreover, further SAR exploration at the C-3 position of fusidic acid should be done through the introduction of disubstitution in the phenyl ring or by varying the positions of substituents from *para*- to *meta*- or *ortho*- and by substituting the phenyl ring with various heterocyclic moieties (Figure 54).

Based on the activity of C-3 amine **3.26**, a diverse range of acyclic or heterocyclic amines should be investigated.

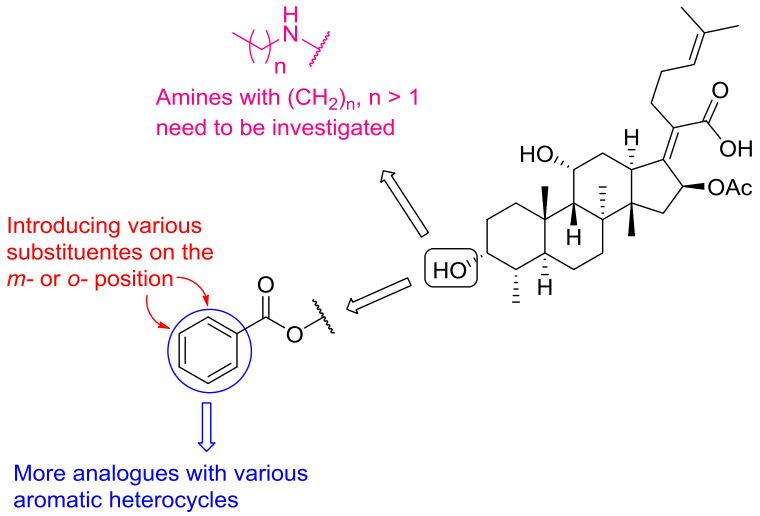

Figure 54: Future recommendation to obtain new derivatives of fusidic acid.

Lastly, fusidic acid and its derivatives have been previously shown to possess antiplasmodial activity against chloroquine-sensitive NF54 and multidrug-resistant K1 strains of the human malaria parasite *Plasmodium falciparum*. Therefore, this set of compounds should also be evaluated for antiplasmodial activity.

CHAPTER 5

Experimental

5.1 Reagents, Solvents and Instruments

Fusidic acid was purchased from AvaChem Scientific while all other reagents were purchased from Sigma-Aldrich, Merck or Combi-Blocks. These reagents were of analytical reagent (AR) grade and were used without further purification. Dry solvents were obtained from a SP-1 stand-alone solvent purification system, from LC Technology Solution Inc. The solvents used for HPLC and LC-MS were bought from Sigma-Aldrich (ammonium acetate as an additive), Merck (glacial acetic acid) and Microsep (acetonitrile and methanol) and were of HPLC grade. The general solvents used for extraction and purification purposes were obtained from Kimix Chemicals and were of AR grade.

Reactions were monitored using aluminum silica pre-coated thin layer chromatography (TLC) plates (60 F_{254} from Merck or Al foils 60 Å medium pore diameter from Sigma-Aldrich) and were visualized by ultraviolent light (UV) at 245 or 365 nm and by using *p*-anisaldehyde stain. The stain solution was prepared by mixing solution A (5% *p*-anisaldehyde in EtOH) to B (5% H_2SO_4 and 20% AcOH in MeOH) in a 1:3 ratio.

Purification of the compounds was done by gravity column chromatography packed with silica gel (60 Å, 70-230 mesh from Sigma-Aldrich) or by preparative TLC (Silica gel GF254, 2000 µm on glass from Analtech). Melting points were determined using the Reichert-Jung Thermovar hot-stage microscope without correction.

Reported compounds were characterized using MS, ^{1}H NMR and ^{13}C NMR. ^{1}H NMR spectra were recorded on a Bruker UltraShield-Plus (400 MHz) spectrometer, with ^{13}C NMR spectrum being recorded on the same instrument at 100 MHz, and referenced to the residual proton or carbon signals of the deuterated solvent with tetramethylsilane (TMS) as an internal

standard. NMR samples were dissolved in either deuterated chloroform ($CDCl_3$), deuterated dimethyl sulfoxide (DMSO-d_6) or deuterated methanol (CD_3OD). Chemical shifts (δ) are reported in part per million (ppm) to two decimal place for ^{1}H NMR and one decimal places for ^{13}C NMR relative to TMS at 0 ppm. Coupling constants (*J*) are reported in Hertz (Hz) to one decimal place. ^{1}H NMR splitting patterns are abbreviated as follows: s (singlet), broad singlet (br s), d (doublet), dd (doublet of doublets), t (triplet), q (quartet) and m (multiplet). The ^{13}C NMR spectra were measured with complete proton decoupling.

Liquid chromatography-mass spectrometric (LC-MS) data of all the compounds were determined on an Agilent HPLC system equipped with the following components: Agilent® 1260 Infinity Binary Pump, Agilent® 1260 Infinity Diode Array Detector (DAD), Agilent® 1290 Infinity Column Compartment, Agilent® 1260 Infinity Standard Auto sampler and Agilent® 6120 Quadrupole LC/MS. The column was a Kinetex Core C18 reverse phase column (2.6 µm particle, 3x50 mm and 100 Å). The column temperature was maintained at 40.00 °C, with an injection volume of 2.0 µL. The mobile phase was made up of 10 mM ammonium acetate in water (A) and 10 mM ammonium acetate in methanol (B). The gradient mode was set to increase gradually to 100% A over 3 min and held constant for 1.5 min. The column was then re-equilibrated to initial mobile phase (80% B: 20% A) over 2.5 min. A flow rate of 0.900 mL/min and high pressure limit of 600.00 bars were maintained.

The purity of the target compounds was determined using the diode array detector (DAD) with absorption wavelength range of 210-640 nm. MS spectra were obtained both by electrospray (ES, spray chamber conditions: gas temperature 310°C, vaporizer 210°C) and atmospheric pressure chemical ionization (APCI).

5.2 Synthesis and characterization

5.2.1 Characterization of fusidic acid

(*Z*)-2-((3*R*,4*S*,5*S*,8*S*,9*S*,10*S*,11*R*,13*R*,14*S*,16*S*)-16-acetoxy-3,11-dihydroxy-4,8,10,14-tetramethylhexadecahydro-17*H*-cyclopenta[*a*]phenanthren-17-ylidene)-6-methylhept-5-enoic acid, [3.1]

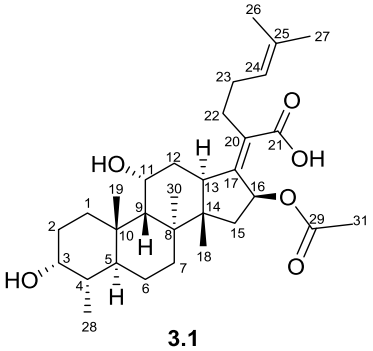

3.1
$C_{31}H_{48}O_6$
Exact Mass: 516.35
MW: 516.72

White solid: m.p. 187 - 189 °C; R_f 0.31 (MeOH:DCM, 0.6:9.4); ^{1}H NMR (400 MHz, $CDCl_3$) δ_H 5.87 (d, *J* = 8.4 Hz, 1H, H^{16}), 5.12 – 5.05 (m, 1H, H^{24}), 4.36 – 4.31 (m, 1H, H^{11}), 3.77 – 3.72 (m, 1H, H^{3}), 3.09 – 3.00 (m, 1H, H^{13}), 2.51 – 2.38 (m, 2H, H^{22}), 2.34 – 2.28 (m, 1H, H^{12a}), 2.21 – 1.99 (m, 5H, $H^{1a,5,15a,23}$), 1.95 (s, 3H, H^{31}), 1.90 – 1.78 (m, 2H, $H^{2a,12b}$), 1.77 – 1.69 (m, 2H, $H^{2b,7a}$), 1.66 (s, 3H, H^{27}), 1.58 (s, 3H, H^{26}), 1.57 – 1.45 (m, 4H, $H^{1b,4,6a,9}$), 1.36 (s, 3H, H^{30}), 1.29 (d, *J* = 14.1 Hz, 1H, H^{15b}), 1.17 – 1.02 (m, 2H, $H^{6b,7b}$), 0.96 (s, 3H, H^{19}), 0.91 (d, *J* = 5.9 Hz, 3H, H^{28}), 0.90 (s, 3H, H^{18}); ^{13}C NMR (100 MHz, $CDCl_3$) δ_C 174.0, 170.6, 150.8, 132.6, 129.6, 123.0, 74.4, 71.5, 68.3, 49.3, 48.7, 44.3, 39.5, 39.0, 37.0, 36.3, 36.1, 35.6, 32.3, 30.2, 29.9, 28.8, 28.4, 25.7, 24.1, 22.8, 20.8, 20.6, 17.9, 17.8, 15.9; purity (LC-MS) 99%, t_R = 5.25 min, MS *m/z* 457.3 $[M\text{-}OAc]^+$; *m/z* 515.3 $[M\text{-}H]^-$.

5.2.2 General procedure for the synthesis and characterization of C-21 bioisosters

Fusidic acid (1.0 eq.) was added to a solution of the respective sulfonamide (4.0 eq. for compound **3.2** and 1.2 eq. for compound **3.3**) in dichloromethane (DCM) followed by a

subsequent addition of EDCI (1.4 eq.) and DMAP (0.4 eq.). The resulting mixture was stirred at 25 °C for 3 to 7 days. After completion of reaction (TLC), the reaction mixture was diluted with DCM and washed with water. The organic layer was dried over anhydrous magnesium sulfate ($MgSO_4$), filtered and concentrated *in vacuo*. The crude product was then purified by column chromatography on silica gel using either EtOAc/DCM or MeOH/DCM as an eluent, which after washing with pentane and recrystallization in pentane/DCM afforded the desired target compound.

(3*R*,4*S*,5*S*,8*S*,9*S*,10*S*,11*R*,13*R*,14*S*,16*S*,*Z*)-17-(1-((4-cyanophenyl)sulfonamido)-6-methyl-1-oxohept-5-en-2-ylidene)-3,11-dihydroxy-4,8,10,14-tetramethylhexadecahydro-1*H*-cyclopenta[*a*]phenanthren-16-yl acetate, [3.2]

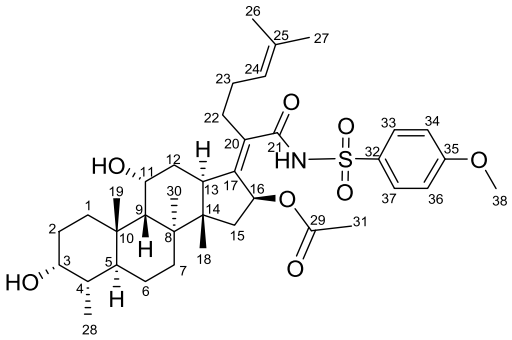

3.2
$C_{38}H_{55}NO_8S$
Exact Mass: 685.36
MW: 685.92

White solid (15 mg, 5% yield); m.p. 198 - 200 °C; R_f 0.39 (MeOH:DCM, 0.7:9.3); ^{1}H NMR (400 MHz, DMSO-d_6) δ_H 11.75 (s, 1H, H^{NH}), 7.84 (d, J = 9.0 Hz, 2H, $H^{33/37}$), 7.11 (d, J = 9.0 Hz, 2H, $H^{34/36}$), 5.58 (d, J = 8.6 Hz, 1H, H^{16}), 4.95 – 4.89 (m, 1H, H^{24}), 4.19 – 4.10 (m, 1H, H^{11}), 3.83 (s, 3H, H^{38}), 3.56 – 3.46 (m, 1H, H^{3}), 2.92 – 2.83 (m, 1H, H^{13}), 2.40 – 2.20 (m, 3H, $H^{12a,22}$), 2.15 – 1.90 (m, 5H, $H^{1a,5,15a,23}$), 1.78 (s, 3H, H^{31}), 1.75 – 1.58 (m, 4H, $H^{2,7a,12b}$), 1.56 (s, 3H, H^{27}), 1.52 – 1.33 (m, 4H, $H^{1b,4,6a,9}$), 1.31 (s, 3H, H^{26}), 1.27 (s, 3H, H^{30}), 1.10 (d, J = 13.9 Hz, 1H, H^{15b}), 1.07 – 0.93 (m, 2H, $H^{6b,7b}$), 0.88 (s, 3H, H^{19}), 0.80 (s, 3H, H^{18}), 0.79 (d, J = 7.2 Hz, 3H, H^{28}); ^{13}C NMR (100 MHz, DMSO-d_6) δ_C 169.7, 168.7, 163.0, 144.6, 131.4,

131.1, 130.9 (2C), 129.9, 122.9, 114.0 (2C), 73.1, 69.2, 65.7, 55.7, 48.6, 48.0, 42.9, 38.8, 38.7, 36.3 (2C), 35.8, 35.1, 31.7, 30.2, 29.4, 28.7, 26.7, 25.2, 23.3, 22.8, 20.7, 20.4, 17.4, 17.2, 16.2; purity (LC-MS) 99%, t_R = 5.19 min, MS *m/z* 626.2 $[M\text{-}OAc]^+$.

(3*R*,4*S*,5*S*,8*S*,9*S*,10*S*,11*R*,13*R*,14*S*,16*S*,*Z*)-3,11-dihydroxy-17-(1-((4-methoxyphenyl) sulfonamido)-6-methyl-1-oxohept-5-en-2-ylidene)-4,8,10,14-tetramethylhexadecahydro-1*H*-cyclopenta[*a*]phenanthren-16-yl acetate, [3.3]

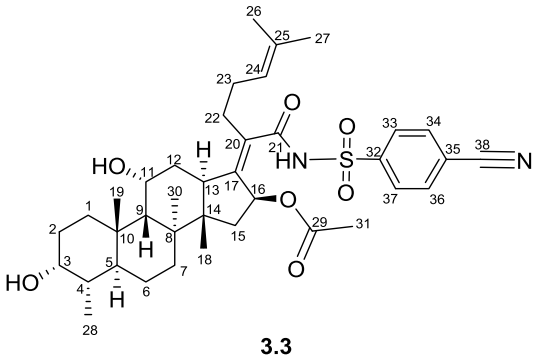

3.3
$C_{38}H_{52}N_2O_7S$
Exact Mass: 680.35
Molecular Weight: 680.90

White solid (20 mg, 3% yield); m.p. 219 – 221 °C; R_f 0.24 (EtOAc:Hex, 8:2); ^{1}H NMR (400 MHz, DMSO-d_6) δ_H 12.24 (s, 1H, H^{NH}), 8.12 (d, *J* = 8.5 Hz, 2H, $H^{33/37}$), 8.06 (d, *J* = 8.5 Hz, 2H, $H^{34/36}$), 5.59 (d, *J* = 8.4 Hz, 1H, H^{16}), 4.98 – 4.85 (m, 1H, H^{24}), 4.18 – 4.02 (m, 1H, H^{11}), 3.55 – 3.46 (m, 1H, H^3), 2.93 – 2.82 (m, 1H, H^{13}), 2.42 – 2.19 (m, 3H, $H^{12a,22}$), 2.19 – 1.89 (m, 5H, $H^{1a,5,15a,23}$), 1.80 (s, 3H, H^{31}), 1.76 – 1.57 (m, 4H, $H^{2,7a,12b}$), 1.55 (s, 3H^{27}), 1.51 – 1.31 (m, 4H, $H^{1b,4,6a,9}$), 1.29 (s, 3H, H^{26}), 1.27 (s, 3H, H^{30}), 1.11 (d, *J* = 14.0 Hz, 1H, H^{15b}), 1.07 – 0.94 (m, 2H, $H^{6b,7b}$), 0.87 (s, 3H, H^{19}), 0.80 (s, 3H, H^{18}), 0.78 (d, *J* = 7.1 Hz, 3H, H^{28}); ^{13}C NMR (100 MHz, DMSO-d_6) δ_C 169.7 (2C), 144.0, 133.1, 132.2 (2C), 131.6, 128.3 (2C), 127.0, 122.8, 117.5, 117.4, 73.1, 69.2, 65.7, 48.6, 48.0, 43.1, 39.5, 38.7, 36.3 (2C), 35.8, 35.1, 31.7, 30.2, 29.4, 28.6, 26.8, 25.2, 23.4, 22.8, 20.7, 20.5, 17.4, 17.2, 16.2; purity (LC-MS) 95%, t_R = 5.04 min, MS *m/z* 621.2 $[M\text{-}OAc]^+$.

5.2.3 Procedures for the synthesis and characterization of C-3 aliphatic esters

5.2.3.1 Intermediates 3.4 and 3.5

(*Z*)-2-((3*R*,4*S*,5*S*,8*S*,9*S*,10*S*,11*R*,13*R*,14*S*,16*S*)-16-acetoxy-11-hydroxy-4,8,10,14-tetramethyl-3-(propionyloxy)hexadecahydro-17*H*-cyclopenta[*a*]phenanthren-17-ylidene)-6-methylhept-5-enoic acid, [3.4]

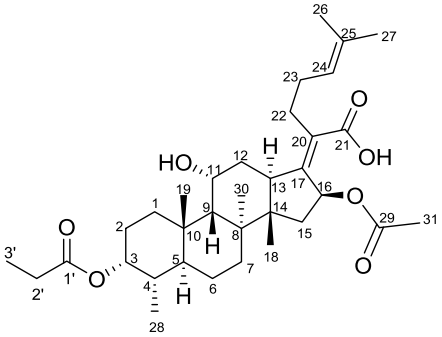

3.4
$C_{34}H_{52}O_7$
Exact Mass: 572.37
MW: 572.78

To a mixture of fusidic acid (3.78 g, 7.32 mmol) and propanoic acid (0.60 mL, 8.05 mmol, d = 0.993 g/mL) in pyridine (4.00 mL), T_3P solution (4.27 ml, 50% w/v in DMF, density = 1.09 g/mL, 14.63 mmol) was added and the resulting reaction mixture was stirred in an ice bath for 3 hrs. and at 25 °C for 21 hrs. After completion of the reaction (TLC), the reaction mixture was diluted with EtOAc (30 mL), washed with 0.5 M aq. HCl (3×30 mL) and water (3×30 mL). The organic layer was dried over anhydrous $MgSO_4$, filtered and concentrated *in vacuo*. The crude product was then purified by column chromatography on silica gel using 50% EtOAc/DCM as eluent, which after washing with pentane afforded white solid (1.32 g, 32% yield); m.p. 176 – 178 °C; R_f 0.42 (EtOAc:DCM, 3:7); ^{1}H NMR (400 MHz, $CDCl_3$) δ_H 5.89 (d, *J* = 8.4 Hz, 1H, H^{16}), 5.14 – 5.04 (m, 1H, H^{24}), 4.97 – 4.90 (m, 1H, H^3), 4.37 – 4.29 (m, 1H, H^{11}), 3.09 – 2.99 (m, 1H, H^{13}), 2.52 – 2.41 (m, 2H, H^{22}), 2.35 (q, *J* = 7.6 Hz, 2H, $H^{2'}$), 2.33 – 2.27 (m, 1H, H^{12a}), 2.22 – 2.00 (m, 5H, $H^{1a,5,15a,23}$), 1.96 (s, 3H, H^{31}), 1.91 – 1.74 (m, 4H, $H^{2,7a,12b}$), 1.73 – 1.67 (m, 1H, H^4), 1.67 (s, 3H, H^{27}), 1.59 (s, 3H, H^{26}), 1.58 – 1.49 (m,

3H, $H^{1b,6a,9}$), 1.37 (s, 3H, H^{30}), 1.32 (d, *J* = 14.2 Hz, 1H, H^{15b}), 1.15 (t, *J* = 7.6 Hz, 3H, $H^{3'}$), 1.13 – 1.01 (m, 2H, $H^{6b,7b}$), 0.98 (s, 3H, H^{19}), 0.91 (s, 3H, H^{18}), 0.81 (d, *J* = 6.7 Hz, 3H, H^{28}); ^{13}C NMR (100 MHz, $CDCl_3$) δ_C 174.3, 174.1, 170.7, 151.3, 132.8, 129.7, 123.1, 74.6, 74.0, 68.4, 49.3, 49.0, 44.5, 39.6, 39.2, 38.0, 37.1, 35.9, 35.0, 33.0, 31.2, 28.9, 28.5, 28.3, 27.6, 25.9, 24.5, 22.7, 20.8, 20.7, 18.2, 17.9, 15.7, 9.6; purity (LC-MS) 98%, t_R = 5.63 min, MS *m/z* 513.3 $[M\text{-}OAc]^+$.

(*Z*)-2-((3*R*,4*S*,5*S*,8*S*,9*S*,10*S*,11*R*,13*R*,14*S*,16*S*)-16-acetoxy-11-hydroxy-4,8,10,14-tetramethyl-3-(pentanoyloxy)hexadecahydro-17*H*-cyclopenta[*a*]phenanthren-17-ylidene)-6-methylhept-5-enoic acid, [3.5]

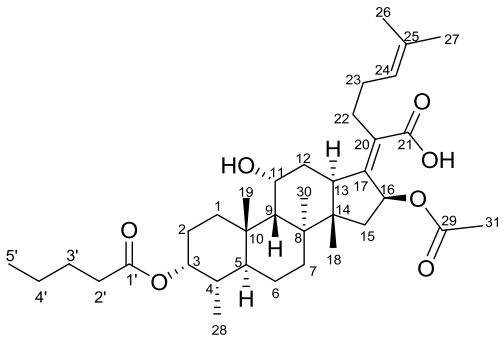

3.5
$C_{36}H_{56}O_7$
Exact Mass: 600.40
MW: 600.84

Valeric anhydride (7.20 mL, 36.74 mmol) was added to a solution of fusidic acid (3.45 g, 6.68 mmol) in pyridine (3.50 mL) and stirred at 25 °C for 6 hrs. After completion of reaction (TLC), the reaction mixture was diluted with DCM (30 mL) and washed with water (3×30 mL). The organic layer was dried over anhydrous $MgSO_4$, filtered and concentrated *in vacuo*. The crude product was then purified by column chromatography on silica gel using 4% MeOH/DCM as eluent, which after pentane wash afforded white solid (1.79 g, 45% yield); m.p. 155 – 157 °C; R_f 0.40 (EtOAc:DCM, 3:7); ^1H NMR (400 MHz, $CDCl_3$) δ_H 5.89 (d, *J* = 8.3 Hz, 1H, H^{16}), 5.15 – 5.05 (m, 1H, H^{24}), 4.97 – 4.90 (m, 1H, H^3), 4.37 – 4.29 (m, 1H, H^{11}), 3.13 – 2.99 (m, 1H, H^{13}), 2.50 – 2.42 (m, 2H, H^{22}), 2.32 (d, *J* = 7.5 Hz, 2H, $H^{2'}$), 2.30 – 2.27

(m, 1H, H^{12a}), 2.21 – 2.00 (m, 5H, $H^{1a,5,15a,23}$), 1.95 (s, 3H, H^{31}), 1.90 – 1.74 (m, 4H, $H^{2,7a,12b}$), 1.66 (s, 3H, H^{27}), 1.64 – 1.61 (m, 1H, H^{4}), 1.59 (s, 3H, H^{26}), 1.60 – 1.49 (m, 5H, $H^{1b,3',6a,9}$), 1.37 (s, 3H, H^{30}), 1.36 – 1.34 (m, 2H, $H^{4'}$), 1.32 (d, J = 14.2 Hz, 1H, H^{15b}), 1.18 – 1.01 (m, 2H, $H^{6b,7b}$), 0.98 (s, 3H, H^{19}), 0.91 (s, 3H, H^{18}), 0.91 (t, J = 7.3 Hz, 3H, $H^{5'}$), 0.81 (d, J = 6.7 Hz, 3H, H^{28}); ^{13}C NMR (100 MHz, $CDCl_3$) δ_C 174.3, 173.7, 170.6, 151.3, 132.8, 129.7, 123.2, 74.6, 74.0, 68.4, 49.3, 49.0, 44.5, 39.6, 39.2, 38.0, 37.1, 35.9, 35.0, 34.7, 33.0, 31.2, 28.9, 28.5, 27.6, 27.5, 25.8, 24.5, 22.7, 22.5, 20.7, 20.7, 18.2, 17.9, 15.8, 13.9; purity (LC-MS) 98%, t_R = 5.69 min, MS *m/z* 541.4 $[M\text{-}OAc]^+$.

5.2.3.2 Intermediates 3.6 and 3.7

To a solution of compound **3.4** or **3.5** (1.0 eq.) in acetonitrile, HOBt (1.0 eq.) and EDCI (1.0 eq.) were added and the resulting mixture was stirred for 3 hrs. at 25 °C. Hydrazine monohydrate (4.0 eq.) was then added after which the reaction mixture was and stirred further for 19 to 24 hrs. After completion of reaction (TLC), the reaction mixture was concentrated under reduced pressure and the resulting residue was taken up in ethyl acetate. The resulting solution was then washed with water, dried over anhydrous $MgSO_4$, filtered and concentrated *in vacuo*. The crude product was then purified by column chromatography on silica gel, which after pentane wash afforded the desired product.

(3*R*,4*S*,5*S*,8*S*,9*S*,10*S*,11*R*,13*R*,14*S*,16*S*,*Z*)-16-acetoxy-17-(1-hydrazinyl-6-methyl-1-oxohept-5-en-2-ylidene)-11-hydroxy-4,8,10,14-tetramethylhexadecahydro-1*H*-cyclopenta[*a*]phenanthren-3-yl propionate, [3.6]

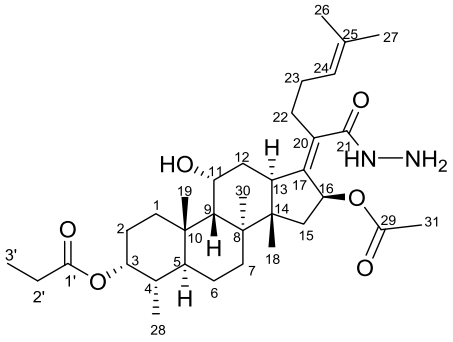

3.6

$C_{34}H_{54}N_2O_6$

Exact Mass: 586.40

MW: 586.81

White solid (536 mg, 78% yield); m.p. 102 – 104 °C; R_f 0.36 (EtOAc:DCM, 3:2); ^{1}H NMR (400 MHz, $CDCl_3$) δ_H 5.78 (d, *J* = 8.2 Hz, 1H, H^{16}), 5.09 – 5.02 (m, 1H, H^{24}), 4.96 – 4.90 (m, 1H, H^{3}), 4.34 – 4.27 (m, 1H, H^{11}), 3.02 – 2.92 (m, 1H, H^{13}), 2.51 – 2.40 (m, 1H, H^{22a}), 2.34 (q, *J* = 7.6 Hz, 2H, $H^{2'}$), 2.29 – 2.22 (m, 2H, $H^{12a,22b}$), 2.15 – 2.03 (m, 5H, $H^{1a,5,15a,23}$), 2.02 (s, 3H, H^{31}), 1.86 – 1.74 (m, 4H, $H^{2,7a,12b}$), 1.73 – 1.68 (m, 1H, H^{4}), 1.67 (s, 3H, H^{27}), 1.59 (s, 3H, H^{26}), 1.58 – 1.48 (m, 3H, $H^{1b,6a,9}$), 1.35 (s, 3H, H^{30}), 1.26 (d, *J* = 14.3 Hz, 1H, H^{15b}), 1.14 (t, *J* = 7.6 Hz, 3H, $H^{3'}$), 1.11 – 0.99 (m, 2H, $H^{6b,7b}$), 0.97 (s, 3H, H^{19}), 0.94 (s, 3H, H^{18}), 0.81 (d, *J* = 6.7 Hz, 3H, H^{28}); ^{13}C NMR (100 MHz, $CDCl_3$) δ_C 174.2, 171.9, 170.8, 143.9, 134.0, 132.8, 123.2, 74.0, 73.6, 68.4, 49.3, 49.0, 43.6, 39.7, 39.5, 38.1, 37.2, 35.9, 34.9, 33.1, 31.3, 29.5, 28.3, 28.0, 27.5, 25.9, 24.5, 22.6, 21.3, 20.7, 18.1, 18.0, 15.7, 9.5; purity (LC-MS) 90%, t_R = 5.53 min, MS *m/z* 527.4 $[M\text{-}OAc]^+$.

(3*R*,4*S*,5*S*,8*S*,9*S*,10*S*,11*R*,13*R*,14*S*,16*S*,*Z*)-16-acetoxy-17-(1-hydrazinyl-6-methyl-1-oxohept-5-en-2-ylidene)-11-hydroxy-4,8,10,14-tetramethylhexadecahydro-1*H*-cyclopenta[*a*]phenanthren-3-yl pentanoate, [3.7]

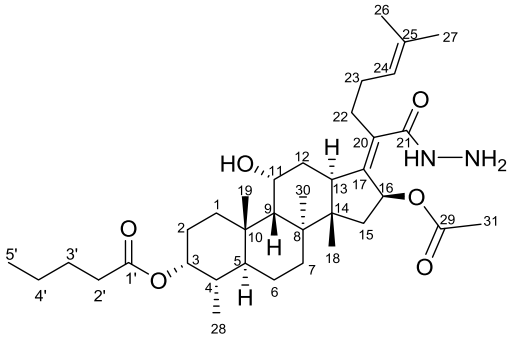

3.7
$C_{36}H_{58}N_2O_6$
Exact Mass: 614.43
MW: 614.87

White solid (615 mg, 58% yield); m.p. 86 – 88 °C; R_f 0.33 (EtOAc:DCM, 3:2); ^{1}H NMR (400 MHz, $CDCl_3$) δ_H 5.78 (d, *J* = 8.3 Hz, 1H, H^{16}), 5.10 – 5.01 (m, 1H, H^{24}), 4.97 – 4.89 (m, 1H, H^{3}), 4.36 – 4.27 (m, 1H, H^{11}), 3.04 – 2.94 (m, 1H, H^{13}), 2.51 – 2.40 (m, 1H, H^{22a}), 2.32 (t, *J* = 7.4 Hz, 2H, $H^{2'}$), 2.29 – 2.22 (m, 2H, $H^{12a,22b}$), 2.16 – 2.04 (m, 5H, $H^{1a,5,15a,23}$), 2.02 (s, 3H, H^{31}), 1.88 – 1.74 (m, 4H, $H^{2,7a,12b}$), 1.67 (s, 3H, H^{27}), 1.64 – 1.60 (m, 1H, H^{4}), 1.59 (s, 3H, H^{26}), 1.58 – 1.49 (m, 5H, $H^{1b,3',6a,9}$), 1.36 (s, 3H, H^{30}), 1.41 – 1.30 (m, 2H, $H^{4'}$), 1.27 (d, *J* = 14.2 Hz, 1H, H^{15b}), 1.18 – 1.00 (m, 2H, $H^{6b,7b}$), 0.97 (s, 3H, H^{19}), 0.94 (s, 3H, H^{18}), 0.91 (t, *J* = 7.3 Hz, 3H, $H^{5'}$), 0.81 (d, *J* = 6.7 Hz, 3H, H^{28}); ^{13}C NMR (100 MHz, $CDCl_3$) δ_C 173.6, 171.9, 170.8, 143.9, 134.0, 132.8, 123.2, 74.0, 73.6, 68.4, 49.3, 49.0, 43.6, 39.7, 39.5, 38.1, 37.2, 35.9, 34.9, 34.7, 33.1, 31.3, 29.5, 28.0, 27.6, 27.5, 25.9, 24.5, 22.6, 22.5, 21.3, 20.7, 18.1, 18.0, 15.8, 13.9; purity (LC-MS) 93%, t_R = 5.82 min, MS *m/z* 555.4 $[M\text{-}OAc]^+$.

5.2.3.3 Target compound 3.8 and 3.9

Methanesulfonyl chloride (1.0 eq.) was added to a solution of compound **3.6** or **3.7** (1.0 eq.) in pyridine with stirring at 25 °C for 2 hrs. After completion of reaction (TLC), the reaction mixture was diluted with ethyl acetate and washed with water and 0.5 M aq. HCl. The

organic layer was dried over anhydrous $MgSO_4$, filtered and concentrated *in vacuo* to afford the crude product which was purified by column chromatography on silica gel using EtOAc/DCM as eluent. The resulting oil was washed with pentane to afford the target compound.

(3*R*,4*S*,5*S*,8*S*,9*S*,10*S*,11*R*,13*R*,14*S*,16*S*,*Z*)-16-acetoxy-11-hydroxy-4,8,10,14-tetramethyl-17-(6-methyl-1-(2-(methylsulfonyl)hydrazinyl)-1-oxohept-5-en-2-ylidene)hexadecahydro-1*H*-cyclopenta[*a*]phenanthren-3-yl propionate, [3.8]

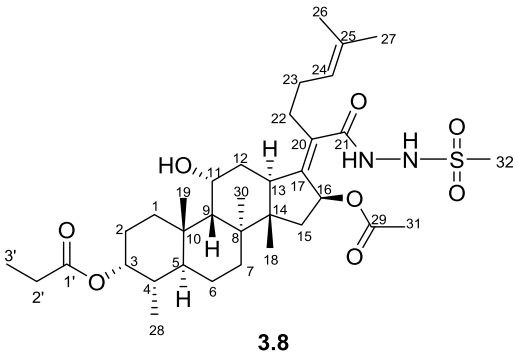

3.8

$C_{35}H_{56}N_2O_8S$

Exact Mass: 664.38

MW: 664.90

White solid (181 mg, 44% yield); m.p. 102 – 104 °C; R_f 0.50 (EtOAc:DCM, 3:7); ^{1}H NMR (400 MHz, $CDCl_3$) δ_H 7.82 (d, *J* = 4.4 Hz, 1H, H^{CONH}), 6.96 (d, *J* = 4.5 Hz, 1H, H^{SO_2NH}), 5.72 (d, *J* = 8.1 Hz, 1H, H^{16}), 5.13 – 5.05 (m, 1H, H^{24}), 4.95 – 4.89 (m, 1H, H^{3}), 4.34 – 4.27 (m, 1H, H^{11}), 3.06 – 2.99 (m, 1H, H^{13}), 2.97 (s, 3H, H^{32}), 2.52 – 2.43 (m, 1H, H^{22a}), 2.33 (q, *J* = 7.6 Hz, 2H, $H^{2'}$), 2.31 – 2.22 (m, 2H, $H^{12a,22b}$), 2.20 – 2.01 (m, 5H, $H^{1a,5,15a,23}$), 1.99 (s, 3H, H^{31}), 1.87 – 1.74 (m, 4H, $H^{2,7a,12b}$), 1.73 – 1.67 (m, 1H, H^{4}), 1.67 (s, 3H, H^{27}), 1.59 (s, 3H, H^{26}), 1.58 – 1.49 (m, 3H, $H^{1b,6a,9}$), 1.35 (s, 3H, H^{30}), 1.30 (d, *J* = 14.3 Hz, 1H, H^{15b}), 1.14 (t, *J* = 7.6 Hz, 3H, $H^{3'}$), 1.13 – 1.00 (m, 2H, $H^{6b,7b}$), 0.97 (s, 3H, H^{19}), 0.93 (s, 3H, H^{18}), 0.80 (d, *J* = 6.7 Hz, 1H, H^{28}); ^{13}C NMR (100 MHz, $CDCl_3$) δ_C 174.0, 170.6 (2C), 146.4, 133.3, 131.9, 122.6, 73.9, 73.8, 68.2, 49.1, 48.9, 43.8, 39.5, 39.3, 39.1, 37.9, 37.0, 35.7, 34.7, 32.9, 31.1,

29.7, 28.2, 28.1, 27.4, 25.7, 24.3, 22.4, 21.1, 20.4, 18.2, 17.8, 15.6, 9.4; purity (LC-MS) 96%, t_R = 5.52 min, MS *m/z* 605.3 $[M\text{-}OAc]^+$.

(3*R*,4*S*,5*S*,8*S*,9*S*,10*S*,11*R*,13*R*,14*S*,16*S*,*Z*)-16-acetoxy-11-hydroxy-4,8,10,14-tetramethyl-17-(6-methyl-1-(2-(methylsulfonyl)hydrazinyl)-1-oxohept-5-en-2-ylidene)hexadecahydro-1*H*-cyclopenta[*a*]phenanthren-3-yl pentanoate, [3.9]

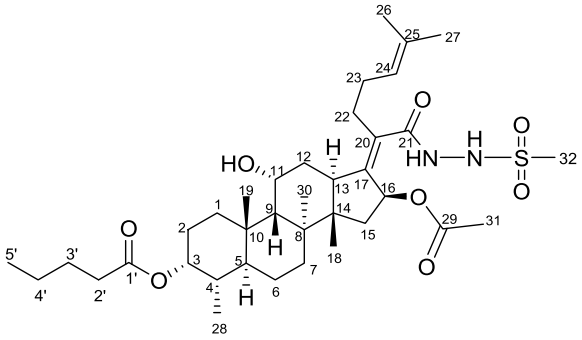

3.9
$C_{37}H_{60}N_2O_8S$
Exact Mass: 692.41
MW: 692.95

White solid (262 mg, 54% yield); m.p. 103 – 105 °C; R_f 0.38 (EtOAc:DCM, 1:9); ^{1}H NMR (400 MHz, $CDCl_3$) δ_H 7.82 (d, *J* = 3.9 Hz, 1H, H^{CONH}), 6.94 (d, *J* = 3.9 Hz, 1H, H^{SO_2NH}), 5.73 (d, *J* = 8.0 Hz, 1H, H^{16}), 5.14 – 5.05 (m, 1H, H^{24}), 4.96 – 4.89 (m, 1H, H^{3}), 4.38 – 4.27 (m, 1H, H^{11}), 3.08 – 3.01 (m, 1H, H^{13}), 2.98 (s, 3H, H^{32}), 2.54 – 2.43 (m, 1H, H^{22a}), 2.32 (t, *J* = 7.5 Hz, 2H, $H^{2'}$), 2.30 – 2.22 (m, 2H, $H^{12a,22b}$), 2.20 – 2.02 (m, 5H, $H^{1a,5,15a,23}$), 2.00 (s, 3H, H^{31}), 1.89 – 1.75 (m, 4H, $H^{2,7a,12b}$), 1.68 (s, 3H, H^{27}), 1.67 – 1.62 (m, 1H, H^{4}), 1.61 (s, 3H, H^{26}), 1.60 – 1.49 (m, 5H, $H^{1b,3',6a,9}$), 1.36 (s, 3H, H^{30}), 1.41 – 1.32 (m, 2H, $H^{4'}$), 1.32 (d, *J* = 14.3 Hz, 1H, H^{15b}), 1.19 – 1.01 (m, 2H, $H^{6b,7b}$), 0.98 (s, 3H, H^{19}), 0.94 (s, 3H, H^{18}), 0.91 (t, *J* = 7.3 Hz, 3H, $H^{5'}$), 0.81 (d, *J* = 6.5 Hz, 3H, H^{28}); ^{13}C NMR (100 MHz, $CDCl_3$) δ_C 173.6, 170.8, 170.7, 146.7, 133.5, 132.0, 122.8, 74.1, 74.0, 68.4, 49.3, 49.1, 44.0, 39.7, 39.5, 39.2, 38.1, 37.2, 35.8, 34.8, 34.7, 33.1, 31.3, 29.9, 28.4, 27.6, 27.5, 25.9, 24.5, 22.6, 22.5, 21.3, 20.6, 18.4, 18.0, 15.8, 13.9; purity (LC-MS) 97%, t_R = 5.73 min, MS *m/z* 633.4 $[M\text{-}OAc]^+$.

5.2.4 General procedure for the synthesis and characterization of C-3 aromatic esters

The respective carboxylic acid (4.0 eq.), DCC (4.0 eq.) and DMAP (0.4 eq.) were added to a solution of fusidic acid (1.0 eq.) in anhydrous DCM. The reaction mixture was stirred at 25 °C under N_2 atmosphere. After completion of reaction (TLC), the reaction mixture was diluted with ethyl acetate, filtered and washed with 2 *N* HCl, saturated aq. $NaHCO_3$, brine and water. The organic layer was then dried over anhydrous $MgSO_4$, filtered and concentrated *in vacuo*. The crude product was then purified by column chromatography on silica gel to afford the corresponding target compound.

(*Z*)-2-((3*R*,4*S*,5*S*,8*S*,9*S*,10*S*,11*R*,13*R*,14*S*,16*S*)-16-acetoxy-3-(benzoyloxy)-11-hydroxy-4,8,10,14-tetramethylhexadecahydro-17*H*-cyclopenta[*a*]phenanthren-17-ylidene)-6-methylhept-5-enoic acid [3.10]

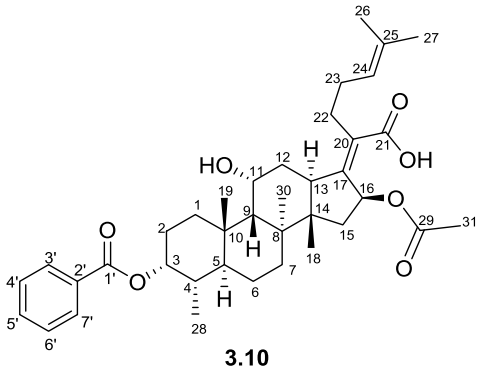

3.10
$C_{38}H_{52}O_7$
Exact Mass: 620.37
MW: 620.83

White solid (19 mg, 10% yield); m.p. 172 – 174 °C; R_f 0.31 (EtOAc:Hex, 1:1); ^{1}H NMR (400 MHz, DMSO-d_6) δ_H 8.00 – 7.92 (m, 2H, $H^{3',7'}$), 7.68–7.62 (m, 1H, $H^{5'}$), 7.57 – 7.50 (m, 2H, $H^{4',6'}$), 5.73 (d, *J* = 8.5 Hz, 1H, H^{16}), 5.11 – 5.02 (m, 2H, $H^{3,24}$), 4.20 – 4.08 (m, 1H, H^{11}), 2.97 – 2.88 (m, 1H, H^{13}), 2.39 – 2.24 (m, 4H, $H^{1a,5,22}$), 2.23 – 2.05 (m, 2H, $H^{12a,23a}$), 2.05 – 1.91 (m, 2H, $H^{15a,23a}$), 1.88 (s, 3H, H^{31}), 1.87 – 1.81 (m, 1H, H^{2a}), 1.81 – 1.67 (m, 4H, $H^{2b,4,7a,12b}$), 1.62 (s, 3H, H^{27}), 1.60 – 1.56 (m, 1H, H^{6a}), 1.55 (s, 3H, H^{26}), 1.54 – 1.43 (m, 2H, $H^{1b,9}$), 1.38 (s, 3H, H^{30}), 1.16 (d, *J* = 14.1 Hz, 1H, H^{15b}), 1.13 – 1.04 (m, 2H, $H^{6b,7b}$), 0.98 (s,

3H, H^{19}), 0.86 (s, 3H, H^{18}), 0.81 (d, *J* = 6.6 Hz, 3H, H^{28}); ^{13}C NMR (100 MHz, DMSO-d_6) δ_C 169.9 (2C), 165.1, 143.7, 133.1, 130.9, 130.5, 129.1, 128.8 (2C), 128.8 (2C), 124.0, 75.0, 73.7, 65.9, 48.5, 48.3, 42.9, 39.0, 38.7, 37.3, 36.3, 36.0, 34.7, 31.9, 30.1, 28.9, 28.3, 26.9, 25.5, 23.7, 22.6, 20.6, 20.5, 17.7 (2C), 15.7; purity (LC-MS) 99%, t_R = 5.31 min, MS *m/z* 619.4 $[M-H]^-$.

(*Z*)-2-((3*R*,4*S*,5*S*,8*S*,9*S*,10*S*,11*R*,13*R*,14*S*,16*S*)-16-acetoxy-3-((4-fluorobenzoyl)oxy)-11-hydroxy-4,8,10,14-tetramethylhexadecahydro-17*H*-cyclopenta[*a*]phenanthren-17-ylidene)-6-methylhept-5-enoic acid [3.11]

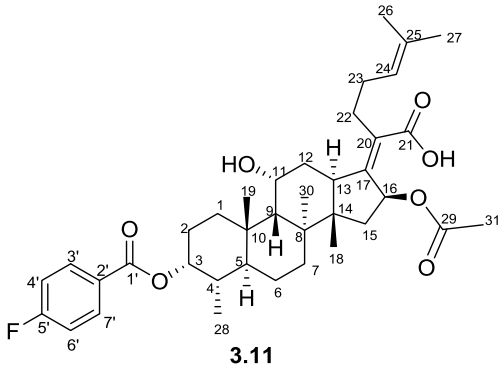

3.11
$C_{38}H_{51}FO_7$
Exact Mass: 638.36
MW: 638.82

White solid (13 mg, 6% yield); m.p. 76 – 78 °C; R_f 0.38 (EtOAc:Hex, 3:7); ^{1}H NMR (400 MHz, $CDCl_3$) δ_H 8.09 – 8.00 (m, 2H, $H^{3'/7'}$), 7.18 – 7.07 (m, 2H, $H^{4'/6'}$), 5.88 (d, *J* = 8.4 Hz, 1H, H^{16}), 5.21 – 5.16 (m, 1H, H^{3}), 5.16 – 5.07 (m, 1H, H^{24}), 4.43 – 4.32 (m, 1H, H^{11}), 3.19 – 3.08 (m, 1H, H^{13}), 2.63 – 2.49 (m, 1H, H^{22a}), 2.37 – 2.23 (m, 4H, $H^{1a,5,12a,22b}$), 2.23 – 2.11 (m, 3H, $H^{15a,23}$), 2.02 (s, 3H, H^{31}), 1.99 – 1.88 (m, 2H, $H^{2a,12b}$), 1.88 – 1.74 (m, 3H, $H^{2b,4,7a}$), 1.66 (s, 3H, H^{27}), 1.66 – 1.60 (m, 3H, $H^{1b,6a,9}$), 1.59 (s, 3H, H^{26}), 1.45 (s, 3H, H^{30}), 1.36 (d, *J* = 14.4 Hz, 1H, H^{15b}), 1.24 – 1.08 (m, 2H, $H^{6b,7b}$), 1.03 (s, 3H, H^{19}), 0.97 (s, 3H, H^{18}), 0.89 (d, *J* = 6.7 Hz, 3H, H^{28}); ^{13}C NMR (100 MHz, $CDCl_3$) δ_C 170.9 (2C), 167.8, 165.1, 153.2, 133.1, 131.9 (2C), 129.0, 125.3, 122.7, 115.5 (2C), 75.1, 74.1, 68.1, 49.1, 48.9, 44.7, 39.6, 39.1,

38.2, 37.0, 35.8, 35.1, 32.8, 31.2, 28.9, 28.6, 27.4, 25.7, 24.5, 22.7, 21.0, 20.6, 18.2, 17.8, 15.8; purity (LC-MS) 98%, t_R = 4.68 min, MS *m/z* 637.3 $[M-H]^-$.

(*Z*)-2-((3*R*,4*S*,5*S*,8*S*,9*S*,10*S*,11*R*,13*R*,14*S*,16*S*)-16-acetoxy-3-((4-chlorobenzoyl)oxy)-11-hydroxy-4,8,10,14-tetramethylhexadecahydro-17*H*-cyclopenta[*a*]phenanthren-17-ylidene)-6-methylhept-5-enoic acid [3.12]

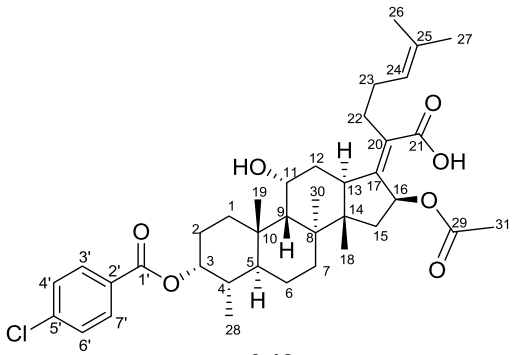

3.12
$C_{38}H_{51}ClO_7$
Exact Mass: 654.33
MW: 655.27

White solid (27 mg, 13% yield); m.p. 118 – 120 °C; R_f 0.24 (EtOAc:Hex, 1:1); ^{1}H NMR (400 MHz, $CDCl_3$) δ_H 7.97 (d, *J* = 8.6 Hz, 2H, $H^{3'/7'}$), 7.42 (d, *J* = 8.6 Hz, 2H, $H^{4'/6'}$), 5.93 (d, *J* = 7.1 Hz, 1H, H^{16}), 5.22 – 5.14 (m, 1H, H^{3}), 5.12 – 5.04 (m, 1H, H^{24}), 4.38 – 4.30 (m, 1H, H^{11}), 3.11 – 2.97 (m, 1H, H^{13}), 2.50 – 2.38 (m, 1H, H^{22a}), 2.35 – 2.24 (m, 4H, $H^{1a,5,12a,22b}$), 2.23 – 2.09 (m, 3H, $H^{15a,23}$), 1.96 (s, 3H, H^{31}), 1.93 – 1.86 (m, 2H, $H^{2a,12b}$), 1.86 – 1.74 (m, 3H, $H^{2b,4,7a}$), 1.70 – 1.66 (m, 1H, H^{6a}), 1.65 (s, 3H, H^{27}), 1.65 – 1.58 (m, 2H, $H^{1b,9}$), 1.58 (s, 3H, H^{26}), 1.43 (s, 3H, H^{30}), 1.33 (d, *J* = 14.2 Hz, 1H, H^{15b}), 1.29 – 1.06 (m, 2H, $H^{6b,7b}$), 1.02 (s, 3H, H^{19}), 0.94 (s, 3H, H^{18}), 0.88 (d, *J* = 6.7 Hz, 3H, H^{28}); ^{13}C NMR (100 MHz, $CDCl_3$) δ_C 174.1, 170.7, 165.3, 150.8, 139.2, 132.6, 130.8 (2C), 129.4, 128.8 (2C), 123.0, 114.3, 75.4, 74.4, 68.2, 49.1, 48.9, 44.3, 39.6, 39.0, 38.2, 37.0, 35.9, 35.1, 32.8, 31.2, 29.7, 28.8, 28.4, 25.7, 24.5, 23.4, 22.6, 20.6, 18.1, 17.8, 15.8; purity (LC-MS) 99%, t_R = 4.71 min, MS *m/z* 653.3/655.3 $[M-H]^-$.

(*Z*)-2-((3*R*,4*S*,5*S*,8*S*,9*S*,10*S*,11*R*,13*R*,14*S*,16*S*)-16-acetoxy-3-((4-bromobenzoyl)oxy)-11-hydroxy-4,8,10,14-tetramethylhexadecahydro-17*H*-cyclopenta[*a*]phenanthren-17-ylidene)-6-methylhept-5-enoic acid [3.13]

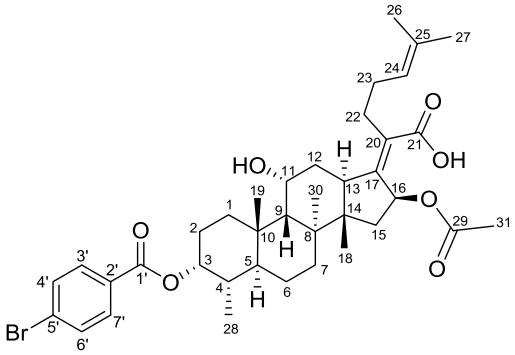

3.13

$C_{38}H_{51}BrO_7$

Exact Mass: 698.28

MW: 699.72

White solid (54 mg, 24% yield); m.p. 179 – 181 °C; R_f 0.31 (MeOH:DCM, 0.4:9.6); ^{1}H NMR (400 MHz, CD_3OD) δ_H 7.94 (d, *J* = 8.7 Hz, 2H, $H^{3'/7'}$), 7.65 (d, *J* = 8.7 Hz, 2H, $H^{4'/6'}$), 5.84 (d, *J* = 8.3 Hz, 1H, H^{16}), 5.19 – 5.11 (m, 2H, $H^{3,24}$), 4.33 – 4.27 (m, 1H, H^{11}), 3.09 – 3.00 (m, 1H, H^{13}), 2.59 – 2.47 (m, 1H, H^{22a}), 2.46 – 2.26 (m, 4H, $H^{1a,5,12a,22b}$), 2.19 – 2.09 (m, 3H, $H^{15a,23}$), 2.01 (s, 3H, H^{31}), 1.98 – 1.75 (m, 5H, $H^{2,4,7a,12b}$), 1.75 – 1.67 (m, 1H, H^{6a}), 1.66 (s, 3H, H^{27}), 1.64 – 1.62 (m, 1H, H^{9}), 1.61 (s, 3H, H^{26}), 1.61 – 1.54 (m, 1H, H^{1b}), 1.46 (s, 3H, H^{30}), 1.24 (d, *J* = 14.1 Hz, 1H, H^{15b}), 1.22 – 1.10 (m, 2H, $H^{6b,7b}$), 1.05 (s, 3H, H^{19}), 0.97 (s, 3H, H^{18}), 0.87 (d, *J* = 6.7 Hz, 3H, H^{28}); ^{13}C NMR (100 MHz, CD_3OD) δ_C 179.5, 173.5, 166.8, 139.3, 138.9, 133.0 (2C), 132.3, 132.1 (2C), 131.2, 128.9, 125.4, 77.3, 76.0, 68.5, 50.6, 50.0, 43.8, 40.7, 40.3, 38.9, 37.9, 37.6, 36.9, 33.3, 31.8, 30.9, 29.2, 28.4, 25.9, 24.3, 23.5, 22.1, 21.2, 18.2, 18.0, 16.3; purity (LC-MS) 99%, t_R = 5.04 min, MS *m/z* 697.3/699.3 $[M-H]^-$.

(*Z*)-2-((3*R*,4*S*,5*S*,8*S*,9*S*,10*S*,11*R*,13*R*,14*S*,16*S*)-16-acetoxy-3-((4-cyanobenzoyl)oxy)-11-hydroxy-4,8,10,14-tetramethylhexadecahydro-17*H*-cyclopenta[*a*]phenanthren-17-ylidene)-6-methylhept-5-enoic acid [3.14]

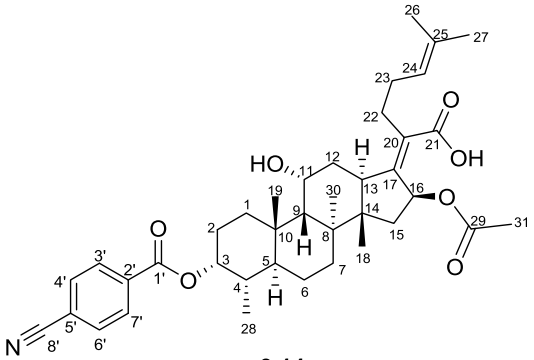

3.14

$C_{39}H_{51}NO_7$

Exact Mass: 645.37

MW: 645.84

White solid (28 mg, 13% yield); m.p. 161 – 163 °C; R_f 0.32 (MeOH:DCM, 0.4:0.96); ^{1}H NMR (400 MHz, CD_3OD) δ_H 8.10 (d, *J* = 8.6 Hz, 2H, $H^{3'/7'}$), 7.79 (d, *J* = 8.6 Hz, 2H, $H^{4'/6'}$), 5.82 (d, *J* = 8.1 Hz, 1H, H^{16}), 5.22 – 5.18 (m, 1H, H^{3}), 5.17 – 5.11 (m, 1H, H^{24}), 4.33 – 4.26 (m, 1H, H^{11}), 3.10 – 3.01 (m, 1H, H^{13}), 2.60 – 2.46 (m, 1H, H^{22a}), 2.46 – 2.26 (m, 4H, $H^{1a,5,12a,22b}$), 2.20 – 2.08 (m, 3H, $H^{15a,23}$), 2.01 (s, 3H, H^{31}), 1.97 – 1.77 (m, 4H, $H^{2,7a,12b}$), 1.76 – 1.67 (m, 1H, H^{4}), 1.66 (s, 3H, H^{27}), 1.65 – 1.62 (m, 3H, $H^{1b,6a,9}$), 1.61 (s, 3H, H^{26}), 1.47 (s, 3H, H^{30}), 1.24 (d, *J* = 14.2 Hz, 1H, H^{15b}), 1.22 – 1.11 (m, 2H, $H^{6b,7b}$), 1.07 (s, 3H, H^{19}), 0.97 (s, 3H, H^{18}), 0.88 (d, *J* = 6.7 Hz, 3H, H^{28}); ^{13}C NMR (100 MHz, CD_3OD) δ_C 173.3 (2C), 166.0, 139.8, 136.1, 133.6 (2C), 132.4, 131.1 (2C), 125.3, 119.0, 117.4, l78.0, 76.0, 68.5, 50.6, 50.0, 43.9, 40.8, 40.3, 38.9, 37.9, 37.6, 36.9, 33.2, 31.7, 30.9, 30.7, 29.1, 28.3, 25.9, 24.3, 23.5, 22.2, 21.0, 18.1, 17.9, 16.3; purity (LC-MS) 99%, t_R = 4.56 min, MS *m/z* 644.3 $[M-H]^-$.

(*Z*)-2-((3*R*,4*S*,5*S*,8*S*,9*S*,10*S*,11*R*,13*R*,14*S*,16*S*)-16-acetoxy-11-hydroxy-4,8,10,14-tetramethyl-3-((4-nitrobenzoyl)oxy)hexadecahydro-17*H*-cyclopenta[*a*]phenanthren-17-ylidene)-6-methylhept-5-enoic acid [3.15]

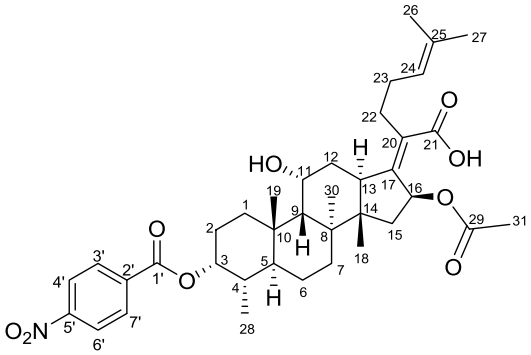

3.15

$C_{38}H_{51}NO_9$

Exact Mass: 665.36

MW: 665.82

Off-white solid (32 mg, 14% yield); m.p. 135 – 137 °C; R_f 0.44 (MeOH:DCM, 0.5:9.5); ^{1}H NMR (400 MHz, CD_3OD) δ_H 8.33 (d, *J* = 9.0 Hz, 2H, $H^{3'/7'}$), 8.25 (d, *J* = 9.0 Hz, 2H, $H^{4'/6'}$), 5.83 (d, *J* = 8.4 Hz, 1H, H^{16}), 5.22 – 5.18 (m, 1H, H^{3}), 5.16 – 5.09 (m, 1H, H^{24}), 4.36 – 4.29 (m, 1H, H^{11}), 3.13 – 3.05 (m, 1H, H^{13}), 2.59 – 2.49 (m, 1H, H^{22a}), 2.48 – 2.28 (m, 4H, $H^{1a,5,12a,22b}$), 2.23 – 2.01 (m, 3H, $H^{15a,23}$), 1.97 (s, 3H, H^{31}), 1.96 – 1.78 (m, 5H, $H^{2,4,7a,12b}$), 1.76 – 1.67 (m, 1H, H^{6a}), 1.66 (s, 3H, H^{27}), 1.65 – 1.61 (m, 2H, $H^{1b,9}$), 1.60 (s, 3H, H^{26}), 1.48 (s, 3H, H^{30}), 1.26 (d, *J* = 14.1 Hz, 1H, H^{15b}), 1.24 – 1.13 (m, 2H, $H^{6b,7b}$), 1.07 (s, 3H, H^{19}), 0.95 (s, 3H, H^{18}), 0.89 (d, *J* = 6.7 Hz, 3H, H^{28}); ^{13}C NMR (100 MHz, CD_3OD) δ_C 174.1, 172.5, 165.6, 152.0, 148.6, 137.5, 133.3, 132.3, 131.6 (2C), 124.7 (2C), 124.4, 78.0, 75.7, 68.3, 50.5, 50.0, 44.9, 40.7, 40.1, 38.8, 37.8, 37.5, 36.9, 33.1, 31.7, 29.9, 29.3, 28.3, 25.9, 24.4, 23.6, 22.1, 20.7, 18.2, 17.9, 16.3; purity (LC-MS) 99%, t_R = 4.76 min, MS *m/z* 664.3 $[M-H]^-$.

(*Z*)-2-((3*R*,4*S*,5*S*,8*S*,9*S*,10*S*,11*R*,13*R*,14*S*,16*S*)-16-acetoxy-11-hydroxy-4,8,10,14-tetramethyl-3-((4-(trifluoromethyl)benzoyl)oxy)hexadecahydro-17*H*-cyclopenta[*a*]phenanthren-17-ylidene)-6-methylhept-5-enoic acid [3.16]

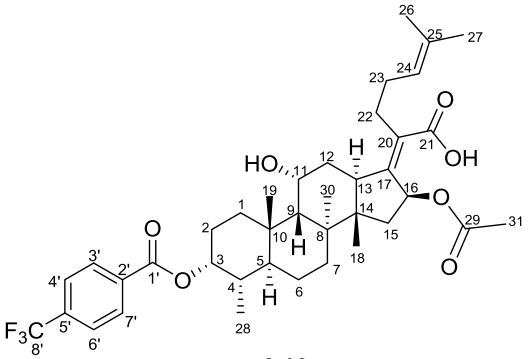

3.16

$C_{39}H_{51}F_3O_7$

Exact Mass: 688.36

MW: 688.83

Off-white solid (71 mg, 35% yield); m.p. 171 – 173 °C; R_f 0.42 (EtOAc:Hex, 1:1); ^{1}H NMR (400 MHz, CD_3OD) δ_H 8.22 (d, *J* = 8.1 Hz, 2H, $H^{3'/7'}$), 7.81 (d, *J* = 8.2 Hz, 2H, $H^{4'/6'}$), 5.83 (d, *J* = 8.3 Hz, 1H, H^{16}), 5.21 – 5.18 (m, 1H, H^{3}), 5.17 – 5.12 (m, 1H, H^{24}), 4.33 – 4.28 (m, 1H, H^{11}), 3.09 – 3.02 (m, 1H, H^{13}), 2.59 – 2.48 (m, 1H, H^{22a}), 2.48 – 2.27 (m, 4H, $H^{1a,5,12a,22b}$), 2.21 – 2.08 (m, 3H, $H^{15a,23}$), 2.01 (s, 3H, H^{31}), 2.00 – 1.77 (m, 5H, $H^{2,4,7a,12b}$), 1.77 – 1.67 (m, 1H, H^{6a}), 1.66 (s, 3H, H^{27}), 1.66 – 1.61 (m, 2H, $H^{1a,9}$), 1.61 (s, 3H, H^{26}), 1.48 (s, 3H, H^{31}), 1.25 (d, *J* = 14.3 Hz, 1H, H^{15b}), 1.22 – 1.11 (m, 2H, $H^{6b,7b}$), 1.07 (s, 3H, H^{19}), 0.97 (s, 3H, H^{18}), 0.89 (d, *J* = 6.7 Hz, 3H, H^{28}); ^{13}C NMR (100 MHz, CD_3OD) δ_C 173.4 (2C), 166.3, 155.6, 140.0, 138.4, 135.7, 132.4, 131.1 (2C), 126.7 (2C), 126.6, 125.3, 77.7, 76.0, 68.5, 50.6, 50.0, 43.9, 40.8, 40.3, 38.9, 37.9, 37.6, 36.9, 33.2, 31.7, 30.8, 29.2, 28.4, 25.9, 24.3, 23.5, 22.2, 21.1, 18.1, 17.9, 16.3; purity (LC-MS) 99%, t_R = 4.96 min, MS *m/z* 687.3 $[M-H]^-$.

(*Z*)-2-((3*R*,4*S*,5*S*,8*S*,9*S*,10*S*,11*R*,13*R*,14*S*,16*S*)-16-acetoxy-11-hydroxy-4,8,10,14-tetramethyl-3-((4-(methylsulfonyl)benzoyl)oxy)hexadecahydro-17*H*-cyclopenta[*a*]phenanthren-17-ylidene)-6-methylhept-5-enoic acid [3.17]

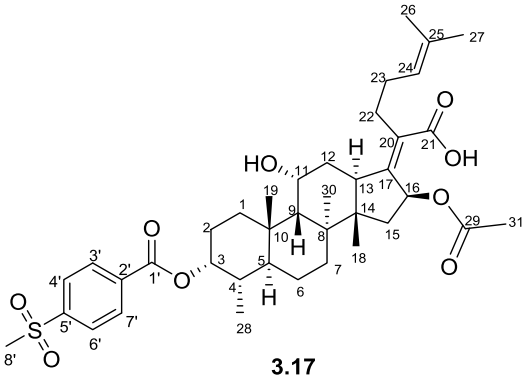

3.17

$C_{39}H_{54}O_9S$

Exact Mass: 698.35

MW: 698.91

White solid (81 mg, 39% yield); m.p. 177 – 179 °C; R_f 0.35 (EtOAc:Hex, 7:3); ^{1}H NMR (400 MHz, CD_3OD) δ_H 8.27 (d, *J* = 8.7 Hz, 2H, $H^{3'/7'}$), 8.09 (d, *J* = 8.7 Hz, 2H, $H^{4'/6'}$), 5.84 (d, *J* = 8.2 Hz, 1H, H^{16}), 5.22 – 5.18 (m, 1H, H^{3}), 5.17 – 5.11 (m, 1H, H^{24}), 4.33 – 4.27 (m, 1H, H^{11}), 3.17 (s, 3H, $H^{8'}$), 3.10 – 3.01 (m, 1H, H^{13}), 2.59 – 2.48 (m, 1H, H^{22a}), 2.48 – 2.27 (m, 4H, $H^{1a,5,12a,22b}$), 2.20 – 2.08 (m, 3H, $H^{15a,23}$), 2.01 (s, 3H, H^{31}), 1.98 – 1.77 (m, 5H, $H^{2,4,7a,12b}$), 1.77 – 1.68 (m, 1H, H^{6a}), 1.66 (s, 3H, H^{27}), 1.66 – 1.62 (m, 2H, $H^{1b,9}$), 1.61 (s, 3H, H^{26}), 1.48 (s, 3H, H^{30}), 1.25 (d, *J* = 14.2 Hz, 1H, H^{15b}), 1.23 – 1.11 (m, 2H, $H^{6b,7b}$), 1.07 (s, 3H, H^{19}), 0.97 (s, 3H, H^{18}), 0.89 (d, *J* = 6.7 Hz, 3H, H^{28}); ^{13}C NMR (100 MHz, CD_3OD) δ_C 173.3 (2C), 166.0, 145.9, 141.2, 137.6, 136.9, 132.6, 131.4 (2C), 128.8 (2C), 125.2, 78.0, 76.0, 68.5, 50.9, 50.0, 44.1 (2C), 40.8, 40.3, 38.9, 37.9, 37.6, 36.9, 33.2, 31.7, 30.7, 29.2, 28.3, 25.9, 24.3, 23.5, 22.1, 21.1, 18.2, 17.9, 16.3; purity (LC-MS) 99%, t_R = 4.21 min, MS *m/z* 697.3 $[M-H]^-$.

(*Z*)-2-((3*R*,4*S*,5*S*,8*S*,9*S*,10*S*,11*R*,13*R*,14*S*,16*S*)-16-acetoxy-11-hydroxy-3-((4-methoxybenzoyl)oxy)-4,8,10,14-tetramethylhexadecahydro-17*H*-cyclopenta[*a*]phenanthren-17-ylidene)-6-methylhept-5-enoic acid [3.18]

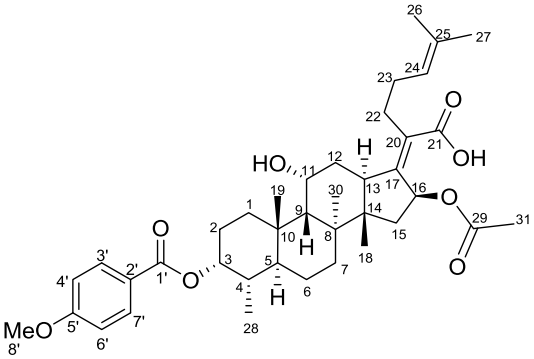

3.18

$C_{39}H_{54}O_8$

Exact Mass: 650.38

MW: 650.85

White solid (13 mg, 6% yield); m.p. 162 – 164 °C; R_f 0.47 (EtOAc:Hex, 7:3); ^{1}H NMR (400 MHz, CD_3OD) δ_H 8.00 (d, *J* = 9.0 Hz, 2H, $H^{3'/7'}$), 7.00 (d, *J* = 9.0 Hz, 2H, $H^{4'/6'}$), 5.84 (d, *J* = 8.5 Hz, 1H, H^{16}), 5.20 – 5.08 (m, 2H, $H^{3,24}$), 4.37 – 4.29 (m, 1H, H^{11}), 3.86 (s, 3H, $H^{8'}$), 3.15 – 3.05 (m, 1H, H^{13}), 2.61 – 2.49 (m, 1H, H^{22a}), 2.48 – 2.26 (m, 4H, $H^{1a,5,12a,22b}$), 2.25 – 2.04 (m, 3H, $H^{15a,23}$), 1.97 (s, 3H, H^{31}), 1.95 – 1.78 (m, 5H, $H^{2,4,7a,12b}$), 1.77 – 1.68 (m, 1H, H^{6a}), 1.67 (s, 3H, H^{27}), 1.61 (s, 3H, H^{26}), 1.61 – 1.56 (m, 2H, $H^{1b,9}$), 1.49 (s, 3H, H^{30}), 1.27 (d, *J* = 13.8 Hz, 1H, H^{15b}), 1.25 – 1.14 (m, 2H, $H^{6b,7b}$), 1.07 (s, 3H, H^{19}), 0.96 (s, 3H, H^{18}), 0.88 (d, *J* = 6.7 Hz, 3H, H^{28}); ^{13}C NMR (100 MHz, CD_3OD) δ_C 172.6 (2C), 167.7, 165.1, 148.4, 133.3 (2C), 132.5 (2C) 124.4, 124.3, 114.9 (2C), 76.5, 75.8, 68.3, 56.0, 50.6, 50.0, 45.0, 40.8, 40.1, 38.9, 37.9, 37.6, 37.0, 33.3, 31.8, 29.9, 29.3, 28.5, 25.9, 24.4, 23.4, 22.1, 20.7, 18.2, 17.9, 16.3; purity (LC-MS) 99%, t_R = 4.57 min, MS *m/z* 649.4 $[M-H]^-$.

(*Z*)-2-((3*R*,4*S*,5*S*,8*S*,9*S*,10*S*,11*R*,13*R*,14*S*,16*S*)-16-acetoxy-11-hydroxy-4,8,10,14-tetramethyl-3-((4-methylbenzoyl)oxy)hexadecahydro-17*H*-cyclopenta[*a*]phenanthren-17-ylidene)-6-methylhept-5-enoic acid [3.19]

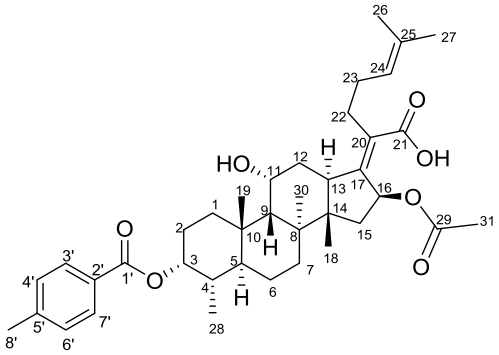

3.19

$C_{39}H_{54}O_7$

Exact Mass: 634.39

MW: 634.85

Off-white solid (24 mg, 12% yield); m.p. 166 – 168 °C; R_f 0.26 (MeOH:DCM, 0.3:9.7); ^{1}H NMR (400 MHz, CD_3OD) δ_H 7.93 (d, *J* = 8.2 Hz, 2H, $H^{3'/7'}$), 7.28 (d, *J* = 8.0 Hz, 2H, $H^{4'/6'}$), 5.82 (d, *J* = 8.2 Hz, 1H, H^{16}), 5.19 – 5.10 (m, 2H, $H^{3,24}$), 4.33 – 4.25 (m, 1H, H^{11}), 3.07 – 2.98 (m, 1H, H^{13}), 2.58 – 2.47 (m, 1H, H^{22a}), 2.40 (s, 3H, $H^{8'}$), 2.40 – 2.25 (m, 4H, $H^{1a,5,12a,22b}$), 2.18 – 2.09 (m, 3H, $H^{15a,23}$), 2.02 (s, 3H, H^{31}), 1.99 – 1.77 (m, 5H, $H^{2,4,7a,12b}$), 1.75 – 1.65 (m, 1H, H^{6a}), 1.65 (s, 3H, H^{27}), 1.63 – 1.61 (m, 2H, $H^{1b,9}$), 1.61 (s, 3H, H^{26}), 1.47 (s, 3H, H^{30}), 1.24 (d, *J* = 14.1 Hz, 1H, H^{15b}), 1.22 – 1.09 (m, 2H, $H^{6b,7b}$), 1.05 (s, 3H, H^{19}), 0.97 (s, 3H, H^{18}), 0.87 (d, *J* = 6.7 Hz, 3H, H^{28}); ^{13}C NMR (100 MHz, CD_3OD) δ_C 173.5 (2C), 167.9, 145.0, 139.5, 138.1, 132.2, 130.5 (2C), 130.2 (2C), 129.2, 125.4, 76.6, 76.0, 68.5, 50.5, 50.0, 43.6, 40.6, 40.3, 39.0, 37.9, 37.5, 36.8, 33.5, 31.8, 30.9, 29.1, 28.4, 25.9, 24.4, 23.3, 22.0, 21.6, 21.2, 18.2, 18.0, 16.3; purity (LC-MS) 98%, t_R = 4.60 min, MS *m/z* 633.4 $[M-H]^-$.

(*Z*)-2-((3*R*,4*S*,5*S*,8*S*,9*S*,10*S*,11*R*,13*R*,14*S*,16*S*)-16-acetoxy-11-hydroxy-3-(isonicotinoyloxy)-4,8,10,14-tetramethylhexadecahydro-17*H*-cyclopenta[*a*]phenanthren-17-ylidene)-6-methylhept-5-enoic acid [3.20]

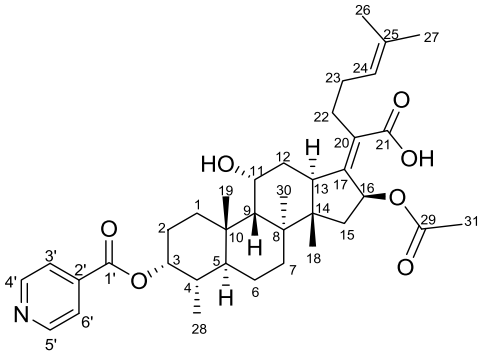

3.20

$C_{37}H_{51}NO_7$

Exact Mass: 621.37

MW: 621.82

White solid (20.1 mg, 11% yield); m.p. 184 – 186 °C; R_f 0.29 (MeOH:DCM, 0.5:9.5); ^{1}H NMR (400 MHz, DMSO-d_6) δ_H 8.83 (d, J = 4.9 Hz, 2H, $H^{4'}$), 7.81 (d, J = 5.7 Hz, 2H, $H^{3'}$), 5.70 (d, J = 8.4 Hz, 1H, H^{16}), 5.20 – 5.01 (m, 2H, $H^{3,24}$), 4.30 – 4.08 (m, 1H, H^{11}), 3.06 – 2.89 (m, 1H, H^{13}), 2.45 – 2.21 (m, 4H, $H^{1a,5,12a,23}$), 2.21 – 1.92 (m, 3H, $H^{15a,23}$), 1.89 (s, 3H, H^{31}), 1.83 – 1.65 (m, 5H, $H^{2,4,7a,12b}$), 1.63 (s, 3H, H^{27}), 1.62 – 1.57 (m, 1H, H^{6a}), 1.55 (s, 3H, H^{26}), 1.54 – 1.41 (m, 2H, $H^{1b,9}$), 1.38 (s, 3H, H^{30}), 1.16 (d, J = 14.0 Hz, 1H, H^{15b}), 1.13 – 1.03 (m, 2H, $H^{6b,7b}$), 0.98 (s, 3H, H^{19}), 0.85 (s, 3H, H^{18}), 0.81 (d, J = 6.6 Hz, 3H, H^{28}); ^{13}C NMR (100 MHz, DMSO-d_6) δ_C 171.1, 169.7, 164.0, 150.8 (2C), 147.0, 137.5, 131.5, 130.4, 123.3, 122.3 (2C), 76.2, 73.5, 65.8, 48.5, 48.3, 43.2, 39.0, 38.6, 37.2, 36.2, 35.9, 34.7, 31.7, 30.0, 28.5, 28.1, 26.7, 25.5, 23.7, 22.7, 20.6, 20.5, 17.6 (2C), 15.7; purity (LC-MS) 98%, t_R = 4.37 min, MS *m/z* 620.4 $[M-H]^-$.

(*Z*)-2-((3*R*,4*S*,5*S*,8*S*,9*S*,10*S*,11*R*,13*R*,14*S*,16*S*)-16-acetoxy-11-hydroxy-4,8,10,14-tetramethyl-3-((pyrazine-2-carbonyl)oxy)hexadecahydro-17*H*-cyclopenta[*a*]phenanthren-17-ylidene)-6-methylhept-5-enoic acid [3.21]

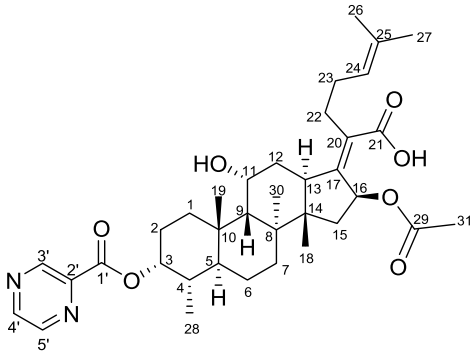

3.21

$C_{36}H_{50}N_2O_7$

Exact Mass: 622.36

MW: 622.80

White solid (20 mg, 9% yield); m.p. 116 – 118 °C; R_f 0.29 (MeOH:DCM, 0.5:9.5); ^{1}H NMR (400 MHz, CD_3OD) δ_H 9.30 (s, 1H, $H^{3'}$), 8.86 – 8.78 (m, 2H, $H^{4',5'}$), 5.85 (d, *J* = 8.4 Hz, 1H, H^{16}), 5.34 – 5.26 (m, 1H, H^{3}), 5.19 – 5.11 (m, 1H, H^{24}), 4.38 – 4.30 (m, 1H, H^{11}), 3.15 – 3.07 (m, 1H, H^{13}), 2.63 – 2.51 (m, 1H, H^{22a}), 2.49 – 2.30 (m, 4H, $H^{1a,5,12a,22b}$), 2.25 – 2.01 (m, 3H, $H^{15a,23}$), 1.99 (s, 3H, H^{31}), 1.98 – 1.80 (m, 4H, $H^{2,4,7a,12b}$), 1.79 – 1.70 (m, 1H, H^{6a}), 1.68 (s, 3H, H^{27}), 1.68 – 1.63 (m, 2H, $H^{1b,9}$), 1.63 (s, 3H, H^{26}), 1.50 (s, 3H, H^{31}), 1.29 (d, *J* = 14.4 Hz, 1H, H^{15b}), 1.27 – 1.15 (m, 2H, $H^{6b,7b}$), 1.10 (s, 3H, H^{19}), 0.98 (s, 3H, H^{18}), 0.94 (d, *J* = 6.8 Hz, 3H, H^{28}); ^{13}C NMR (100 MHz, CD_3OD) δ_C 174.3, 172.6, 164.8, 149.1, 148.5, 146.8, 146.1, 145.1, 133.3, 132.4, 124.4, 78.8, 75.7, 68.3, 50.6, 50.0, 44.9, 40.7, 40.1, 38.8, 37.8, 37.5, 36.9, 33.1, 31.7, 29.9, 29.3, 28.3, 25.9, 24.3, 23.5, 22.1, 20.7, 18.2, 17.9, 16.2; purity (LC-MS) 97%, t_R = 4.28 min, MS *m/z* 621.4 $[M-H]^-$.

(Z)-2-((3R,4S,5S,8S,9S,10S,11R,13R,14S,16S)-16-acetoxy-4,8,10,14-tetramethyl-3,11-bis((pyrazine-2-carbonyl)oxy)hexadecahydro-17*H*-cyclopenta[*a*]phenanthren-17-ylidene)-6-methylhept-5-enoic acid [3.22]

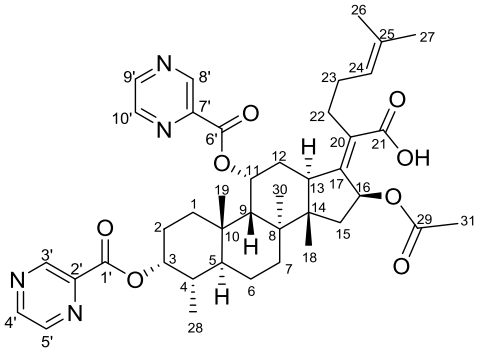

3.22
$C_{41}H_{52}N_4O_8$
Exact Mass: 728.38
MW: 728.89

White solid (32 mg, 12% yield); m.p. 134 – 136 °C; R_f 0.29 (MeOH:DCM, 0.5:9.5); ^{1}H NMR (400 MHz, CD_3OD) δ_H 9.18 (d, *J* = 1.2 Hz, 1H, $H^{3'}$), 9.06 (d, *J* = 1.4 Hz, 1H, $H^{8'}$), 8.80 (d, *J* = 2.4 Hz, 1H, $H^{5'}$), 8.73 (dd, *J* = 2.5, 1.4 Hz, 1H, $H^{4'}$), 8.71 – 8.68 (m, 2H, $H^{9',10'}$), 5.84 (d, *J* = 8.5 Hz, 1H, H^{16}), 5.76 – 5.66 (m, 1H, H^{11}), 5.28 – 5.18 (m, 1H, H^{3}), 5.04 – 4.95 (m, 1H, H^{24}), 3.04 – 2.90 (m, 1H, H^{13}), 2.66 – 2.57 (m, 1H, H^{22a}), 2.54 – 2.42 (m, 2H, $H^{5,12a}$), 2.41 – 2.31 (m, 1H, H^{12b}), 2.31 – 2.21 (m, 1H, H^{15a}), 2.09 – 1.99 (m, 2H, $H^{9,22b}$), 1.98 (s, 3H, H^{31}), 1.97 – 1.85 (m, 6H, $H^{1a,2a,4,7a,23}$), 1.85 – 1.74 (m, 2H, $H^{2b,6a}$), 1.69 (s, 3H, H^{27}), 1.44 (s, 3H, H^{26}), 1.43 (s, 3H, H^{30}), 1.42 – 1.39 (m, 2H, $H^{1b,7b}$), 1.36 (d, *J* = 14.2 Hz, 1H, H^{15b}), 1.34 – 1.21 (m, 1H, H^{6b}), 1.16 (s, 3H, H^{19}), 1.04 (s, 3H, H^{18}), 0.92 (d, *J* = 6.7 Hz, 3H, H^{28}); ^{13}C NMR (100 MHz, CD_3OD) δ_C 173.7, 172.4, 164.8, 164.5, 149.0, 148.8, 147.2, 146.5, 146.3 (2C), 146.1, 144.8, 144.7, 133.4, 132.7, 123.7, 78.0, 75.4, 74.4, 49.9, 49.8, 45.1, 40.8, 39.9, 38.6, 37.9, 36.6, 33.1, 32.9, 31.0, 29.6, 28.6, 28.0, 25.8, 24.5, 23.3, 21.7, 20.7, 18.2, 17.7, 16.1; purity (LC-MS) 90%, t_R = 4.17 min, MS *m/z* 727.3 $[M-H]^-$.

5.2.5 Procedure for the synthesis and characterization C-3 amine series

5.2.5.1 Intermediate 3.23

(3*R*,4*S*,5*S*,8*S*,9*S*,10*S*,11*R*,13*R*,14*S*,16*S*,*Z*)-17-(1-hydrazineyl-6-methyl-1-oxohept-5-en-2-ylidene)-3,11-dihydroxy-4,8,10,14-tetramethylhexadecahydro-1*H*-cyclopenta[*a*]phenanthren-16-yl acetate [3.23]

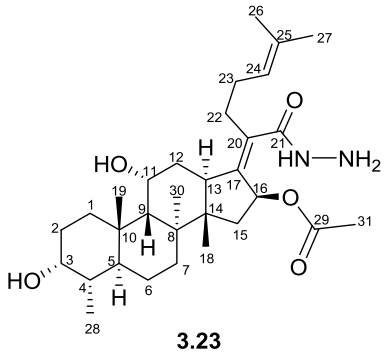

3.23
$C_{31}H_{50}N_2O_5$
Exact Mass: 530.37
MW: 530.75

To a solution of fusidic acid (4.26 g, 8.24 mmol) in acetonitrile (10 mL), HOBt (1.47 g, 9.89 mmol) and EDCI (1.85 g, 9.89 mmol) were added subsequently while stirring at 25 °C for 3 hrs. Hydrazine hydrate (1.60 mL, 32.96 mmol) was then added with continuous stirring at 25 °C. After completion of reaction (TLC), the reaction mixture was concentrated under reduced pressure and the residue taken up in DCM (30 mL) and washed with water (3×30 mL). The organic layer was dried over anhydrous $MgSO_4$, filtered and concentrated *in vacuo*. The crude product was then purified by column chromatography on silica gel using 70% EtOAc/Hexane as eluent, which after washing with pentane afforded white solid (4.05 g, 86% yield); m.p. 113 – 115 °C; R_f 0.37 (MeOH:DCM:NH_4OH, 0.9:9:0.1); ^{1}H NMR (400 MHz, CD_3OD) δ_H 5.78 (d, J = 8.4 Hz, 1H, H^{16}), 5.18 – 5.07 (m, 1H, H^{24}), 4.35 – 4.28 (m, 1H, H^{11}), 3.71 – 3.62 (m, 1H, H^3), 3.10 – 2.99 (m, 1H, H^{13}), 2.59 – 2.48 (m, 1H, H^{22a}), 2.32 – 2.21 (m, 2H, $H^{12a,22b}$), 2.21 –2.03 (m, 5H, $H^{1a,5,15a,23}$), 1.99 (s, 3H, H^{31}), 1.89 – 1.69 (m, 4H, $H^{2,7a,12b}$), 1.68 (s, 3H, H^{27}), 1.61 (s, 3H, H^{26}), 1.61 – 1.58 (m, 1H, H^9), 1.58 – 1.44 (m, 3H, $H^{1b,4,6a}$),

1.39 (s, 3H, H^{30}), 1.20 (d, *J* = 14.2 Hz, 1H, H^{15b}), 1.18 – 1.07 (m, 2H, $H^{6b,7b}$), 1.00 (s, 3H, H^{19}), 0.95 (s, 3H, H^{18}), 0.90 (d, *J* = 6.8 Hz, 3H, H^{28}); ^{13}C NMR (100 MHz, CD_3OD) δ_C 173.1, 172.4, 144.9, 133.9, 133.2, 124.4, 75.0, 72.4, 68.5, 50.7, 49.9, 44.6, 40.7, 40.2, 38.2, 37.8, 37.3, 36.8, 32.9, 31.0 (2C), 30.4, 28.7, 25.9, 23.8 (2C), 22.4, 21.1, 17.9 (2C), 16.5; purity (LC-MS) 99%, MS *m/z* 529.3 $[M-H]^-$.

5.2.5.2 Intermediate 3.24

(3*R*,4*S*,5*S*,8*S*,9*S*,10*S*,11*R*,13*R*,14*S*,16*S*,*Z*)-3,11-dihydroxy-4,8,10,14-tetramethyl-17-(6-methyl-1-(2-(methylsulfonyl)hydrazinyl)-1-oxohept-5-en-2-ylidene)hexadecahydro-1*H*-cyclopenta[*a*]phenanthren-16-yl acetate [3.24]

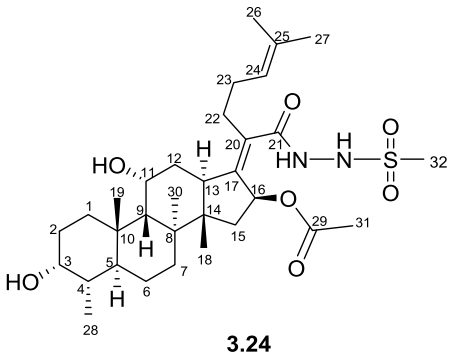

3.24
$C_{32}H_{52}N_2O_7S$
Exact Mass: 608.35
MW: 608.84

Methanesulfonyl chloride (0.63 mL, 8.12 mmol) was added to a solution of compound **3.23** (4.31 g, 8.12 mmol) in pyridine (20 mL) while stirring at 25 °C. After completion of reaction (TLC), the reaction mixture was diluted with ethyl acetate (30 mL) and washed with water (3×30 mL) and 0.5 M aq. HCl (3×30 mL). The organic layer was dried over anhydrous $MgSO_4$, filtered and concentrated *in vacuo*. The crude product was then purified by column chromatography on silica gel using 70% EtOAc/Hexane as eluent, which after washing with pentane afforded white solid (4.46 g, 90% yield); m.p. 125 – 127 °C; R_f 0.42 (EtOAc:DCM, 8:2); ^{1}H NMR (400 MHz, $CDCl_3$) δ_H 8.16 (s, 1H, H^{CONH}), 7.10 (br s, 1H, H^{SO_2NH}), 5.73 (d, *J* = 8.2 Hz, 1H, H^{16}), 5.15 – 5.05 (m, 1H, H^{24}), 4.39 – 4.30 (m, 1H, H^{11}), 3.79 – 3.70 (m, 1H,

H^{3}), 3.06 – 3.00 (m, 1H, H^{13}), 3.00 (s, 3H, H^{32}), 2.49 – 2.40 (m, 1H, H^{22a}), 2.38 – 2.22 (m, 2H, $H^{12a,22b}$), 2.21 – 2.07 (m, 5H, $H^{1a,5,15a,23}$), 1.99 (s, 3H, H^{31}), 1.93 – 1.69 (m, 4H, $H^{2,7a,12b}$), 1.67 (s, 3H, H^{27}), 1.60 (s, 3H, H^{26}), 1.58 – 1.53 (m, 3H, $H^{4,6a,9}$), 1.52 – 1.46 (m, 1H, H^{1b}), 1.37 (s, 3H, H^{30}), 1.27 (d, *J* = 14.2 Hz, 1H, H^{15b}), 1.17 – 1.04 (m, 2H, $H^{6b,7b}$), 0.97 (s, 3H, H^{19}), 0.93 (s, 3H, H^{18}), 0.91 (d, *J* = 6.9 Hz, 3H, H^{28}); ^{13}C NMR (100 MHz, $CDCl_3$) δ_C 170.8, 170.6, 145.9, 133.1, 131.7, 122.7, 73.8, 71.5, 68.3, 49.4, 48.8, 43.8, 39.6, 39.4, 39.3, 37.0, 36.4, 36.0, 35.5, 32.1, 30.2, 29.8, 29.7, 28.3, 25.7, 23.9, 23.0, 21.2, 20.8, 17.9, 17.8, 15.9; purity (LC-MS) 83%, t_R = 4.49 min, MS *m/z* 549.3 $[M\text{-}OAc]^+$.

5.2.5.3 Intermediate 3.25

(4*S*,5*S*,8*S*,9*S*,10*S*,11*R*,13*R*,14*S*,16*S*,*Z*)-11-hydroxy-4,8,10,14-tetramethyl-17-(6-methyl-1-(2-(methylsulfonyl)hydrazinyl)-1-oxohept-5-en-2-ylidene)-3-oxohexadecahydro-1*H*-cyclopenta[*a*]phenanthren-16-yl acetate [3.25]

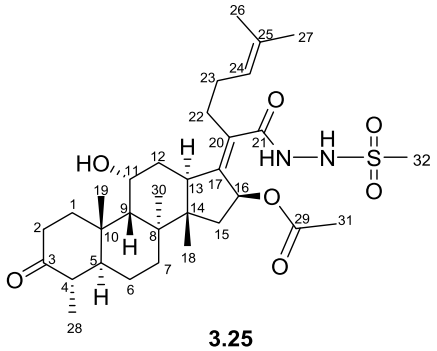

3.25
$C_{32}H_{50}N_2O_7S$
Exact Mass: 606.33
MW: 606.82

Jones reagent (0.35 mL, 1.06 mmol, 2.98 mM) was added dropwise to a solution of compound **3.24** (2.48 g, 4.08 mmol) in acetone (8.00 mL) with stirring in an ice bath over 30 mins after which the reaction was stirred for an additional 10 mins, before being diluted with water (30 mL) and extracted with EtOAc (3×30 mL). The organic layer was then dried over anhydrous $NaSO_4$, filtered and concentrated under reduced pressure. The crude product was then purified by column chromatography on silica gel using 50% EtOAc/Hexane as eluent,

which after washing with pentane afforded a white solid (730 mg, 29% yield); m.p. 123 – 125 °C; R_f 0.31 (EtOAc:DCM, 1:1); ^{1}H NMR (400 MHz, $CDCl_3$) δ_H 7.96 (d, *J* = 4.5 Hz, 1H, H^{CONH}), 6.98 (d, *J* = 4.5 Hz, 1H, H^{SO_2NH}), 5.73 (d, *J* = 8.0 Hz, 1H, H^{16}), 5.16 – 5.06 (m, 1H, H^{24}), 4.43 – 4.35 (m, 1H, H^{11}), 3.07 – 3.00 (m, 1H, H^{13}), 3.00 (s, 3H, H^{32}), 2.53 – 2.41 (m, 3H, $H^{2,22a}$), 2.38 – 2.23 (m, 4H, $H^{1a,5,12a,22b}$), 2.19 – 2.08 (m, 3H, $H^{15a,23}$), 2.00 (s, 3H, H^{31}), 1.99 – 1.83 (m, 4H, $H^{1b,4,7a,12b}$), 1.68 (s, 3H, H^{27}), 1.66 – 1.61 (m, 2H, $H^{6a,9}$), 1.60 (s, 3H, H^{26}), 1.32 (d, *J* = 14.2 Hz, 1H, H^{15b}), 1.29 (s, 3H, H^{30}), 1.28 – 1.16 (m, 2H, $H^{6b,7b}$), 1.15 (s, 3H, H^{19}), 1.00 (d, *J* = 6.6 Hz, 3H, H^{28}), 0.96 (s, 3H, H^{18}); ^{13}C NMR (100 MHz, $CDCl_3$) δ_C 213.5, 170.6, 170.5, 146.1, 133.3, 132.1, 122.6, 73.8, 68.1, 48.9, 48.4, 45.7, 45.4, 43.8, 39.5, 39.3, 39.2, 38.0, 37.0, 36.0, 35.4, 33.6, 29.7, 28.2, 25.7, 24.7, 22.6, 21.8, 21.2, 18.2, 17.8, 12.3; purity (LC-MS) 99%, t_R = 4.25 min, MS *m/z* 605.3 $[M-H]^-$.

5.2.5.4 Target compound 3.26

(4*S*,5*S*,8*S*,9*S*,10*S*,11*R*,13*R*,14*S*,16*S*,*Z*)-11-hydroxy-4,8,10,14-tetramethyl-17-(6-methyl-1-(2-(methylsulfonyl)hydrazineyl)-1-oxohept-5-en-2-ylidene)-3-(methylamino)hexadecahydro-1*H*-cyclopenta[*a*]phenanthren-16-yl acetate [3.26]

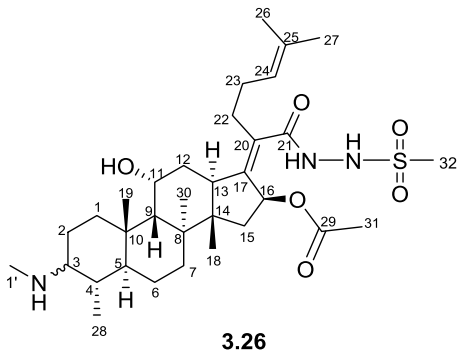

3.26
$C_{33}H_{55}N_3O_6S$
Exact Mass: 621.38
MW: 621.88

To a solution of **3.25** (90 mg, 0.15 mmol) in DCE (4.00 mL), methylamine (0.02 mL, 0.44 mmol), $Na(OAc)_3BH$ (319 mg, 1.48 mmol) and AcOH (0.02 mL, 0.30 mmol) were added and the mixture stirred under N_2 atmosphere at 60 °C for 48 hrs. After completion of reaction

(TLC), the reaction mixture was quenched with 1 N aq. $NaHCO_3$, extracted with EtOAc (30 mL) and washed with water (3×30 mL). The organic layer was dried over anhydrous $MgSO_4$, filtered and concentrated *in vacuo*. The crude product was then purified by prep-TLC using 9% MeOH/DCM as eluent, which after washing with pentane afforded a white solid (10.8 mg, 12% yield); m.p. 137 – 139 °C; R_f 0.20 (MeOH:DCM:NH_4OH, 0.9:9.05:0.05); a 1:1 mixture of diastereomers; ^{1}H NMR (400 MHz, $CDCl_3$) δ_H 7.11 (d, *J* = 8.7 Hz, 1H, H^{CONH}), 6.80 (d, *J* = 8.8 Hz, 1H, H^{SO_2NH}), 5.73 (d, *J* = 8.3 Hz, 1H, H^{16}), 5.18 – 5.03 (m, 1H, H^{24}), 4.50 – 4.34 (m, 1H, H^{11}), 2.98 (s, 3H, H^{32}), 2.96 – 2.92 (m, 1H, H^{13}), 2.51 – 2.43 (m, 1H, H^3), 2.37 (s, 3H, $H^{1'}$), 2.35 – 2.24 (m, 1H, H^{22a}), 2.23 – 2.03 (m, 8H, $H^{1,5,12a,15a,22b,23}$), 2.01 (s, 3H, H^{31}), 1.98 – 1.83 (m, 2H, H^2), 1.83 – 1.72 (m, 1H, H^{12b}), 1.65 (s, 3H, H^{27}), 1.64 – 1.58 (m, 3H, $H^{4,6a,9}$), 1.58 (s, 3H, H^{26}), 1.47 – 1.41 (m, 1H, H^{7a}), 1.39 (s, 3H, H^{30}), 1.19 (d, *J* = 14.4 Hz, 7H, H^{15b}), 1.15 – 1.00 (m, 2H, $H^{6b,7b}$), 0.99 (s, 3H, H^{19}), 0.92 (s, 3H, H^{18}), 0.88 (d, *J* = 6.8 Hz, 3H, H^{28}); ^{13}C NMR (100 MHz, $CDCl_3$) δ_C 172.0, 170.4, 143.4, 132.6, 132.5, 123.1, 73.9, 68.1, 61.5, 49.9, 48.6, 43.5, 40.3, 39.7, 39.1, 36.6, 36.4, 35.5, 35.3, 35.0, 30.1, 29.8, 29.7, 28.3, 25.6, 24.9, 24.2, 22.8, 21.6, 21.3, 17.7, 17.1, 15.9; purity (LC-MS) 80%, t_R = 3.44 min, MS *m/z* 620.3 $[M-H]^-$.

5.3 Biological assay procedure

The minimum inhibitory concentration (MIC) was determined using the standard broth micro dilution method on a single 96-well microtiter plate.[118,119] A 10 mL culture of *Mycobacterium tuberculosis* H37RvMa is grown for the Alamar Blue assay.[120] The cultures are grown to an optical density (OD_{600}) of 0.6 – 0.7.

The media used are:

(i) GAST/Fe (glycerol–alanine–salts) medium pH 6.6, supplemented with 0.05% Tween- 80 and 1% Glycerol.[121,122]

(ii) 7H9 supplemented with 10% Albumin Dextrose Catalase supplement (ADC), 0.05% Tween-80 and 0.2% D-glucose.[123]

Cultures grown in GAST/Fe are diluted to 1:100, and cultures grown in 7H9 ADC are diluted to 1:500, prior to inoculation of the MIC assay.

The compounds to be tested are reconstituted to a concentration of 10 mM in DMSO. Two-fold serial dilutions of the test compound are prepared across a 96-well micro titre plate, after which, 50 µL of the diluted respective *M. tuberculosis* culture was added to each well from rows 2-12 in a serial dilution. The plate layout is a modification of the method previously described.[124] Assay controls used are a minimum growth control (Rifampicin at 2x MIC) and a maximum growth control (5% DMSO).

The micro titre plates are sealed in a secondary container and incubated at 37 °C with 5% CO_2 and humidification to prevent evaporation of the liquid. The lowest concentration of drug that inhibits growth of more than 99 % of the bacterial population is considered to be the MIC_{99}. The MIC values were then recorded at 7- and 14-days post inoculation of the assay, by observing the presence or absence of a bacterial pellet. 10 µL of Alamar Blue (resazurin) is added at day 13 and the assay plate is re-incubated for another 24 hrs. A visual score is obtained by observation of a color change, from blue (no bacterial growth) to pink (growth), at day-14.

REFERENCE

1. World Health Organization *Global Tuberculosis Report*; Geneva, **2016**.

2. Marriner, G. A.; Nayyar, A.; Uh, E.; Wong, S. Y.; Mukherjee, T.; Via, L. E.; Carroll, M.; Edwards, R. L.; Gruber, T. D.; Choi, I.; Lee, J.; Arora, K.; England, K. D.; Boshoff, H. I. M.; Barry III, C. E. *Top. Med. Chem.* **2011**, *7*, 47–124.

3. Migliori, G. B.; Loddenkemper, R.; Blasi, F.; Raviglione, M. C. *Eur. Respir. J.* **2007**, *29*, 423–427.

4. Todar, K. Mycobacterium tuberculosis and Tuberculosis http://textbookofbacteriology.net/tuberculosis.htm (accessed May 24, 2017).

5. Gengenbacher, M.; Kaufmann, S. H. E. *FEMS Microbiol. Rev.* **2012**, *36*, 514–532.

6. Lawn, S. D.; Zumla, A. I. *Lancet* **2011**, *378*, 57–72.

7. Rivers, E. C.; Mancera, R. L. *Drug Discov. Today* **2008**, *13*, 1090–1098.

8. Lee, B.; Clemens, D. L.; Silva, A.; Dillon, B. J.; Maslesa-Galic, S.; Nava, S.; Ding, X.; Ho, C. M.; Horwitz, M. A. *Nat. Commun.* **2017**, *8*, In press DOI:10.1038/ncomms14183.

9. Kinchen, J. M.; Ravichandran, K. S. *Nat. Rev. Mol. Cell Biol.* **2008**, *9*, 781–95.

10. Guirado, E.; Schlesinger, L. S. *Front. Immunol.* **2013**, *4*, 1–7.

11. Cohen, T.; Jenkins, H. E.; Lu, C.; McLaughlin, M.; Floyd, K.; Zignol, M. *Drug Resist. Updat.* **2014**, *17*, 105–123.

12. World Health Organization *Global Tuberculosis Report*; Geneva, **2013**.

13. Zumla, A.; Raviglione, M.; Hafner, R.; Reyn, F. C. V. *N. Engl. J. Med.* **2013**, *368*, 745–755.

14. Janin, Y. L. *Bioorg. Med. Chem.* **2007**, *15*, 2479–513.

15. Jassal, M.; Bishai, W. R. *Lancet Infect. Dis.* **2009**, *9*, 19–30.

16. World Health Organization *Treatment of tuberculosis: guidelines*; 4th ed.; Geneva, **2010**.

17. Dube, D.; Agrawal, G. P.; Vyas, S. P. *Drug Discov. Today* **2012**, *17*, 760–773.

18. Jnawali, H. N.; Ryoo, S. In *Tuberculosis-Current issues in diagnosis and management*; Bassam, H. M.; Mayank, G. V., Eds.; InTech: Janeza Trdine, **2013**; pp. 163–180.

19. Sloan, D. J.; Lewis, J. M. *Trans. R. Soc. Trop. Med. Hyg.* **2016**, *110*, 163–172.

20. Chetty, S.; Ramesh, M.; Singh-Pillay, A.; Soliman, M. E. S. *Bioorg. Med. Chem. Lett.* **2017**, *27*, 370–386.

21. Lienhardt, C.; Raviglione, M.; Spigelman, M.; Hafner, R.; Jaramillo, E.; Hoelscher, M.; Zumla, A.; Gheuens, J. *J. Infect. Dis.* **2012**, S1–9S.

22. World Health Organization *Treatment of tuberculosis: Guidelines for national programmes*; 3rd ed.; Geneva, **2003**.

23. Zignol, M.; Dean, A. S.; Falzon, D.; Gemert, W. Van; Wright, A.; Deun, A. Van; Portaels, F.; Laszlo, A.; Espinal, M. A.; Pablos-Méndez, A.; Bloom, A.; Aziz, M. A.; Weyer, K.; Jaramillo, E.; Nunn, P.; Floyd, K.; Raviglione, M. C. *N. Engl. J. Med.* **2016**, *375*, 1081–1089.

24. Francis J Curry National Tuberculosis Center *Tuberculosis Infection Control: a*

practical manual for preventing TB; Francis J Curry: San Francisco, **2007**.

25. Souza, M. V. N. D. *Fitoterapia* **2009**, *80*, 453–60.

26. World Health Organization *Multidrug-resistant tuberculosis (MDR-TB)*; **2013**.

27. Falzon, D.; Jaramillo, E.; Schünemann, H. J.; Arentz, M.; Bauer, M.; Bayona, J.; Blanc, L.; Caminero, J. A.; Daley, C. L.; Duncombe, C.; Fitzpatrick, C.; Gebhard, A.; Getahun, H.; Henkens, M.; Holtz, T. H.; Keravec, J.; Keshavjee, S.; Khan, A. J.; Kulier, R.; Leimane, V.; Lienhardt, C.; Lu, C.; Mariandyshev, A.; Migliori, G. B.; Mirzayev, F.; Mitnick, C. D.; Nunn, P.; Nwagboniwe, G.; Oxlade, O.; Palmero, D.; Pavlinac, P.; Quelapio, M. I.; Raviglione, M. C.; Rich, M. L.; Royce, S.; Rüsch-Gerdes, S.; Salakaia, A.; Sarin, R.; Sculier, D.; Varaine, F.; Vitoria, M.; Walson, J. L.; Wares, F.; Weyer, K.; White, R. A.; Zignol, M. *Eur. Respir. J.* **2011**, *38*, 516–528.

28. World Health Organization *Anti-tuberculosis drug reistance in the world*; Geneva, **2004**.

29. World Health Organization *"Totally Drug-Resistant TB": a WHO consultation on the diagnostic definition and treatment options*; Geneva, **2012**.

30. Srivastava, S.; Peloquin, C. A.; Sotgiu, G.; Migliori, G. B. *Eur. Respir. J.* **2013**, *42*, 1449–1453.

31. Ma, Z.; Lienhardt, C.; McIlleron, H.; Nunn, A. J.; Wang, X. *Lancet* **2010**, *375*, 2100–2109.

32. Banuls, A. L.; Sanou, A.; Van Anh, N. T.; Godreuil, S. *J. Med. Microbiol.* **2015**, *64*, 1261–1269.

33. Chaudhari, K.; Surana, S.; Jain, P.; Patel, H. M. *Eur. J. Med. Chem.* **2016**, *124*, 160–185.

34. Fears, R.; Kaufmann, S.; Meulen, T. V.; Zumla, A. *Tuberculosis* **2010**, *90*, 182–187.

35. Zumla, A. I.; Gillespie, S. H.; Hoelscher, M.; Philips, P. P. J.; Cole, S. T.; Abubakar, I.; McHugh, T. D.; Schito, M.; Maeurer, M.; Nunn, A. J. *Lancet Infect. Dis.* **2014**, *14*, 327–340.

36. Working Group on new TB Drugs. Global TB drug pipeline http://www.newtbdrugs.org/pipeline/clinical (accessed May 26, 2017).

37. Muliaditan, M.; Davies, G. R.; Simonsson, U. S. H.; Gillespie, S. H.; Pasqua, O. D. *Drug Discov. Today* **2017**, *22*, 481–486.

38. Kakkar, A. K.; Dahiya, N. *Tuberculosis* **2014**, *94*, 357–362.

39. Manjunatha, U.; Boshoff, H. I. M.; Barry III, C. E. *Commun. Integr. Biol.* **2009**, *2*, 215–218.

40. Lechartier, B.; Rybniker, J.; Zumla, A.; Cole, S. T. *EMBO Mol. Med.* **2014**, *6*, 158–168.

41. Dooley, K. E.; Phillips, P. P. J.; Nahid, P.; Hoelscher, M. *Adv. Drug Delivery Rev.* **2016**, *102*, 116–122.

42. Kishore, N.; Mishra, B. B.; Tripathi, V.; Tiwari, V. K. *Fitoterapia* **2009**, *80*, 149–163.

43. Balunas, M. J.; Kinghorn, A. D. *Life Sciences* **2005**, *78*, 431–441.

44. Dias, D. A.; Urban, S.; Roessner, U. *Metabolites* **2012**, *2*, 303–336.

45. Garcia, A.; Bocanegra-Garcia, V.; Palma-Nicolas, J. P.; Rivera, G. *Eur. J. Med. Chem.* **2012**, *49*, 1–23.

46. Zhang, A.; Sun, H.; Wang, X. *Eur. J. Med. Chem.* **2013**, *63*, 570–577.

47. Cragg, G. M.; Newman, D. J. *Biochim. Biophys. Acta* **2013**, *1830*, 3670–3695.

48. Dong, M.; Pfeiffer, B.; Altmann, K. H. *Drug Discov. Today* **2017**, *22*, 585–591.

49. Newman, D. J.; Cragg, G. M. *J. Nat. Prod.* **2016**, *79*, 629–661.

50. Peláez, F. *Biochem. Pharmacol.* **2006**, *71*, 981–990.

51. Njuguna, N. M.; Masimirembwa, C.; Chibale, K. *J. Nat. Prod.* **2012**, *75*, 507–513.

52. Espinoza-Moraga, M.; Njuguna, N. M.; Mugumbate, G.; Caballero, J.; Chibale, K. *J. Chem. Inf. Model.* **2013**, *53*, 649–660.

53. Patridge, E.; Gareiss, P.; Kinch, M. S.; Hoyer, D. *Drug Discov. Today* **2016**, *21*, 204–207.

54. Newman, D. J.; Cragg, G. M. *J. Nat. Prod.* **2012**, *75*, 311–335.

55. Godtfredsen, W. O.; Daehne, V. W.; Tybring, L.; Vangedal, S. *J. Med. Chem.* **1966**, *9*, 15–22.

56. Godtfredsen, W. O.; Vangedal, S. *Acta Chem. Scand.* **1966**, *20*, 1599–1607.

57. Curbete, M. M.; Salgado, H. R. N. *Crit. Rev. Anal. Chem.* **2015**, *46*, 352–360.

58. Long, B. H. *Acta Derm. Venereol, Suppl.* **2008**, *88*, 14–20.

59. Duvold, T.; Jørgensen, A.; Andersen, N. R.; Henriksen, A. S.; Sørensen, D. M.;

Björkling, F. *Bioorg. Med. Chem. Lett.* **2002**, *12*, 3569–72.

60. Von Daehne, W.; Godtfredsen, W. O.; Rasmussen, P. R. *Adv. Appl. Microbiol.* **1979**, *25*, 95–146.

61. Chain, E.; Florey, H. W.; Jennings, M. A.; Williams, T. I. *Brit. J. Exp. Pathol.* **1943**, *24*, 108–119.

62. O'Neill, A. J.; Bostock, J. M.; Moita, A. M.; Chopra, I. *J. Antimicrob. Chemother.* **2002**, *50*, 839–848.

63. Perry, M. J.; Hendricks-Gittings, A.; Stacey, L. M.; Adlard, M. W.; Noble, W. C. *J. Antibiot.* **1983**, 1659–1663.

64. Zhao, M.; Gödecke, T.; Gunn, J.; Duan, J. A.; Che, C. T. *Molecules* **2013**, *18*, 4054–4080.

65. Pushkin, R.; Iglesias-Ussel, M. D.; Keedy, K.; MacLauchlin, C.; Mould, D. R.; Berkowitz, R.; Kreuzer, S.; Darouiche, R.; Oldach, D.; Fernandes, P. *Clin. Infect. Dis.* **2016**, *63*, 1599–1604.

66. Liang, R.; Yong, X.; Duan, Y.; Tan, Y.; Zeng, P.; Zhou, Z.; Jiang, Y.; Wang, S.; Jiang, Y.; Huang, X.; Dong, Z.; Hu, T.; Shi, H.; Li, N. *World J. Microbiol. Biotechnol.* **2014**, *30*, 2861–2869.

67. Christiansen, K. *Int. J. Antimicrob. Agents* **1999**, *12*, S3–S9.

68. Payne, A. J.; Neal, L. M.; Knoll, L. J. *Parasitol. Res.* **2013**, *112*, 3859–3863.

69. Leo Pharma *FUCIDIN ® Fusidic acid Product Monograph*; Thornhill, **2013**.

70. Johnson, R. A.; McFadden, G. I.; Goodman, C. D. *PLoS One* **2011**, *6*, 1–6.

71. Duvold, T.; Sørensen, M. D.; Bjorkling, F.; Henriksen, A. S.; Rastrup-Andersen, N. *J. Med. Chem.* **2001**, *44*, 3125–3131.

72. Cicek-Saydam, C.; Cavusoglu, C.; Burhanoglu, D.; Hilmioglu, S.; Ozkaly, N.; Bilgic, A. *Clin. Microbiol. Infect.* **2001**, *7*, 700–702.

73. National Center for Biotechnology Information . *PubChem BioAssay Database; AID=1332.https://pubchem.ncbi.nlm.nih.gov/bioassay/1332 (accessed May 26, 2017).*

74. Aubé, J. *ACS Med. Chem. Lett.* **2012**, *3*, 442–444.

75. Kigondu, E. M.; Wasuna, A.; Warner, D. F.; Chibale, K. *Bioorg. Med. Chem.* **2014**, *22*, 4453–4461.

76. Wolfson, J. S.; Hooper, D. C. *Clin. Microbiol. Rev.* **1989**, *2*, 378–424.

77. Lu, Y.; Zheng, M.; Wang, B.; Fu, L.; Zhao, W.; Li, P.; Xu, J.; Zhu, H.; Jin, H.; Yin, D.; Huang, H.; Upton, A. M.; Ma, Z. *Antimicrob. Agents Chemother.* **2011**, *55*, 5185–5193.

78. Wallis, R. S.; Dawson, R.; Friedrich, S. O.; Venter, A.; Paige, D.; Zhu, T.; Silvia, A.; Gobey, J.; Ellery, C.; Zhang, Y.; Eisenach, K.; Miller, P.; Diacon, A. H. *PLoS ONE* **2014**, *9*, 1–9.

79. Koul, A.; Arnoult, E.; Lounis, N.; Guillemont, J.; Andries, K. *Nature* **2011**, *469*, 483–490.

80. Ashburn, T. T.; Thor, K. B. *Nat. Rev. Drug Discovery* **2004**, *3*, 673–683.

81. Maitra, A.; Kolvekar, T.; Devarajan, P. V; Guzman, J. D.; Bhakta, S. *Int. J. Infect. Dis.* **2015**, *32*, 50–55.

82. Findon, G.; Miller, T. E.; Rowe, L. C. *Lab. Anim. Sci.* **1991**, *41*, 462–5.

83. Johnson, M. D.; MacDougall, C.; Ostrosky-Zeichner, L.; Perfect, J. R.; Rex, J. H. *Antimicrob. Agents Chemother.* **2004**, *48*, 693–715.

84. Omollo, C. PhD Thesis, University of Cape Town, **2017**.

85. Kaur, G. PhD Thesis, Univeristy of Cape Town, **2016**.

86. Wasuna, A. PhD Thesis, University of Cape Town, **2017**.

87. Lemaire, S.; Van Bambeke, F.; Pierard, D.; Appelbaum, P. C.; Tulkens, P. M. *Clin. Infect. Dis.* **2011**, *52*, S493–S503.

88. Turnidge, J. *Int. J. Antimicrob. Agents* **1999**, *12*, S23–S34.

89. Njoroge, M. PhD Thesis, University of Cape Town, **2014**.

90. Janssen, G.; Vanderhaeghe, H. *J Med. Chem.* **1967**, *10*, 205–208.

91. Diacon, A. H.; Pym, A.; Grobusch, M.; Patientia, R.; Rustomjee, R.; Page-Shipp, L.; Pistorius, C.; Krause, R.; Bogoshi, M.; Churchyard, G.; Venter, A.; Allen, J.; Palomino, J. C.; Marez, T. D.; Heeswijk, R. P. G. Van; Lounis, N.; Meyvisch, P.; Verbeeck, J.; Parys, W.; Beule, K. de; Andries, K.; McNeeley, D. F. *N. Engl. J. Med.* **2009**, *360*, 2397–2405.

92. Metushi, I. G.; Nakagawa, T.; Uetrecht, J. *Chem. Res. Toxicol.* **2012**, *25*, 2567–2576.

93. Sinha, B. K.; Mason, R. P. *J. Drug Metab. Toxicol.* **2014**, *5*, 30–31.

94. Strydom, N. PhD Thesis, University of Cape Town, **2016**.

95. Mindermann, T.; Zimmerli, W.; Rajacic, Z.; Gratzl, O. *Acta Neurochir. (Wien)* **1993**,

121, 12–14.

96. Meanwell, N. A. *J. Med. Chem.* **2011**, *54*, 2529–2591.

97. Ballatore, C.; Huryn, D. M.; Smith III, A. B. *ChemMedChem* **2014**, *8*, 385–395.

98. Zawilska, J. B.; Wojcieszak, J.; Olejniczak, A. B. *Pharmacol. Rep.* **2013**, *65*, 1–14.

99. Huttunen, K. M.; Raunio, H.; Rautio, J. *Pharmacol. Rev.* **2011**, *63*, 750–71.

100. Mori, G.; Chiarelli, L. R.; Riccardi, G.; Pasca, M. R. *Drug Discov. Today* **2017**, *22*, 519–525.

101. Craig, P. N. *J. Med. Chem.* **1971**, *14*, 680–684.

102. Espinoza-Moraga, M.; Singh, K.; Njoroge, M.; Kaur, G.; Okombo, J.; De Kock, C.; Smith, P. J.; Wittlin, S.; Chibale, K. *Bioorg. Med. Chem. Lett.* **2016**, *27*, 658–661.

103. Kaur, G.; Singh, K.; Pavadai, E.; Njoroge, M.; Espinoza-Moraga, M.; De Kock, C.; Smith, P. J.; Wittlin, S.; Chibale, K. *Med. Chem. Commun.* **2015**, *6*, 2023–2028.

104. Montalbetti, C. A. G. N.; Falque, V. *Tetrahedron* **2005**, *61*, 10827–10852.

105. Tsakos, M.; Schaffert, E. S.; Clement, L. L.; Villadsen, N. L.; Poulsen, T. B. *Nat. Prod. Rep.* **2015**, 605–632.

106. Rastrup-Andersen, N.; Duvold, T. *Magn. Reson. Chem.* **2002**, *40*, 471–473.

107. Duvold, T.; Bretting, C. A. S.; Rasmussen, P. R.; Bouerat, L.; Thorhauge, J. Novel fusidic acid derivatives **2005**, WO 2005/007669 A1.

108. Vishwanatha, T. M.; Panguluri, N. R.; Sureshbabu, V. V *Synthesis* **2013**, *45*, 1569–1601.

109. Dunetz, J. R.; Xiang, Y.; Baldwin, A.; Ringling, J. *Org. Lett.* **2011**, *13*, 5048–5051.

110. Xu, J. Q.; Shen, Q.; Li, J.; Hu, L. H. *Bioorg. Med. Chem.* **2010**, *18*, 3934–9.

111. Jursic, B. S.; Upadhyay, S. K.; Creech, C. C.; Neumann, D. M. *Bioorg. Med. Chem. Lett.* **2010**, *20*, 7372–5.

112. Abdel-Magid, A. F.; Carson, K. G.; Harris, B. D.; Maryanoff, C. A.; Shah, R. D. *J. Org. Chem.* **1996**, *61*, 3849–3862.

113. Panfilov, A. V; Markovich, Y. D.; Zhirov, A. A.; Ivashev, I. P.; Kirsavon, A. T.; Kondrat'ev, V. B. *Pharm. Chem. J.* **2000**, *34*, 371–373.

114. Klein, D. *Organic chemistry*; 2nd ed.; John Wiley & Sons: Hoboken, **2015**.

115. Tojo, G.; Fernandez, M. *Oxidation of Alcohols to Aldehydes and Ketones*; 1st ed.; Springer: New York, **2006**.

116. Clayden, J.; Greeves, N.; Warren, S. *Organic Chemistry*; 2nd ed.; Oxford University Press: New York, **2012**.

117. Prideaux, B.; Via, L. E.; Zimmerman, M. D.; Eum, S.; Sarathy, J.; O'Brien, P.; Chen, C.; Kaya, F.; Weiner, D. M.; Chen, P.; Song, T.; Lee, M.; Shim, T.; Cho, J. S.; Kim, W.; Cho, N. S.; Olivier, K. N.; Barry III, C. E.; Dartois, V. *Nat. Med.* **2015**, *21*, 1223–1227.

118. Collins, L. A.; Franzblau, S. G. *Antimicrob. Agents Chemother.* **1997**, *41*, 1004–1009.

119. Collins, L. A.; Torrero, M. N.; Franzblau, S. G. *Antimicrob. Agents Chemother.* **1998**, *42*, 344–347.

120. Ioerger, T. R.; Feng, Y.; Ganesula, K.; Chen, X.; Dobos, K. M.; Fortune, S.; Jacobs, J.

W. R.; Mizrahi, V.; Parish, T.; Rubin, E.; Sassetti, C.; Sacchettini, J. C. *J. Bacteriol.* **2010**, *192*, 3645–3653.

121. De Voss, J. J.; Rutter, K.; Schroeder, B. G.; Su, H.; Zhu, Y.; Barry III, C. E. *Proc. Natl. Acad. Sci. U.S.A.* **2000**, *97*, 1252–1257.

122. Franzblau, S. G.; DeGroote, M. A.; Cho, S. H.; Andries, K.; Nuermberger, E.; Orme, I. M.; Mdluli, K.; Angulo-Barturen, I.; Dick, T.; Dartois, V.; Lenaerts, A. J. *Tuberculosis* **2012**, *92*, 453–88.

123. Pethe, K.; Sequeira, P. C.; Agarwalla, S.; Rhee, K.; Kuhen, K.; Phong, W. Y.; Patel, V.; Beer, D.; Walker, J. R.; Duraiswamy, J.; Jiricek, J.; Keller, T. H.; Chatterjee, A.; Tan, M. P.; Ujjini, M.; Rao, S. P. S.; Camacho, L.; Bifani, P.; Mak, P. A.; Ma, I.; Barnes, S. W.; Chen, Z.; Plouffe, D.; Thayalan, P.; Ng, S. H.; Au, M.; Lee, B. H.; Tan, B. H.; Ravindran, S.; Nanjundappa, M.; Lin, X.; Goh, A.; Lakshminarayana, S. B.; Shoen, C.; Cynamon, M.; Kreiswirth, B.; Dartois, V.; Peters, E. C.; Glynne, R.; Brenner, S.; Dick, T. *Nat. Commun.* **2010**, *1*, 1–8.

124. Ollinger, J.; Bailey, M. A.; Moraski, G. C.; Casey, A.; Florio, S.; Alling, T.; Miller, M. J.; Parish, T. *PLoS ONE* **2013**, *8*, 1–9.

Appendices

Appendix 1: Key COSY correlations of fusidic acid (**3.1**) in $CDCl_3$

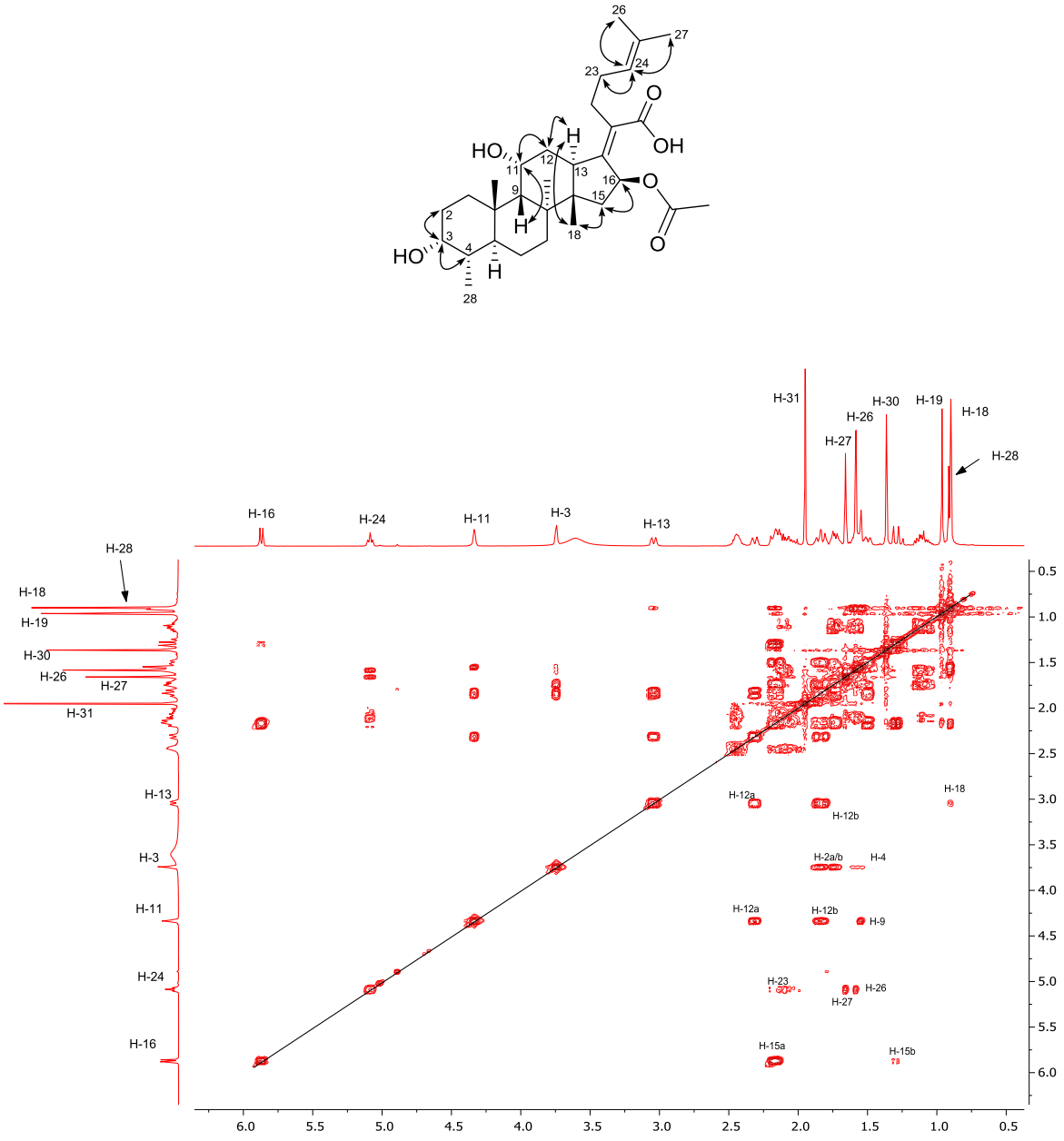

Appendix 2: Stacked ^{1}H-NMR spectra of compounds **3.1** and **3.2** in DMSO-d_6

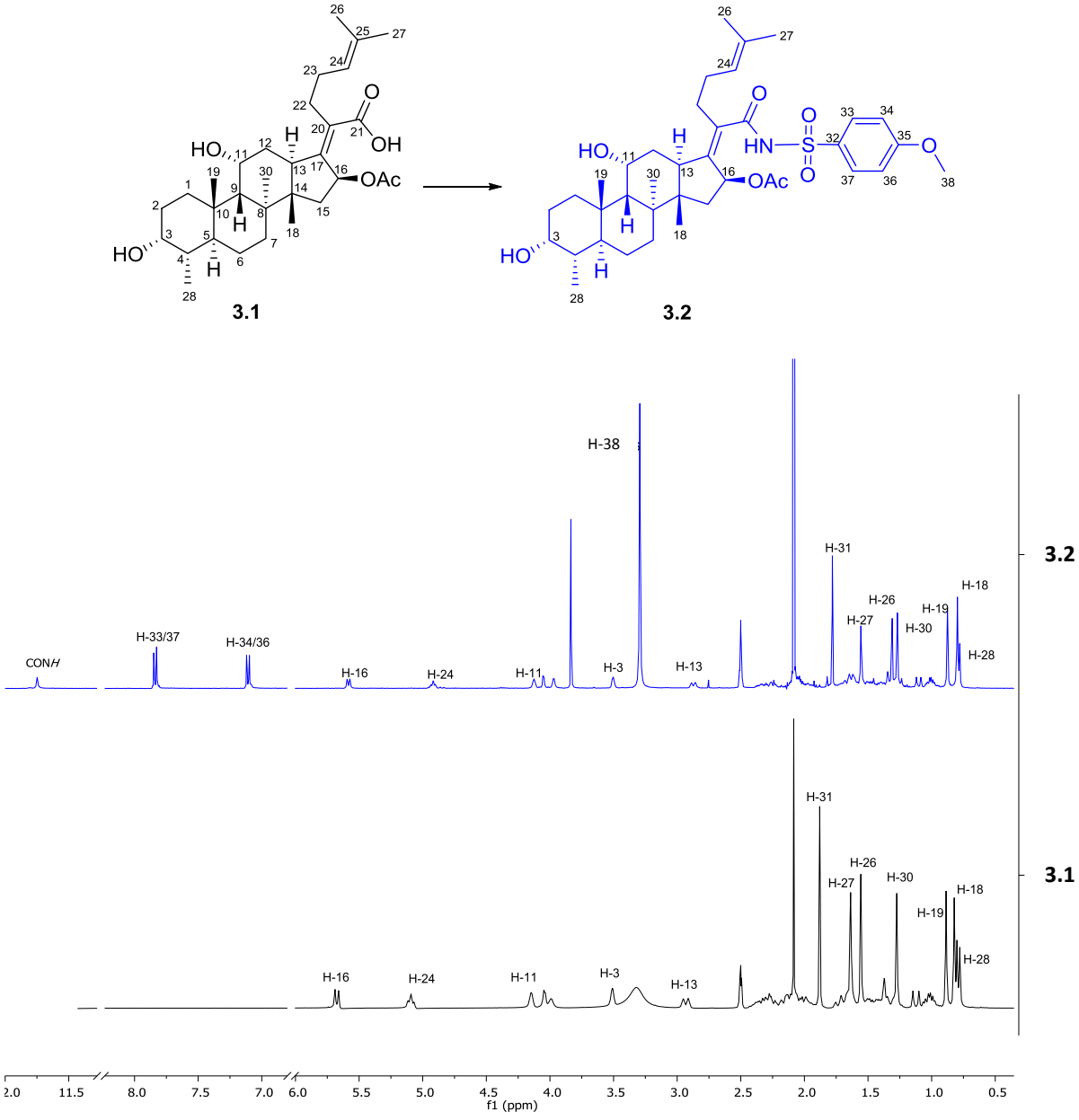

Appendix 3: Stacked ^{1}H-NMR spectra of compounds **3.1, 3.4, 3.6** and **3.8** in $CDCl_3$

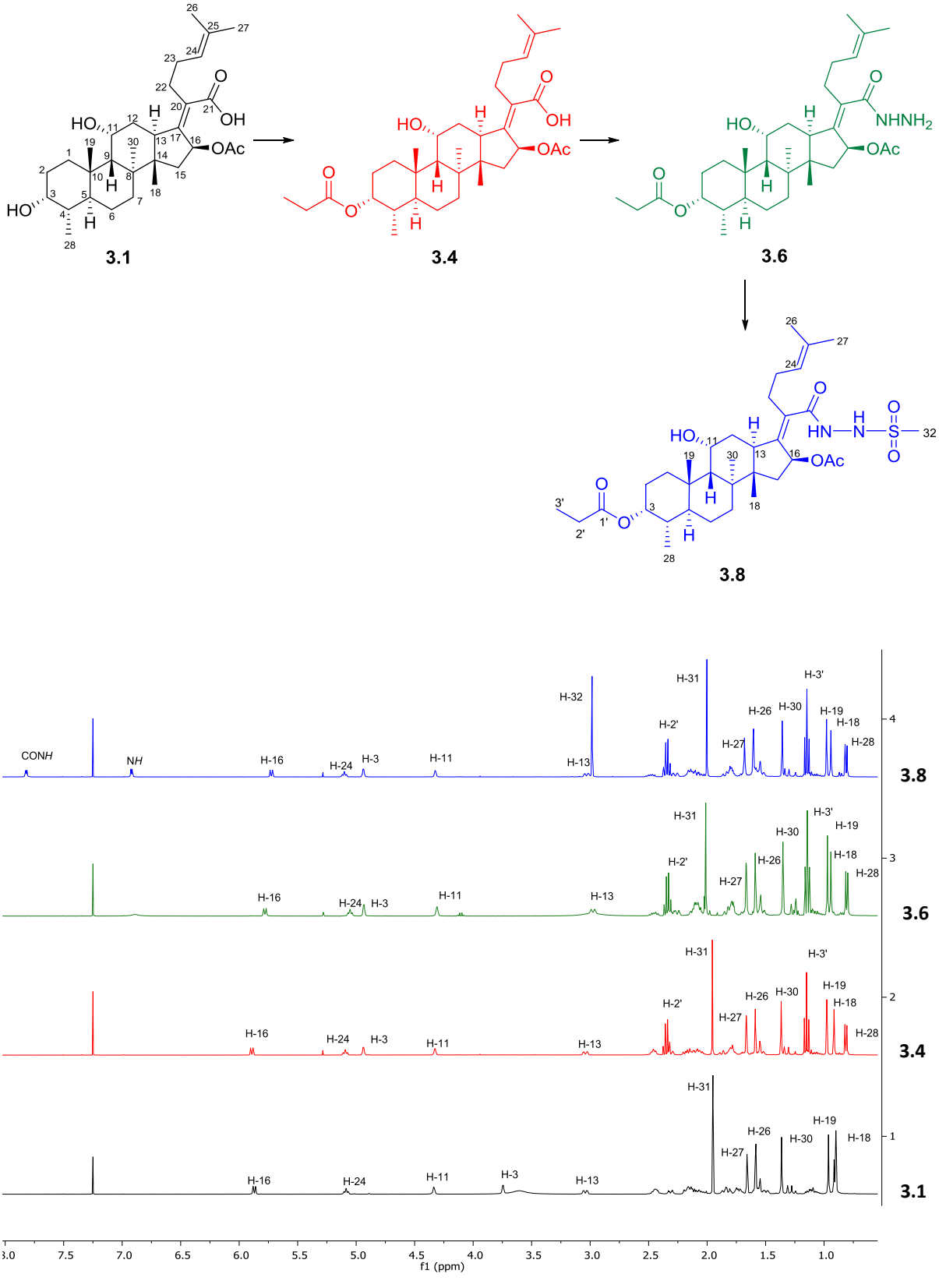

Appendix 4: Stacked ^{1}H-NMR spectra of compounds **3.1** and **3.13** in CD_3OD

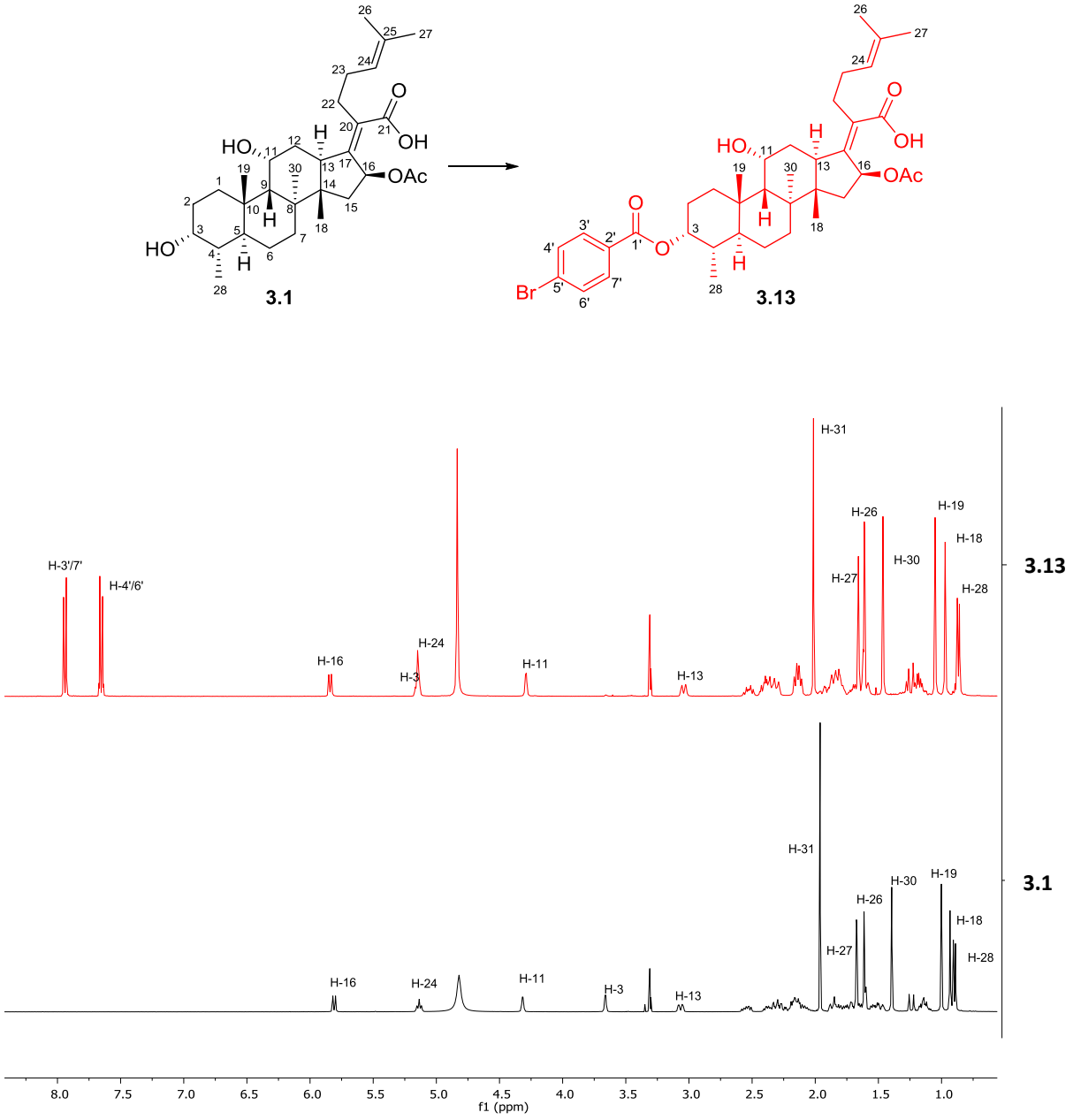

Appendix 5: Stacked ^{1}H-NMR spectra of compounds **3.1, 3.21** and **3.22** in CD_3OD

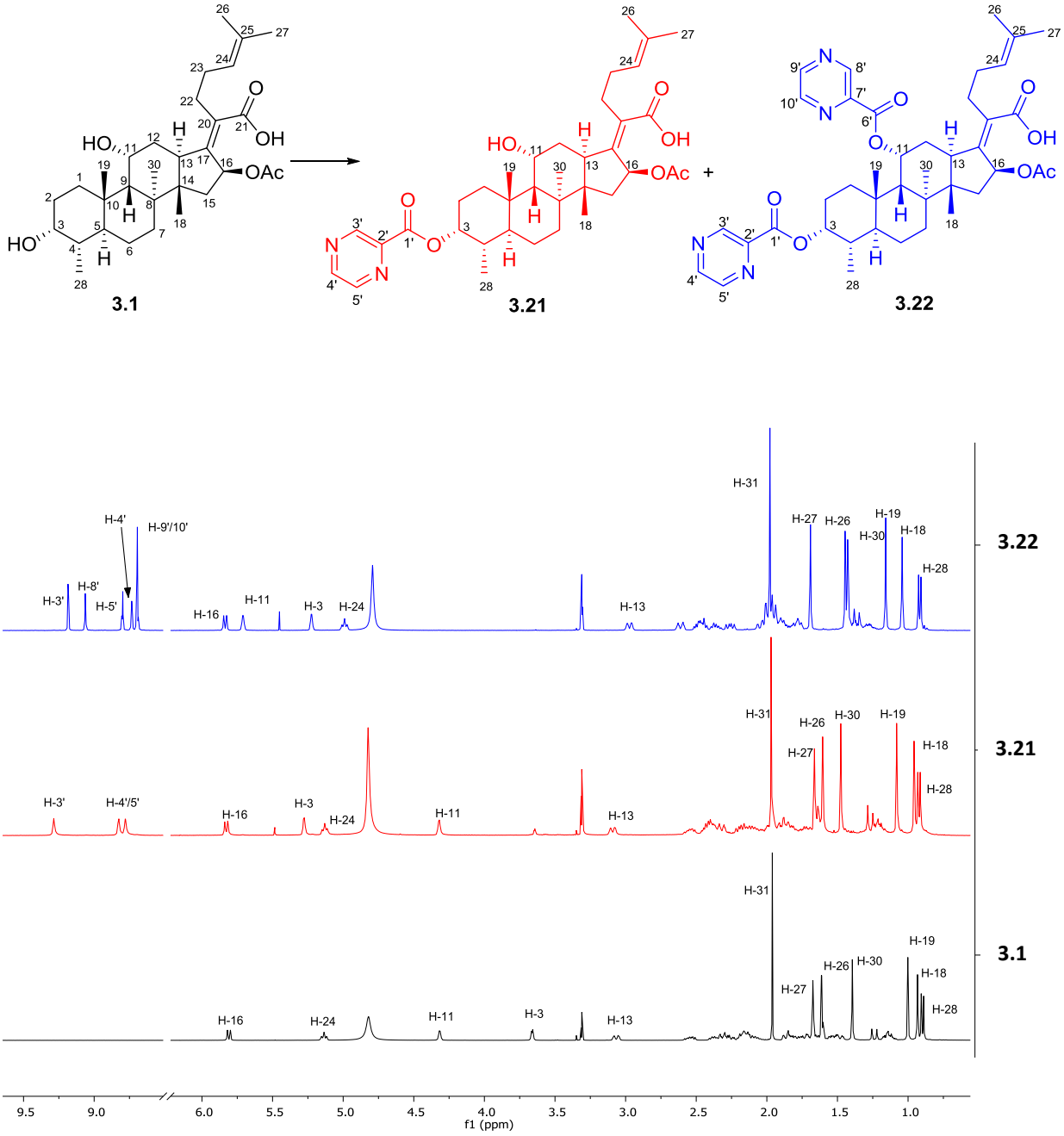

Appendix 6: Stacked ^{1}H-NMR spectra of compounds **3.1, 3.24, 3.25** and **3.26** in $CDCl_3$